Producing A Peptide For Use In A Blood Biosensor For Injury

Detection

By

Errek Mạnh Trung Phạm

Submitted in Partial Fulfillment of the Requirements

for the Degree of

Master of Science

in the

Biological Sciences

Program

YOUNGSTOWN STATE UNIVERSITY

December 2020

Producing A Peptide For Use In A Blood Biosensor For Injury Detection

Errek Mạnh Trung Phạm

I hereby release this thesis to the public. I understand that this thesis will be made available from the OhioLINK ETD Center and the Maag Library Circulation Desk for public access. I also authorize the University or other individuals to make copies of this thesis as needed for scholarly research.

Signature: _____

                     Errek M.T. Phạm, Master's Student   Date

Approvals: _____

                     Dr. Diana L. Fagan, Thesis Advisor   Date

                     _____

                     Dr. Jonathan J. Caguiat, Committee Member   Date

                     _____

                     Dr. David K. Asch, Committee Member   Date

                     _____

                     Dr. Salvatore A. Sanders, Dean of Graduate Studies   Date

Abstract

Conventional hybridoma technology has been used for the selection and production of proteins for biosensor development. However, hybridoma technology is typically a slower and more costly procedure than phage display and produces a less durable end-product. Quicker and more efficient production of a small peptide using phage display has been studied at Youngstown State University for use in a blood biosensor. A heptapeptide BR-1 had been selected to bind to human serum albumin (HSA) with high specificity and was sequenced and inserted into a pMAL-c5X expression vector. In this study, biotinylation with biotin-PEG$_4$-hydrazide and EDC chemistry, indirect enzyme-linked immunosorbent assays (ELISAs) with HSA target and biotinylated peptide (B-BR-1), and competitive inhibition peptide ELISAs with HSA target, soluble or bound Inhibition HSA, and B-BR-1 were used to confirm peptide specificity for HSA. The pMAL-c5X protein production and purification system, amylose resin affinity chromatography, 8–16% and 16.5% SDS-PAGE, and UV-Vis spectrophotometry were used to evaluate BR-1 production and purity. Binding of 2 μg B-BR-1 to 1 μg HSA target was significantly reduced by 0.01 and 0.1 μg bound Inhibition HSA ($p < 0.05$). Bound Inhibition HSA was found to inhibit B-BR-1 more strongly than soluble HSA. A fusion of maltose binding protein to BR-1 was produced and purified by affinity chromatography with a high yield of 2.23 mg/mL MBP/BR-1. However, evaluation of protein cleavage by SDS-PAGE and UV-Vis spectrophotometry was unable to detect soluble BR-1 peptide after cleavage. Optimization of BR-1 production and purification methods will enable future mass production of a small, durable peptide to develop a wearable blood biosensor to save the lives of military and law enforcement personnel.

Acknowledgements

Table of Contents

Abbreviations/Terms

γ – wavelength

ε – extinction coefficient

Ω – Ohms

A – absorbance

A_{500} – absorbance at 500 nm

A_{600} – absorbance at 600 nm

Ab – antibody

AH – Alexander Huber

ALT – alanine aminotransferase

b – cell path

BR – William (Bill) Rees

BR-1 – peptide discovered by Bill Rees

B-BR-1 – biotinylated BR-1 peptide

Boc – butyloxycarbonyl

BSA – bovine serum albumin

CNT – carbon nanotube

CSA – chicken serum albumin

CVD – chemical vapor deposition

Da – Dalton

DCCD – 1,3-dicyclohexylcarbodiimide

dH_2O – deionized water

DMSO – dimethyl sulfoxide

EDC – 1-ethyl-3-(3-dimethylaminopropyl) carbodiimide

EDTA – ethylenediaminetetraacetic acid

EIS – electrical impedance spectroscopy

ELISA – enzyme-linked immunosorbent assay

EP – Errek Pham

FET – field-effect transistor

FK – Floyd Kenney

Fmoc – fluorenylmethyloxycarbonyl

h – Hill coefficient of cooperativity of binding

HABA – 4'-hydroxyazobenzene-2-carboxylic acid

HRP – horseradish peroxidase

HRP/Anti-M13 – horseradish peroxidase-anti-M13 conjugate

HRP/SA – horseradish peroxidase-streptavidin conjugate

HSA – human serum albumin

g – gravitational acceleration

IPTG – isopropyl β-D-1-thiogalactopyranoside

K_d – dissociation constant

LB – Luria-Bertani

M – molarity (moles/L)

MBP – maltose binding protein

MES – N-morpholino ethanesulfonic acid

MSTN – myostatin

MWCNT – multiwalled carbon nanotube

MWCO – molecular weight cutoff

N – normality (equivalent moles of hydrogen ions per mole acid/base)

NFDM – nonfat dry milk

NHS – *N*-hydroxysuccinimide

NMR – nuclear magnetic resonance

OVA – ovalbumin

PBS – phosphate buffered saline

PBST – PBS + 0.05% Tween-20

PCR – polymerase chain reaction

PEDOT – poly(3,4 ethylenedioxythiophene)

PEG – poly(ethylene glycol)

PEG_4 – four units of PEG

PES – polyethersulfone

pfu – plaque-forming unit

PSS – poly(sodium 4-styrene sulfonate)

QCM – quartz crystal microbalance

RbSA – rabbit serum albumin

RF – replicative form

RP-HPLC – reversed-phase high performance liquid chromatography

RPM – revolutions per minute

SA – streptavidin

SDS – sodium dodecyl sulfate

SDS-PAGE – sodium dodecyl sulfate polyacrylamide gel electrophoresis

Sulfo-NHS – sulfo-*N*-hydroxysuccinimide

SWCNT – single-walled carbon nanotube

TBS – Tris buffered saline

TFA – trifluoroacetic acid

TMB – 3,3,5,5-Tetramethylbenzidine

Tween-20 – polyoxyethylene-sorbitan monolaurate

X-gal – 5-bromo-4-chloro-3-indolyl β-D-galactopyranoside

Figures

Tables

A. Introduction

As modern technology continues to advance and improve quality of life around the world, it also makes the taking of life much easier through the production of new weapons of war. Once an individual has been injured in the line of duty, medical personnel must be notified of that person's need for medical attention. This can be done by the injured person him/herself or by another person at the scene, but the amount of time that elapses during the notification and the distance medical personnel must travel may be too great. The injured could also be incapacitated and no other person is around to observe the event. In order to address this problem, one solution that has been researched for various uses around the world is the development of wearable biosensors.

A problem that arises from conventional use of larger proteins in biosensors is protein degradation. Proteins used in research are meant to be stored long-term in cold conditions of 4°C or less, preferably in sterile containers (Pierce Biotechnology 2003). These conditions are not representative of those that are encountered in the field, so longevity of the biosensor must be increased. Exposure to substances such as sweat, dust, airborne pathogens, and food—which are different from the target—may cause a false positive reading in the biosensor. This thesis seeks to produce a small, novel peptide that binds specifically to human serum albumin (HSA) through the uses of phage display technology and a bacterial protein expression vector. The small size of the peptide ought to be more resistant to conformational changes due to changes in temperature while maintaining its specificity for the HSA target.

The significance of this project is the production and use of a peptide that can be used in the development of a blood biosensor. The processes used will be more efficient

in both time and costs than conventional hybridoma technology or purchasing peptide from another lab—especially when large amounts of peptide are needed—with an end-product that will be more durable while maintaining specificity for the HSA target. A wearable blood biosensor can be developed using this peptide that will detect injury in military and law enforcement units, quickly notify medical personnel of the event, and ultimately decrease medical response times and improve survival rates of the individuals who protect and serve their countries.

Biosensors have been intensively and continually researched and produced for various uses across the world in the areas of medicine, food industry, and environmental safety (as reviewed in Yang et al. 2015). Scientists have sought to develop and improve upon old designs in efforts to produce increasingly affordable, sensitive, and fast biosensors that can detect a multitude of biological and chemical compounds. Biosensors are comprised of a transducing element that converts and propagates a signal upon binding of a biological element to its target analyte. Optical, thermal, and electrically conductive fibers have been used on multiple platforms and functionalized with proteins, peptides, and enzymes discovered through hybridoma and phage display technologies (Barozzi et al. 2017; Fischer et al. 2016; McKnight et al. 2016). These transducing elements have multiple properties of interest that enable swift and efficient transmission of signals, while the biological components are selected to bind to target substrates with high specificity and avidity. The methods of selection for—and subsequent functionalization with—the biological elements have been thoroughly studied and modified to develop more efficient protocols that increase the purity and affinity of the selected specific binding elements, yet nonspecific binders remain an issue (Rahbarnia et

al. 2016).

1. Overview of Biosensors

Biosensors are an example of increasingly useful applications of modern technological advancements across many areas including healthcare, diagnosis of disease markers, drug delivery, detection of food-borne pathogens, and probing for environmental contaminants (as reviewed in Yang et al. 2015). One definition of a biosensor given by the Merriam-Webster dictionary is "a device that monitors and transmits information about a life process; especially, a device consisting of a biological component (such as an enzyme or bacterium) that reacts with a target substance and an electrochemical or optical component that detects the resulting products or by-products and emits a signal" (Merriam-Webster 2018). In general, biosensors utilize a biological component and a transducing element through which chemical or physical means detect the presence of other biological molecules upon binding. They must be durable, reliable, inexpensive, specific for analytes of interest, and quick in analyzing data so that they can be commercialized for widespread use in the named areas above, hopefully increasing rates of diagnosis and improving the quality of life for many or even all individuals. **Figure 1** shows the different elements of a biosensor.

Elements of a Biosensor

Samples	Transducers		Data Acquisition System
Cell Cultures	**Nucleic Acids**	**FETs**	**3) Signal Amplifier**
Food Samples	**Cells**	**Nanowire Array**	
Human Samples (Blood, Saliva, Urine)	**Enzymes**	**Nanoparticles** **Electrodes**	**4) Signal Processor**
	Proteins +	**Carbon Nanotubes**	
Environmental Samples (Air, Water, Plants, Soil)	**Antibodies**	**Optical Fibers**	
	1) Bioreceptors	**2) Electrical Interfaces**	**5) Display**

Figure 1: Basic elements of a biosensor.

1.1. Transducing Elements

Transducing elements in biosensor systems are essential in the propagation of a signal upon binding of the target analyte to the sensor. Examples of transducing elements that have been used include optical fibers, steel fibers, 3D-printed polymeric conductive fibers, activated carbon mixed with graphite and metallic conductive ink screen printed on paper substrate, and carbon nanotubes (Barozzi et al. 2017; Fischer et al. 2016; McKnight et al. 2016). These elements vary in their physical, chemical, and mechanical properties, propagate signals through different methods, and have unique functions in their respective biosensor systems. The transducing element of choice for this project is carbon nanotubes.

1.2. Overview of Carbon Nanotubes

Carbon nanotubes are classified as nanomaterials with favorable physical, chemical, and mechanical properties due to their structures. They have been intensely

studied over the past two decades and used in a variety of applications. Carbon nanotubes can differ in structure depending on their method of synthesis and specific structures which affect their properties. Different methods of functionalizing the nanotubes have been utilized to attach chemical or biological molecules that bind to different targets of interest, or analytes. Depending on the functionalized carbon nanotubes and molecules attached, the biosensors in which they are incorporated function based on different working principles to propagate a signal upon binding to their targets, each with a different purpose in their own research fields. This diversity in modifying carbon nanotubes and measuring signal propagation has led to the development of multiple types of biosensors with many applications.

1.2.1. Structures of Carbon Nanotubes

Carbon nanotubes are carbon materials which consist of rolled graphite sheets resembling seamless hollow tubes. The two main types of carbon nanotubes available are single-walled carbon nanotubes (SWCNTs) and multi-walled carbon nanotubes (MWCNTs). SWCNTs can be thought of as a single molecular sheet of graphite rolled up into a seamless cylinder with diameters ranging 0.75–3 nm and lengths ranging 1–50 μm (as reviewed in Yang et al. 2015). MWCNTs consist of at least two layers of curled graphite sheets which may either reach all the way around the structure to make a complete layer or remain separated from each other. Because of their larger size and increased structural integrity, MWCNTs have diameters ranging 2–30 nm or even to more than 100 nm with an approximate distance of 0.42 nm between layers.

Graphite sheets, also called graphene, are sheets of hexagonal sp^2 carbon-carbon

bonds. These carbon-carbon bonds are very strong and, although they have planar geometries, their structure does not experience deformation from being rolled into cylinders. For SWCNTs, the three structural configurations for the cylinders are armchair type, zigzag type, and chiral type where they differ in spiral angle and subsequently differ in electrical properties depending on their diameter. For MWCNTs, different combinations of the structural configurations may be present, but the differences in electrical properties also depend on diameter of the cylinder. **Figure 2** shows the rolling of graphene sheets into CNTs.
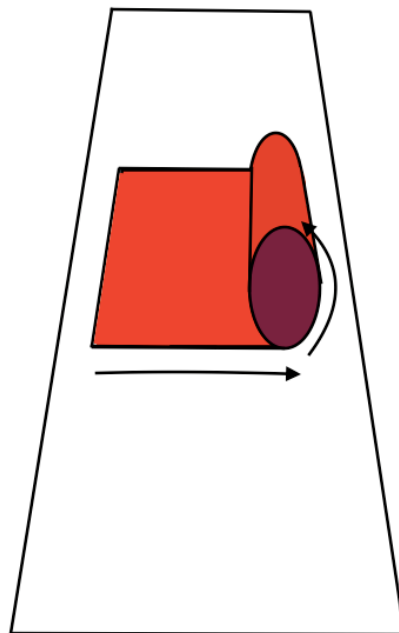
Figure 2: Example of the rolling of two-dimensional graphene sheets (white) into cylindrical CNTs (red) (from Kenney 2018).

1.2.2. *Synthesis of Carbon Nanotubes*

With the demand for carbon nanotubes increasing due to their widespread study and use, additional methods for synthesizing them have been developed and refined.

Companies specializing in nanotechnology have sprung up to meet this increased demand. Many methods have been utilized in the production of SWCNTs and MWCNTs, including the most popular methods of arc discharge, laser ablation, and chemical vapor deposition (as reviewed in Yang et al. 2015).

In arc discharge, carbon nanotubes are grown by deposition on graphite cathodes that undergo a current in a vacuum reactor. Large graphite rods are used as cathodes while smaller graphite rods with metal catalysts such as Ferrocene are used as anodes, all of which are contained in a vacuum reactor with an inert gas that avoids oxidation of the nanotubes. Conditions are varied for efficient production of the nanomaterial and include current, voltage, temperature, reduced pressure, and cooling speed. As the graphite and metal catalyst are subjected to the current, the anode is vaporized, consumed in the presence of high-temperature plasma, and subsequently cooled. The resulting carbon nanotubes are deposited on the cathode and vary in defects, diameter, and purity. Arc discharge, however, is a difficult and expensive synthesis method to maintain, generally yields less product, and requires additional studies to formulate the best conditions conducive for high-yield and efficient production of carbon nanotubes.

In laser ablation, graphite mixed with a metal catalyst is placed into a high temperature vacuum furnace that is likewise filled with an inert gas. A high energy laser beam irradiates the graphite/catalyst mixture, causing them to evaporate due to the temperature of the environment and deposit onto a collector to form carbon nanotubes. The advantage of laser ablation over arc discharge is that the resulting nanotubes are higher in purity and have less defects, but the process is expensive and requires a lot of energy (as reviewed in Yang et al. 2015).

In chemical vapor deposition (CVD), a thermal dehydrogenation reaction occurs in the presence of a transition metal catalyst. A gas containing the carbon source is placed in a reaction chamber along with an inert gas under high temperature, resulting in the decomposition of the carbon source gas and deposition of carbon nanotubes on a catalyst substrate. Carbon sources used include methane, ethanol, ethylene, acetylene, and benzene, while metal catalysts include cobalt, iron, nickel, copper, chromium, and molybdenum. The advantages of CVD include the ability for carbon nanotubes to directly grow on a substrate and the use of simpler and more cost-effective equipment. Most of the nanotubes produced, however, are MWCNTs, so further assessment of CVD synthesis conditions is needed (as reviewed in Yang et al. 2015).

1.2.3. Properties of Carbon Nanotubes

Carbon nanotubes have multiple properties that make them favorable for use in the development of biosensor systems. Carbon nanotubes have tensile strengths greater than steel and Kevlar along with a lower density and high thermal stability (as reviewed in Olszewski 2013). They can act as both thermal and electrical conductors with low resistance, depending on cylindrical diameter, and are thus able to conduct high currents (Holzinger et al. 2011; as reviewed in Yang et al. 2015). Along with their chemically inert nature and high specific surface areas because of their small size, carbon nanotubes can be functionalized to accommodate and utilize chemical and biological molecules to produce functional biosensing systems (as reviewed in Nagaraju et al. 2015). Despite their insolubility and tendency to aggregate in aqueous solutions due to their hydrophobic nature, functionalization solubilizes the nanotubes and increases the number of molecules

that can be conjugated to them.

1.3. Biological Elements

Carbon nanotube-based biosensors have utilized a wide range of biological molecules (as reviewed in Nagaraju et al. 2015 and Yang et al. 2015). The nanotube propagates a signal upon binding of the biological component to its target analyte. Different types of biomolecules and bioreceptors have been used in the production of biosensors. Enzymes can bind to a substrate of interest and produce chemical reactions. Cell receptors, antibodies, antibody fragments, and even peptides can bind to target antigens or pathogens, while nucleotides can bind to DNA or RNA. These molecules can thus act either in aqueous solution or extracellular matrices, at cell membrane surfaces, or inside cells if the transducing element is able to penetrate the cell membrane.

1.4. Functionalization of Carbon Nanotubes

Since carbon nanotubes are hydrophobic and need further "processing" for use in biological systems, they must be functionalized to increase solubility and to introduce biological molecules needed to detect specific analytes. Functionalization can occur through physical processes such as ultrasonication, milling, crushing, and friction to modify the surface of the nanotubes (as reviewed in Yang et al. 2015). Functionalization can also occur through chemical processes which include noncovalent or covalent means to introduce other nanomaterials and/or functional groups and increase biocompatibility. Carbon nanotubes typically have improved characteristics that make them even more desirable for use in creating biosensors and include higher sensitivities, faster response

times, and an increased range of target analytes.

Noncovalent functionalization of carbon nanotubes preserves the original physical and chemical structure and takes advantage of π–π stacking effects and a large surface area to which functional groups can be attached (as reviewed in Yang et al. 2015). Different conjugated polymers or biological molecules have been used to modify the carbon nanotubes, including DNA, peptides, enzymes, and cyclic aromatic hydrocarbons (Holzinger et al. 2011). Proteins are typically used to functionalize and disperse the nanotubes in aqueous solution because they are polar and hydrophilic molecules. The simplest method of noncovalent functionalization is dip coating where the carbon nanotubes are placed in a solution of one or more molecules to be adsorbed. This method is effective at attaching multiple biological molecules and thus enabling the sensor to detect multiple analytes at weaker maximum values, a significant improvement from past biosensors. Although noncovalent functionalization requires less work, the bonds between the molecules and carbon nanotubes are significantly weaker than in covalent functionalization.

Covalent functionalization allows a greater range of molecules to be attached to the carbon nanotubes, but at the expense of structural integrity through the formation of physical defects and the partial destruction of the sp^2 C–C bonds (Kenney 2018; as reviewed in Yang et al. 2015). Oxidation is the first step in functionalization followed by attachment of functional groups and subsequent derivation to produce functional groups and bonds needed for different biosensing applications. The introduction of functional groups improves biosensor sensitivity, interaction with biomolecules, sensing speed, and biological compatibility (as reviewed in Nagaraju et al. 2015).

The carbon nanotubes are oxidized by high concentration acids, such as sulfuric acid or nitric acid, which opens the tubes by creating holes to which functional groups can be attached (as reviewed in Nagaraju et al. 2015). These functional groups include carboxyl, hydroxyl, and sulfate groups which can be further derivatized into amide or ester bonds upon attachment of biological molecules (as reviewed in Yang et al. 2015). Coupling agents are needed, however, to form those bonds between the functionalized carbon nanotubes and the biological molecules. Placing the functionalized carbon nanotubes in solutions of molecules alone, especially those of proteins and peptides, may not attach the nanotubes to the desired part of the biological molecule. The most used coupling agents are hydroxybenzotriazole and the carbodiimides 1-ethyl-3-(3-dimethylaminopropyl) carbodiimide (EDC) and 1,3-dicyclohexylcarbodiimide (DCCD). **Figure 3** shows the oxidation of a SWCNT with a mixture of nitric and sulfuric acids to introduce carboxyl groups.
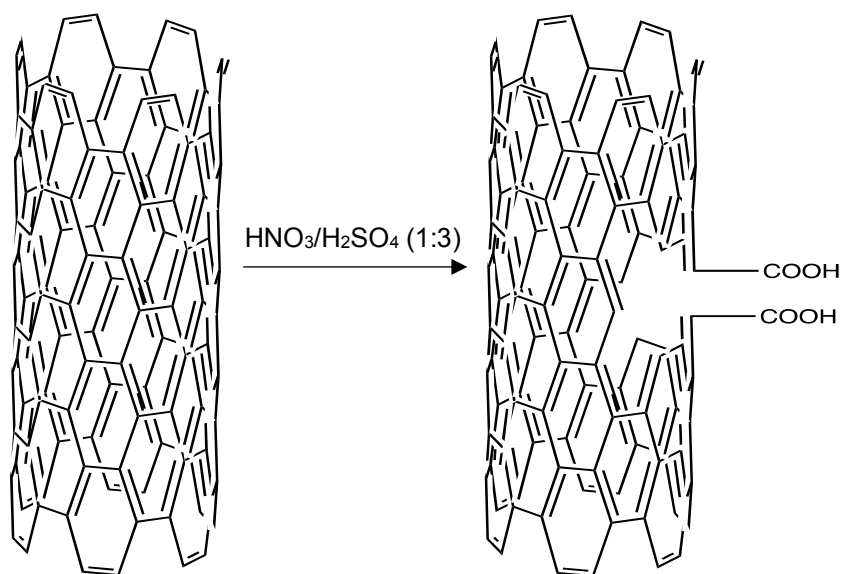
Figure 3: Oxidation of a SWCNT with nitric and sulfuric acids (from Kenney 2018).

Covalent functionalization in which oxidation by nitric acid followed by coupling a peptide through the EDC linker is of interest to this project. Since the short-chain peptide has an amino end (the N-terminus), and the functionalized carbon nanotubes have carboxyl groups introduced, a very strong amide bond can be formed after the EDC cross-linker reaction occurs. The EDC reaction first takes place between the EDC and the carboxyl group to form an amine-reactive *O*-acylisourea intermediate which then reacts with an amino group to form a stabile amide bond, releasing an isourea by-product in the process (as reviewed in Gao and Kyratzis 2008; Thermo Fisher Scientific, Inc. 2011 EDC). The intermediate formed is unstable in aqueous solutions and thus requires *N*-hydroxysuccinimide (NHS) or sulfo-*N*-hydroxysuccinimide (sulfo-NHS) to stabilize the reaction through a two-step conjugation procedure or else the intermediate undergoes hydrolysis. NHS and sulfo-NHS have been conjectured to stabilize the *O*-acylisourea intermediate through conversion to a more stable amine-reactive NHS ester with an increase in efficiency of the reaction. **Figure 4** shows the reaction mechanism for EDC.
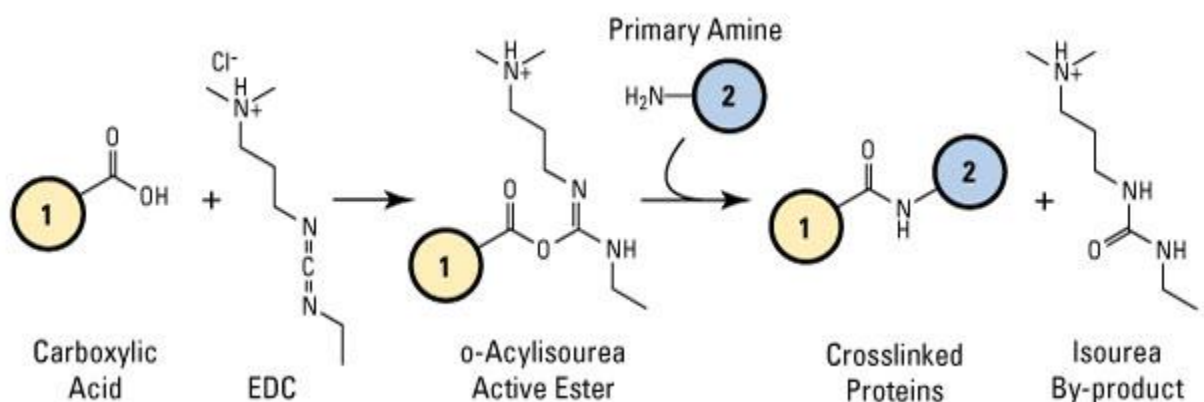
Figure 4: EDC Reaction. Reaction of carboxyl functional group with EDC to attach a peptide with a primary amine (from Thermo Fisher Scientific 2011 EDC).

Peptide/protein functionalized carbon nanotubes have been used in medical applications. Proteins used for functionalization include bovine serum albumin (BSA), streptavidin, and even enzymes such as lysozyme (as reviewed in Nagaraju et al. 2015). Nanotube arrays have been observed to be formed after functionalization with peptides, indicating that biological molecules can be attached to the oxidized carbon nanotubes and interact with other biological species in a solution as well.

1.5. Types and Working Principles of Biosensor Systems

Upon binding of the biological element to its target analyte and converting the binding action into a detectable signal, the two main types of biosensor systems propagate the signal according to either chemical or physical means and can be further subdivided according to their working principles. The detectable signals that can be propagated include current, absorbance, and fluorescence (as reviewed in Yang et al. 2015).

Three types of biosensors which function through chemical means are amperometric-based, potentiometric-based, and impedimetric-based. These sensors typically utilize an enzyme electrode which binds to analytes and produces a reaction (as reviewed in Yang et al. 2015). These biosensors work well because of the carbon nanotubes' hollow structure, their ability to adsorb large amounts of enzymes, and their conversion of the enzymatic reactions into detectable signals such as current, potential, or resistance. The potential to adsorb different enzymes allows the biosensors to be designed to select for a wide variety of analytes.

Other biosensors which function through physical means better represent carbon

nanotubes' desirable properties for use in such systems and include optical, piezoresistive, and calorimetric sensors. Optical biosensors rely on the nanotubes' optimal luminescence properties and easily detectable changes in emission after adsorbing biological molecules, quickly generating results when the sensor is placed in a spectrophotometer (as reviewed in Yang et al. 2015). Piezoresistive biosensors produce changes in resistance when an external force is applied to the carbon nanotubes. The nanotubes can withstand greater stress forces than steel and Kevlar, and they can undergo moderate deformations without loss of function. Calorimetric biosensors take advantage of the carbon nanotubes' excellent thermal stability and conductivity in measuring the corresponding heat changes produced by chemical reactions, namely enzymatic reactions.

1.5.1. *Applications of Carbon Nanotube-Based Biosensors*

After functionalization, the carbon nanotubes and their attached molecules can then be used in biosensors. The nanotubes are functionalized using various methods such as dipping, DNA wrapping, and amidation, amination, and glutaraldehyde cross-linking (as reviewed in Nagaraju et al. 2015 and Yang et al. 2015). Depending on the desired setup, a monitoring device or other method gives a signal or reading which indicates binding of the target analyte to the sensor. Examples of carbon nanotube-based biosensors include enzyme, DNA, and immune sensors. These sensors have been used to successfully detect blood glucose levels, human hormones (androsterone), specific sequences of DNA, activity and concentrations of biological enzymes (DNA methyltransferase), proteins (streptavidin), drugs, adenoviruses, and toxic compounds (hydrogen peroxide, ethanol).

2. Human Serum Albumin

Human serum albumin (HSA) is the most abundant protein in plasma, constituting about 60% of the total proteins in plasma, or an estimated 2.5 % of total blood volume, with normal concentrations ranging 35–50 g/L, or 74.6–522 μM (Peters 1996; Russell et al. 2008). HSA has multiple functions in the body that include balancing osmotic concentrations, buffering pH levels, and transporting substances such as hormones, drugs, and toxic metabolic waste products (Campbell et al. 2000). In individuals who have experienced blood loss from injuries or surgery, HSA levels and blood volumes are decreased, so these individuals require additional HSA for protein replacement therapy and restoring blood volume (Sato et al. 2002). HSA has been purified for these clinical applications and produced in commercial quantities, although they contain impurities which may negatively affect patient health and recovery.

More efficient methods of HSA purification have been evaluated using phage display. Sato et al. utilized phage display and biopanning on HSA-bound polystyrene plates to screen for a peptide which bound with high affinity to HSA, determining binding specificity through ELISA and tested on Sepharose beads to purify HSA (Sato et al. 2002). To account for the conformational changes that HSA experiences upon binding to hydrophobic surfaces such as the polystyrene plates that are typically used in biopanning, Sato et al. also selected for specific phage with biotinylated HSA and magnetic streptavidin beads that more closely mimicked HSA in solution, and they then likewise evaluated phage binding specificity through enzyme-linked immunosorbent assays (ELISAs). Specific binding phage DNA was sequenced, the peptides were synthesized, and then the peptides were tested again to ensure favorable binding to HSA.

One confounding factor, however, was revealed when conducting affinity tests in solution with a near physiological concentration of 140 mM NaCl. Sato et al. found that some of the screened peptides increased or decreased in HSA affinity to varying degrees, indicating that the different peptides are binding to different sites on HSA.

3. Phage Display

Phage display technology has been a significant advancement with many applications across a wide range of research fields. It has been intensively evaluated to display and select for peptides or proteins on the surface of bacteriophage, viruses that infect bacteria and utilize the host's molecular mechanisms to produce new viral proteins and DNA which will assemble to form new viruses (Barbas et al. 2001; as reviewed in Willats 2002). Through modification of the bacteriophage genes, the peptides or proteins that are expressed can be used to probe for various biological or chemical targets. Due to the ability and versatility of the phage genome for modification and the different vehicles through which genetic modification and viral replication can occur, whole libraries of bacteriophages have been constructed to display a multitude of clones with up to 10^{10} diversity, increasing the effectiveness of screening methods for high affinity binders.

3.1. Filamentous Bacteriophages

Bacteriophages, or simply phages, perform viral replication either through a lytic cycle in which the virus is assembled inside the cell and the host bacterium is destroyed in the process, or through a nonlytic cycle in which viral components are exported through the host cell membrane and cell wall to then assemble new viruses. Filamentous

phages have been primarily studied because of their nondestructive, nonlytic cycle and include the Ff class phages f1, fd, and M13 (Barbas et al. 2001). Ff filamentous phages utilize an F pilus on the bacterium for attachment and subsequent entry into the host cell.

The structure of Ff phages consists of a circular genome of single-stranded DNA inside a cylindrical capsid composed of five different viral coat proteins. The main body of the phage consists of approximately 2700 pVIII protein molecules with one end containing about five molecules each of pVII and pIX proteins and the other end similarly containing about five molecules each of pIII and pVI proteins (Barbas et al. 2001). The pVIII major coat proteins are tightly arranged in an overlapping pattern spanning most of the cylindrical phage body. Depending on the size of the phage genome after the insertion of genes of interest, the capsid can increase in length by utilizing more pVIII to accommodate the increase in genetic material. The pVII and pIX minor coat proteins at the one end of the phage are small, hydrophobic molecules that form a pointed end. The pIII and pVI minor coat proteins at the other end of the phage are larger and form a cone-shaped end, with pIII consisting of three domains designated N1, N2, and CT. The N1 amino terminus is required by the phage during infection and the N2 amino terminus binds to the F pilus, thus giving the phage the ability to infect bacteria (Rakonjac et al. 1999). The CT carboxy terminus of pIII interacts with pVI and pVIII to form the cone-shaped end. The remaining viral proteins have other functions related to the phage life cycle. pII, pV, and pX are proteins that bind single-stranded DNA and function in DNA replication, while pI, pIV, and pXI are proteins involved in assembly of the phage at the bacterial membrane. **Figure 5** shows the basic structure of an M13 bacteriophage.
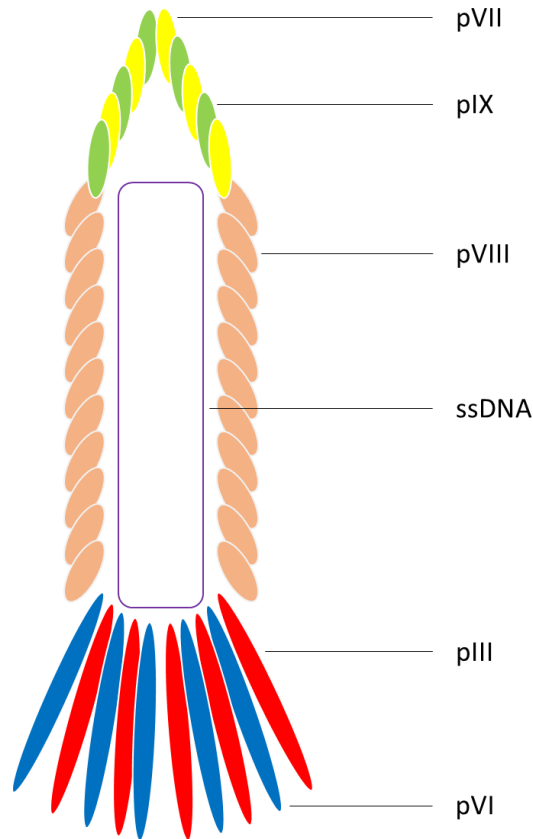
Figure 5: Structure of an M13 bacteriophage.

3.1.1. *Phage Life Cycle*

The phage life cycle consists of infection, replication, and assembly of the new viruses, usually occurring in *Escherichia coli* in the laboratory setting. Infection must first begin with interaction of the phage with the F pilus and bacterial cytoplasmic membrane proteins TolQ, TolR, and TolA (Barbas et al. 2001). The F pilus of an F^+ bacterium containing the F plasmid is used in the process of conjugation between bacteria where the pilus pulls the bacteria together and DNA is transferred from the donor bacterium to a recipient F^- bacterium that lacks the F plasmid. After conjugation, the recipient bacterium becomes F^+ and can go on to conjugate with other bacteria. The TolQRA cytoplasmic membrane proteins, on the other hand, function in maintaining the

integrity of the bacterial outer membrane and span the membrane multiple times to form a complex.

Phages take advantage of the F pilus' action of pulling a target toward the bacterium by attaching to the pilus. The N2 domain of minor coat protein pIII attaches to the F pilus, releasing the N1 domain, and the bacterium pulls the phage towards itself (Barbas et al. 2001). After the phage has been pulled toward the outer membrane of the bacterium, the free N1 domain attaches to TolA which acts as a coreceptor. The coat proteins pVIII, pVII, and pIX then dissociate from each other and enter the cytoplasmic membrane of the bacterium as the phage DNA undergoes translocation into the bacterial cytoplasm.

After these infection steps, the phage takes advantage of the bacterium's enzymes to synthesize complementary DNA and produce double-stranded DNA called the parental replicative form (RF) DNA (Barbas et al. 2001). The synthesized complement strand of DNA is used to transcribe mRNAs which are then translated by ribosomes to produce all 11 phage proteins. The RF DNA is then used to continually produce mRNAs and proteins until the end of the phage replicative cycle is signaled by binding of pV dimers to new phage single-stranded DNA and effectively preventing the formation of RF DNA. The phage coat and assembly proteins are inserted into the cytoplasmic and outer bacterial membranes to facilitate translocation of phage material.

Assembly of new phages occurs at the cytoplasmic and outer bacterial cell membranes. pV is removed from the phage DNA and allows the DNA to be packaged into a new capsid (Barbas et al. 2001). Initiation of assembly occurs when pVII, pIX, and pVIII interact with the newly synthesized DNA and its packaging signal to form the

capsid's pointed end and protrude during a pIV-formed "exit pore." pV is continually removed from the DNA, moving the DNA into the newly forming capsid as pVIII is added on to elongate the phage. pIII and pVI terminate assembly by adding on to the end of the phage DNA and detaching the newly formed phage from the bacterium while maintaining the cell membrane integrity. The CT domain of pIII is important in the release of the phage from the bacterium (Rakonjac et al. 1999).

3.1.2. *Proteins and Peptides Displayed on Phage*

Through insertion of DNA sequences into the genes that encode phage coat proteins, researchers have studied the attachment of other proteins or peptides to the amino and carboxy termini of multiple coat proteins, most notably pVIII and pIII (Barbas et al. 2001). Methods have been selected to introduce proteins or peptides with small enough sizes which allow the phages to retain infectivity and propagation of the phage cycle. A larger number of smaller proteins can be displayed on pVIII while a smaller number of larger proteins can be displayed on pIII (as reviewed in Willats 2002). Since peptides are smaller, they are generally displayed without detrimentally affecting the phage cycle.

There are two methods through which proteins and peptides can be displayed on the pVIII and pIII coat proteins. The first is through a direct fusion of the nucleotide sequence encoding the peptide to be displayed by inserting it between the signal sequence for the coat protein and the amino terminus coding region (Barbas et al. 2001). All the resulting pVIII or pIII proteins are fusion proteins and no wildtype protein is retained, although this can negatively affect the stability, efficiency of packaging, and infectivity

of the phage (as reviewed in Sidhu et al. 2001). To overcome this issue, hybrid phage and phagemid systems (plasmids with a phage origin of replication located within a helper phage) have been developed to retain phage stability, efficiency, and infectivity (as reviewed in Willats 2002). Hybrid phage systems are created such that both the wildtype phage coat protein gene is retained while a modified gene is inserted elsewhere in the phage genome in addition to an antibiotic resistance gene used to select phages displaying the desired fusion proteins (as reviewed in Bazan et al. 2012). In phagemid systems, a helper phage encodes all the phage coat proteins except for an inducible promoter which allows control of the phage cycle and the incorporation of both wildtype and fusion proteins into the capsid. The phagemid replicates as a double-stranded plasmid while the helper phage coinfects and produces single-stranded phagemid DNA that is then incorporated into the newly produced phages. Both hybrid display systems have been used in demonstrating the fusion of proteins to all five phage coat proteins in M13 bacteriophage, namely on the amino termini of pVIII, pIII, pVII, and pIX, and on the carboxy termini of pVI, pIII, and pVIII.

pIII has been most widely used in the development of phage library displaying proteins and peptides. Because only about five of the minor coat protein molecules are displayed on each phage instead of the 2700 pVIII major coat proteins, larger inserts are tolerated in the phage cycle (Barbas et al. 2001). Most sequences are inserted in the N1 domain of the pIII protein, but again, there is a limit to the size of the inserts since very large proteins or peptides can affect the infectivity of the phage. Constructing hybrid phage, however, mediates this problem so that there is less crowding at the cone-shaped end of the phage capsid where one fusion pIII protein is displayed (with the protein or

peptide attached to the amino or carboxy terminus) and the rest are wildtype pIII encoded by the helper phage.

3.2. Biopanning

Biopanning, or simply panning, is a screening procedure in which specific phage binders are selected to find phage clones which bind with high affinity to a target of interest. The process typically coats a target on a plastic microtiter plate either through direct adsorption or, after biotinylating the target, through indirect binding to another protein such as streptavidin that binds very tightly to the support (as reviewed in Bazan et al. 2012; New England BioLabs 2016). Using biotinylation and a streptavidin-coated support can prevent denaturation or blocking of binding sites on the target that would otherwise occur if the target were bound to the support alone. Biotinylation and streptavidin capture supports allow affinity discrimination in which higher affinity and avidity phages bind to the target, although the yield per clone is low (Barbas et al. 2001). Other supports to which the target and/or streptavidin can be attached include column matrices, magnetic beads, or even whole cells.

The type of support, antigen concentration, phage concentration, blocking agents, incubation time, detergents, and number of washing steps used all affect the yield and presence of phage clones that do not bind with high affinity (Barbas et al. 2001; as reviewed in Bazan et al. 2012). Several troubleshooting methods are used to remove nonbinding background phages, plate-binding phage, and low affinity phage. Repeated washing steps dilute the solution in the wells so that the nonbinding phage can be removed through aspiration. After enough washings, the number of nonbinding phages

should be minimized. Meanwhile, preadsorption steps, in which the phage solution is

exposed to blocking agents such as BSA or casein, remove blocking agent binders

through a negative selection process and leaves the rest of the phage library in solution

for transfer to the next set of wells for additional preadsorption steps (if more than one

blocking agent is used) or for binding to the target molecule (New England BioLabs

2016). Increasing the concentration of the detergent used (usually Tween-20) can remove

low affinity specific binding phage by disrupting their weaker bonding and displacing

them into solution for aspiration. Furthermore, additional rounds of panning can be

performed to increase the number of high affinity specific binding phage and decrease

low affinity specific or nonspecific binding phage. Amplification of the phage eluates

between each panning round can increase the number of high affinity specific phages at

the cost of also increasing the number of nonspecific or low affinity specific phages.

Figure 6 shows the basic biopanning process to select for specific phage.
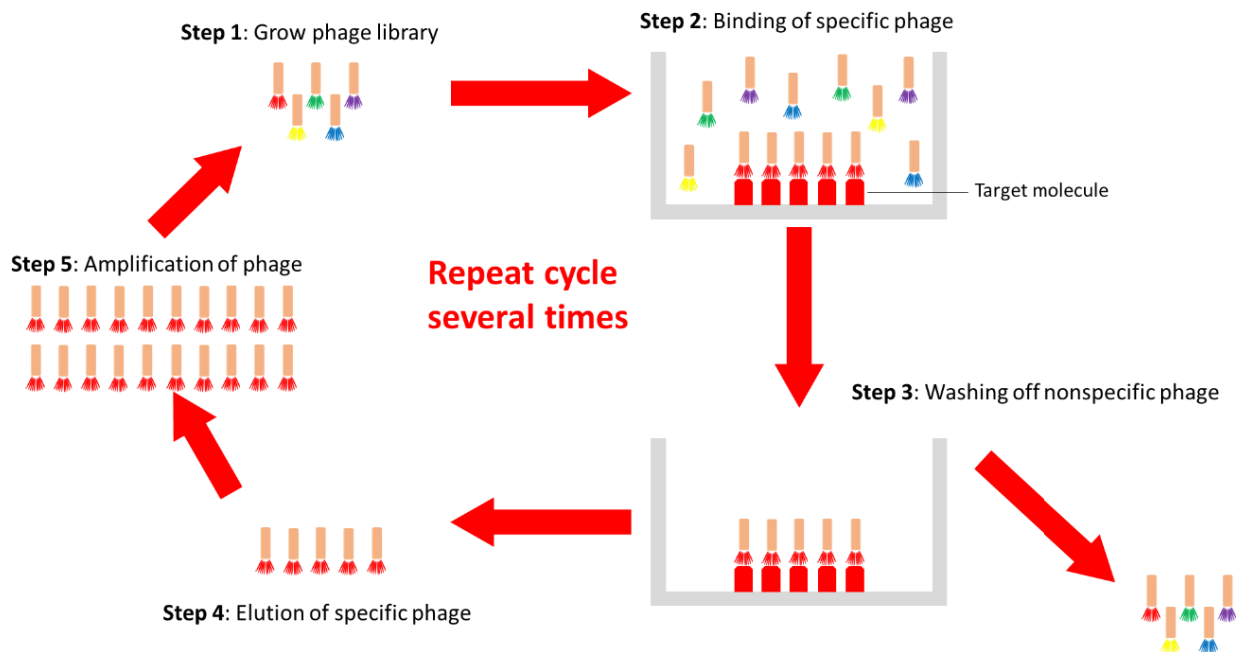
Figure 6: Biopanning in the selection of specific phage.

4. Focus

The project of this thesis focuses on the development of a wearable blood biosensor for detecting injury in law enforcement or military applications. The sequenced BR-1 peptide that was selected by a previous graduate student through phage display technology (Rees 2016) will be evaluated by indirect and competitive inhibition peptide enzyme-linked immunosorbent assays (ELISAs) for preferential binding to HSA. BR-1 will then be produced and purified using a pMAL-c5X expression vector.

5. Hypotheses

The hypotheses of this project are that 1) the BR-1 peptide will be found to bind to HSA with high specificity, 2) that the BR-1 peptide can be produced through use of a pMAL-c5X expression vector, and 3) that the BR-1 peptide can be attached to carboxylated SWCNTs and tested for preferential binding to HSA over other substances.

B. Materials

10X Tris/Glycine/SDS Running Buffer (Cat. No. 161-0372), 2X Laemmli Sample Buffer (161-0737), 2X Tricine Sample Buffer (161-0739), Criterion TGX Precast Midi Protein Gels, 8–16% polyacrylamide, 18 well comb (5671104), Criterion Tris-Tricine Precast Gels, 16.5% polyacrylamide, 18 well comb (3450064), Coomassie Brilliant Blue R-250 Staining Solution (161-0436), and SYPRO Ruby Protein Gel Stain (170-3125) were purchased from Bio-Rad Laboratories, Inc. (Hercules, CA). 7X-O-Matic Solution (Cat. No. ICN7667493), Acetic Acid, Glacial (A38S-500), Agar (BP1423-500), Regenerated Cellulose Dialysis Tubing, 12–14 kDa MWCO (21-152-14), Tris Base (BP154-1), and Tris-HCl (PR-H5121) were purchased from Fisher Scientific International, Inc. (Pittsburgh, PA). 1 mg/mL BR-1 peptide was purchased from GenScript USA, Inc. (Piscataway, NJ). ProSieve Color Protein Marker, 10-190 kDa (Cat. No. 50550) was purchased from Lonza Group (Alpharetta, GA). 1 mg/mL Factor Xa Protease (Cat. No. P8010S) M13KE Phage (N0316S), Ph.D.-7 Phage Display Library Kit (E8100S), and pMAL-c5X Protein Fusion and Purification System (E8200S) were purchased from New England BioLabs, Inc. (Beverly, MA). Ethyl Alcohol 200 Proof (Cat. No. 111HPLC200) and Methyl Alcohol 200 Proof (339000ACS) were purchased from Pharmco-AAPER (Shelbyville, KY). 0.22 μm Polyethersulfone (PES) Membrane Syringe Filter (Cat. No. SLGP033RS), 1 M Ammonium Hydroxide Solution (09859), 1 M/2 N Sulfuric Acid (1.60313), 1.0 N Sodium Hydroxide Solution (S2770), 5-Bromo-4-chloro-3-indolyl β-D-galactopyranoside,β-Mercaptoethanol (444203), X-gal (203782), Acetonitrile (271004), Agar (A1296), Albumin from Bovine Serum (A1009), Albumin from Human Serum (A8763), Corning Costar 96-well PVC Round-bottom Assay Plate, Non-treated

(CLS2797), D-(+)-Glucose (G7021), D-(+)-Maltose Monohydrate (M9171), Dimethyl

Sulfoxide (D2650), Ethylenediaminetetraacetic Acid Disodium Salt Dihydrate (324503),

Formic Acid (33015), Glycerol (G5516), Guanidine Hydrochloride (G4505), HRP/Anti-

M13 Monoclonal Conjugate (GE27-9421-01), Isopropyl β-D-1-thiogalactopyranoside

(I5502), Sodium Carbonate (S4019), Sodium Bicarbonate (S5761), Sodium Chloride

(S271-1), Sodium Dodecyl Sulfate (L3771), Sodium Hydroxide Pellets (SX0590-1),

Sodium Phosphate Dibasic Heptahydrate (S9390), Sodium Phosphate Monobasic

Monohydrate (S9638), Streptavidin-Peroxidase Polymer (S2438), Tetracycline

Hydrochloride (T3383), Trifluoroacetic Acid (T6508), Tryptone (T7293),

Polyoxyethylene-sorbitan monolaurate (P9416), and Yeast Extract (Y1625) were

purchased from Sigma Chemical Co. (St. Louis, MO). 1% Casein in TBS (37532), 1-

ethyl-3-(3-dimethylaminopropyl)carbodiimide hydrochloride (22981), 4'-

hydroxyazobenzene-2-carboxylic acid (28010), Ampicillin Sodium Salt (11593027),

BupH™ MES Buffered Saline Packs (28390), Coomassie Plus Protein Assay Reagent,

aka Bradford Reagent (1856210), EZ-Link™ Hydrazide-PEG4-Biotin (21360), M13

Phage Coat Protein Monoclonal Antibody (E1), Biotin (MA1-34468), Nunc MaxiSorp™

96-well Flat-bottom Immuno Plate (44-2404-21), Pierce™ Avidin (21121), Pierce™

Graphite Spin Columns, 0.5 mL (88302), TMB (3,3,5,5-Tetramethylbenzidine) Liquid

Substrate System for ELISA (T0440), and Zeba™ Spin Desalting Columns, 5 mL

(89891) were purchased from Thermo Fisher Scientific, Inc. (Waltham, MA). Great

Value Instant Nonfat Dry Milk (SKU 9292811) and Clorox Concentrated Germicidal

Bleach (Mfg. No. 30966) were purchased from Walmart Inc. (Boardman, OH). AH3

ER2523 *E. coli* was prepared at Youngstown State University (Youngstown, OH).

C. Methods

1. *E. coli* ER2738 Bacterial Growth and Storage

E. coli strain ER2738 (F' *proA$^+$B$^+$ lacI^q Δ(lacZ) M15 zzf::Tn10(Tet^R)/fhuA2 glnV Δ(lac proAB) thi-1 Δ(hsdS-mcrB)5*) stock was streaked onto LB agar plates and incubated overnight at 37°C. The plate was wrapped in parafilm to ensure an airtight seal and prevent drying out before storage at 4°C for up to four weeks. The *E. coli* was streaked again onto new plates and sealed as needed. (Chung et al. 1989; New England BioLabs 2016)

2. *E. coli* ER2738 Overnight Culture

E. coli strain ER2738 was taken from the storage plate and inoculated into 20 mL of LB broth and 20 μL of 20 mg/mL tetracycline in a 125-mL Erlenmeyer flask to ensure the growth of ER2738 *E. coli* expressing the F plasmid containing a tetracycline resistance gene. The medium was incubated at 37°C overnight in an orbital shaker at 250 RPM on a MaxQ 4000 benchtop orbital shaker (Thermo Fisher Scientific, Waltham, MA) (New England BioLabs 2016; Rees 2016). This same method was used to prepare transformed AH3 ER2523 containing the MBP/BR-1 fusion protein prepared by Alexander Huber prior to protein purification (Huber 2019).

3. Phage Titering

To determine the number of plaque-forming units (pfu) per mL of solution, the phage from storage was titered. Sterile culture tubes were placed into a water bath preheated to 55°C. LB agar plates were maintained at 37°C in an incubator until needed.

Top agar was completely melted using a microwave and 3 mL of the top agar was placed into the culture tubes. Forty microliters of 40 mg/mL X-gal and 40 µL of 40 mg/mL IPTG were added to each culture tube. One hundred-fold serial dilutions of phage were made in 1X PBS (10 mM Phosphate, 150 mM NaCl, pH 7.4) in a sterile hood. Twenty microliters of each phage dilution was transferred into 200 µL of overnight bacteria culture, vortexed, and incubated for one minute to ensure infection by the phage. The infected bacteria were transferred into the culture tubes containing the top agar/X-gal/IPTG mixture, vortexed, and poured into the LB agar plates prior to 5 minutes of incubation with the bacteria. After cooling to room temperature, the plates were incubated overnight at 37°C and blue plaques were counted (Barbas et al. 2001; New England BioLabs 2016).

4. Biotinylation of BR-1 Peptide

Five hundred millimolar EDC in reaction buffer (10 mg EDC in 100 µL 0.1 M MES, pH 4.85) was prepared immediately before use. Twenty-five microliters of 50 mM biotin hydrazide in DMSO was added to 1 mL of 0.5 mg/mL BR-1 peptide in Milli-Q ultrapure water in a plastic test tube and rocked to mix. Three microliters of the EDC in reaction buffer was added and mixed. The sample solution was diluted 1:1 in 2.5% TFA and stored at room temperature (Rees 2016; Thermo Fisher Scientific 2011 *EZ-Link*).

A Pierce graphite spin column (one column per 500 µL of sample solution) was placed into a 15-mL conical tube and centrifuged at 2,000 x *g* in an Allegra 6R Centrifuge (Beckman Coulter, Brea, CA) for one minute to remove the storage buffer. One hundred microliters of 1 M NH_4OH was added to the column and centrifuged at

2,000 x *g* for one minute. The flow-through was discarded and this step was repeated

once. To activate the spin column, 100 μL of acetonitrile was added and the column

centrifuged at 2,000 x *g* for one minute. The flow-through was discarded and this step

was repeated once. After preparation, the column was placed into a new collection tube.

Five hundred microliters of sample solution was added to the column and the column was

capped. The column was periodically vortexed for 10 minutes to keep the graphite

suspended and ensure binding. The column was then centrifuged at 1,000 x *g* for three

minutes and the flow-through discarded. After placing the column into a new collection

tube, the column was washed with 200 μL of 1.0% TFA and centrifuged at 2,000 x *g* for

one minute. The flow-through was discarded and this step was repeated once. The

column was placed into a new collection tube and 100 μL of 0.1% formic acid in 50%

acetonitrile was added to elute the sample. The column was centrifuged at 2,000 x *g* for

one minute and the eluate was reapplied to the column and centrifuged three more times.

The sample was then gently dried in a makeshift vacuum evaporator (**Figure 7**) over the

course of three days (vacuum Erlenmeyer flask with a rubber stopper, placed on a hot

plate set on low, the sample wrapped in aluminum foil to trap and conduct heat, with a

Fisher Maxima Dry 15 PSI, 40 L/min, 65 torr vacuum attached). Once the sample was

thoroughly dried, it was resuspended in 1 mL Milli-Q ultrapure water (final concentration

0.5 mg/mL EP B-BR-1) and stored at −20°C in a labelled screw-top microfuge tube (Rees

2016; Thermo Fisher Scientific 2011 *Graphite*).

4.1. Zeba Spin Desalting Columns

The EP B-BR-1 sample was thawed before the desalting procedure. The Zeba

Spin Desalting Columns were first prepared by twisting off the bottom tab and removing the cap. The spin column was then placed into a 15-mL Falcon tube and centrifuged at 1,000 x *g* in an Allegra 6R Centrifuge (Beckman Coulter, Brea, CA) for two minutes to remove the storage solution. The flow-through was then discarded. Milli-Q ultrapure water (2.5 mL) was placed in the column before centrifuging again at 1,000 x *g* for two minutes and discarding the flow-through. This process was repeated twice to wash the column a total number of three times. The spin column was placed in a new 15-mL Falcon tube. The EP B-BR-1 sample was slowly loaded dropwise into the center of the column resin bed. The assembly was then centrifuged at 1,000 x *g* for two minutes. The column was discarded while the flow-through containing desalted biotinylated peptide was placed in a labelled screw-top microfuge tube. The sample was stored at –20°C (Kenney 2018; Thermo Fisher Scientific 2013).

4.2. HABA/Avidin Biotin Incorporation Assay

To determine the amount of biotin bound to the peptide sample, a biotin incorporation assay using HABA/Avidin was performed (Rees 2016; Thermo Fisher Scientific 2012). Since a concentration of 0.5 mg/mL of peptide is too high for the assay to work properly, the biotinylated peptide sample (EP B-BR-1) was diluted to 0.05 mg/mL by adding 10 μL of sample to 90 μL of 0.1 M MES (in a second biotin incorporation assay, the AH B-BR-1 peptide sample was diluted to a working concentration of 4 mg/mL). Five milliliters of HABA/avidin solution was then prepared. First, the 10 M HABA solution was prepared by adding 24.2 mg of HABA to 9.9 mL of Milli-Q ultrapure water and 0.1 mL of 1 N NaOH. An additional 0.1 mL of 1 N NaOH

was added to help completely dissolve the HABA, and then the solution was syringe filtered before use (stored at 4°C). The 10 mg/mL avidin solution was prepared by adding 20 mg of avidin to 2 mL of MilliQ ultrapure water and stored at -20°C. After preparing the HABA and avidin solutions, 5 mL of HABA/avidin solution was made by adding 150 μL of 10 M HABA solution and 250 μL of 10 mg/mL avidin solution to 4.6 mL of PBS.

Before measuring the absorbance of the biotinylated peptide sample on an Agilent 8453 UV-Vis spectrophotometer (Hewlett-Packard, Palo Alto, CA), a 1-cm glass cuvette was blanked with 1 mL of dH_2O at 500 nm wavelength. The cuvette was emptied and dried with a Kimwipe before adding 900 μL of the HABA/avidin solution to the cuvette. The absorbance was then measured at 500 nm and recorded as A_{500} HABA/avidin. This process was repeated nine times and averaged to ensure consistency. To obtain the HABA/avidin/MES blank, the cuvette was emptied, rinsed five times with dH_2O, and dried with a Kimwipe. Nine hundred microliters of HABA/avidin solution was added to the cuvette. One hundred microliters of MES was added to the cuvette containing HABA/avidin and inverted to mix. The absorbance at 500 nm was measured and recorded as A_{500} HABA/avidin/MES until the value remained constant for 15 seconds. This process was repeated nine times and averaged to ensure consistency. To measure the biotinylated peptide sample, the cuvette was emptied, rinsed five times with dH_2O, and dried with a Kimwipe. Nine hundred microliters of HABA/avidin solution was added to the cuvette. One hundred microliters of sample was added to the cuvette containing HABA/avidin and inverted to mix. The absorbance at 500 nm was measured and recorded as A_{500} HABA/avidin/B-BR-1 until the value remained constant for 15 seconds. This process was repeated nine times and averaged to ensure consistency (Rees 2016;

Thermo Fisher Scientific 2012).

Calculations for biotin incorporated into the peptide sample were performed using Beer's Law (Aγ = $\varepsilon\gamma$bC). **A** is the absorbance of the sample at a particular wavelength, γ, of 500 nm. ε is the extinction coefficient of the wavelength, also known as absorptivity. For HABA/avidin samples at 500 nm with a pH of 7.0, the extinction coefficient is equal to 34,000 $M^{-1}\cdot cm^{-1}$. **b** is the cell path expressed in cm. In a 1-cm cuvette, **b** = 1 cm. **C** is the concentration of the sample expressed in molarity (mol/L or mmol/mL). Four calculations were performed to determine the concentration of biotin in the peptide sample. Calculation #1 gave the concentration of the original solution of biotinylated molecules in mmol/mL (before dilution for the assay), where

$$mmol\ biotinylated\ peptide\ per\ mL\ = \frac{peptide\ concentration\ (\frac{mg}{mL})}{MW\ of\ peptide\ (\frac{mg}{mmol})}.$$ Calculation #2 gave

the change in absorbance at 500 nm, where $\Delta A_{500} = (A_{500}\ HABA/avidin - A_{500}\ HABA/avidin/B\text{-}BR\text{-}1) - (A_{500}\ HABA/avidin - A_{500}\ HABA/avidin/MES\ Blank)$. Calculation #3 gave the concentration of biotin in mmol/mL of reaction mixture, where $mmol\ biotin/mL\ reaction\ mixture = \frac{\Delta A_{500}}{\varepsilon \cdot b} = \frac{Calculation\ \#2}{\varepsilon \cdot b}$.

Calculation #4 gave the mmol biotin per mmol peptide, where

$$\frac{mmol\ biotin\ in\ original\ sample}{mmol\ peptide\ in\ original\ sample} = \frac{(mmol/mL\ biotin\ in\ reaction\ mixture)(10)(dilution\ factor)}{mmol/mL\ peptide\ in\ original\ sample} =$$

$\frac{(Calculation\ \#3)(10)(10)}{Calculation\ \#1}$ (Rees 2016; Thermo Fisher Scientific 2012).

5. Peptide ELISA

To test the binding of biotinylated peptide (B-BR-1) to HSA, an indirect peptide ELISA was performed with HSA as the target. A 96-well polyvinyl chloride microtiter

plate was used. The HSA (in triplicate) and Streptavidin Blank (in triplicate) wells were

coated with 100 μL of 10 μg/mL HSA (10 mg/mL HSA stock solution diluted 1:1,000) in

0.05 M Na_2CO_3, pH 9.6 buffer. The Phage Positive Control well was coated with 100 μL

of 1.57 x 10^{11} pfu/mL M13KE phage in 0.05 M Na_2CO_3, pH 9.6. Two hundred

microliters of PBST (PBS + 0.05% Tween-20) + 1% Yeast Extract blocking buffer was

added to the No HSA (in triplicate) and Ab Blank (in triplicate) wells, and a water jacket

was placed around all wells to prevent evaporation, and the plate was incubated at 4°C

overnight in a humidified chamber. All wells were aspirated and washed once with PBST

wash buffer. Two hundred microliters of blocking buffer was added to each of the HSA,

Streptavidin, and Phage Positive Control wells. The plate was incubated at 37°C for 30

minutes in a humidified chamber. All wells were aspirated and washed three times with

wash buffer. One hundred microliters of 10 μg/mL BR B-BR-1 was added to each of the

HSA and No HSA wells. One hundred microliters of wash buffer was added to the

Streptavidin Blank, Antibody Blank, and Phage Positive Control wells. The plate was

incubated at room temperature for two hours on a rocker table. All wells were aspirated

and washed six times with wash buffer. One hundred microliters of horseradish

peroxidase conjugated to anti-M13 monoclonal antibody (HRP/Anti-M13, diluted

1:5,000 in PBST + 0.1% Yeast Extract sample buffer) was added to the Phage Positive

Control and Antibody Blank wells. One hundred microliters of horseradish peroxidase-

conjugated streptavidin (HRP/SA, diluted 1:10,000 in sample buffer) was added to the

HSA Alone, HSA Competition, Biotin Positive Control, and Streptavidin Blank wells.

The plate was incubated at 4°C overnight in a humidified chamber. All wells were

aspirated and washed six times with wash buffer. One hundred microliters of TMB

colorimetric substrate was added to each well and incubated at room temperature for up to 15 minutes until a suitable blue color formed. Fifty microliters of 2 N H_2SO_4 stop solution was added to each well to stop the reaction. The absorbance was measured at 450 nm wavelength using a Microplate Autoreader (Bio-Tek Instruments, Winooski, Vermont) (Dennis et al. 2002; Rees 2016).

6. Competitive Inhibition Peptide ELISA

To further test the specificity of binding of biotinylated peptide (B-BR-1) to HSA, competitive inhibition peptide ELISAs were performed with HSA as the competing reagent. A 96-well polyvinyl chloride microtiter plate was used. For the first ELISA (**Figure 10**; three replicas were performed with minor changes), the HSA Alone (in duplicate), HSA Competitive (in duplicate), Streptavidin Blank (in triplicate), and Antibody Blank (in triplicate) wells were coated with 100 μL of 10 μg/mL HSA (10 mg/mL HSA stock solution diluted 1:1,000) in 0.05 M Na_2CO_3, pH 9.6 buffer. The Phage Positive Control well was coated with 100 μL of 1.57 x 10^{11} pfu/mL M13KE phage in 0.05 M Na_2CO_3, pH 9.6. The Biotin Positive Control well was coated with 100 μL of 10 μg/mL B-BR-1 in 0.05 M Na_2CO_3, pH 9.6. A water jacket was placed around all wells to prevent evaporation, and the plate was incubated at 37°C for 30 minutes in a humidified chamber. All wells were aspirated and washed once with PBST (PBS + 0.05% Tween-20) wash buffer. Two hundred microliters of PBS + 1% yeast extract blocking buffer was added to the previous wells as well as the Preincubation wells. The plate was incubated at 37°C for 30 minutes in a humidified chamber. All wells were aspirated and washed three times with wash buffer. HSA + B-BR-1 Preincubation dilutions (50 μL of 0.02, 0.2, and 2

μg/mL HSA + 50 μL of 20 μg/mL B-BR-1 in PBS + 0.1% Tween-20 sample buffer) were

mixed in the blocked Preincubation wells. The HSA + B-BR-1 dilutions were then

transferred to the HSA Competition wells, and 100 μL of 10 μg/mL B-BR-1 in sample

buffer was added to the HSA Alone and No HSA wells. One hundred microliters of wash

buffer was added to the positive controls and blank wells. The plate was incubated at

room temperature for two hours in a humidified chamber. All wells were aspirated and

washed six times with wash buffer. One hundred microliters of horseradish peroxidase-

conjugated anti-M13 monoclonal antibody (HRP/Anti-M13, diluted 1:5,000 in PBS +

0.1% Tween-20 sample buffer) was added to the Phage Positive Control and Antibody

Blank wells. One hundred microliters of horseradish peroxidase-conjugated streptavidin

(HRP/SA, diluted 1:10,000 in sample buffer) was added to the HSA Alone, HSA

Competition, Biotin Positive Control, and Streptavidin Blank wells. The plate was

incubated at 4°C overnight in a humidified chamber. All wells were aspirated and washed

six times with wash buffer. One hundred microliters of TMB colorimetric substrate was

added to each well and incubated at room temperature for up to 15 minutes until a

suitable blue color formed. Fifty microliters of 2 N H_2SO_4 stop solution was added to

each well to stop the reaction. The absorbance was measured at 450 nm wavelength using

a Microplate Autoreader (Bio-Tek Instruments, Winooski, Vermont) (Rees 2016).

Subsequent competitive inhibition peptide ELISAs were performed with a couple

changes. The Preincubation wells of **Figures 12** and **13** had increasing concentrations of

HSA (0.01, 0.1, and 1 μg/mL HSA in 0.05 M Na_2CO_3, pH 9.6) bound to them first before

blocking, and B-BR-1 was incubated in them to deplete peptide from the preincubation

solution before transferring the solution to the HSA Competition wells. The concentration

of B-BR-1 added to the preincubation wells was also increased from 10 µg/mL to 20 µg/mL (**Figure 13**) and 100 µg/mL (**Figure 11**).

7. Phage Binding ELISA

As another method to determine the specificity of the peptide and whether the original HSA-6 phage and its displayed peptide still bound to HSA, an indirect phage binding ELISA with various concentrations of phage was performed. A 96-well polyvinyl chloride microtiter plate was used. The HSA + X HSA-6 Phage (in duplicate) and Antibody Blank (in triplicate) wells were coated with 100 µL of 10 µg/mL HSA (10 mg/mL HSA stock solution diluted 1:1,000) in 0.05 M Na_2CO_3, pH 9.6. The Phage Positive Control well was coated with 100 µL of 1.57 x 10^{11} pfu/mL M13KE phage in 0.05 M Na_2CO_3, pH 9.6. A water jacket was placed around all wells to prevent evaporation, and the plate was incubated at room temperature for two hours in a humidified chamber. All wells were aspirated and washed once with PBS (no Tween-20) wash buffer. Two hundred microliters of TBS (Tris-buffered saline) + 1% Casein blocking buffer was added to all wells. The plate was incubated at room temperature for two hours in a humidified chamber. All wells were aspirated and washed three times with wash buffer. One hundred microliters of the phage solutions (10^6, 10^8, and 10^{10} pfu/mL HSA-6 in TBS sample buffer) was added to the HSA + X HSA-6 Phage and No HSA + X HSA-6 Phage wells. One hundred microliters of wash buffer was added to the positive control and blank wells. The plate was incubated at 4°C overnight in a humidified chamber. All wells were aspirated and washed six times with wash buffer. One hundred microliters of horseradish peroxidase conjugated to anti-M13 monoclonal antibody

36

(HRP/Anti-M13, diluted 1:5,000 in PBS + 0.1% Casein sample buffer) was added to all wells. The plate was incubated at 4°C overnight in a humidified chamber. All wells were aspirated and washed six times with wash buffer. One hundred microliters of TMB colorimetric substrate was added to each well and incubated at room temperature for up to 15 minutes until a suitable blue color formed. Fifty microliters of 2 N H_2SO_4 stop solution was added to each well to stop the reaction. The absorbance was measured at 450 nm wavelength using a Microplate Autoreader (Bio-Tek Instruments, Winooski, Vermont) (Dennis et al. 2002; Rees 2016).

8. Protein Purification from Bacterial Cytoplasm

Since the BR-1 peptide was expressed as a cytoplasmic fusion protein, Method I (Total Cell Extract) from the pMAL-c5X manual was used (New England BioLabs 2011). One liter of rich broth (LB-based) containing 11.1 mM glucose and 100 μg/mL ampicillin was inoculated with 10 mL of AH3 ER2523, BR-1 peptide sequence in pMAL-c5X transformed into ER 2523 *E. coli* (Huber, 2019). An overnight culture was performed in a 2-L Erlenmeyer flask with baffles for aeration. The bacteria were grown for 2.5 hours to a density of 2 x 10^8 cells/mL ($A_{600} \approx 0.5$) at 37°C with shaking at 200 RPM on an Incu-Shaker 10L (Benchmark Scientific, Sayreville, NJ). The absorbance was checked with a BioPhotometer Plus (Eppendorf, Framingham, MA). Three milliliters of 0.1 M IPTG stock was added to a final concentration of 0.3 mM. The medium was then incubated for an additional two hours at 37°C with shaking at 200 RPM. After incubation and induction of fusion protein production, the medium was poured into pre-weighed and labelled Oak Ridge tubes and centrifuged at 4,000 x *g* at 4°C for 20 minutes in a Sorvall

RC5B Plus Refrigerated Centrifuge (Thermo Fisher Scientific, Waltham, MA). The cells were then resuspended in approximately 5 mL Column Buffer (20 mM Tris-HCl, 200 mM NaCl, 1 mM EDTA; 5 mL/5 g of cells) and transferred to a 15-mL conical tube before freezing overnight at –20°C.

The sample was thawed in cold water and placed in an ice-water bath for sonication using a Microson™ Ultrasonic Cell Disruptor (Misonix, Farmingdale, NY) on Level 2 with short, remote pulses of ≤ 15 seconds. Protein release was monitored using a Bradford assay by adding 5 μL of sonicate to 1 mL Bradford reagent and absorbance was read at 595 nm wavelength using a Microplate Autoreader (Bio-Tek Instruments, Winooski, Vermont). Sonication was continued until the released protein reached a maximum at about two total minutes of sonication. The sonicate was then centrifuged at 20,000 x g for 20 minutes at 4°C. The supernatant (crude extract) was saved and diluted 1:6 with 150 mL Column Buffer before storing at –20°C (New England BioLabs 2011).

The affinity chromatography equipment was prepared by soaking a 1.5 x 15 cm chromatography column, column plugs, and stopcock in a 70% MeOH bath for 10 minutes. They were then thoroughly rinsed with sterile dH_2O and dried. Three-millimeter inner diameter flexible tubing was placed into 7X detergent with 10% bleach. The tubing was rolled to remove as much of the deposits as possible, soaked for 10 minutes, thoroughly rinsed with sterile dH_2O, and dried. The tubing was soaked again in a 10% bleach solution for 15 minutes, thoroughly rinsed with sterile dH_2O, and dried. Erlenmeyer flasks were washed with 7X detergent, thoroughly rinsed with dH_2O, and autoclaved for 20 minutes.

The amylose resin was mixed gently in sterile water in a graduated cylinder and

allowed to settle. The top layer was aspirated to remove the fine particles. Additional water was added, and this procedure was repeated until no obvious fines were visible. After removal of the fines, the resin was mixed in 20% EtOH and poured into a vacuum Erlenmeyer flask. A rubber stopper was placed on top and the flask connected to a Fisher Maxima Dry 15 PSI, 40 L/min, 65 torr vacuum pump. The vacuum was then turned on and the mixture allowed to sit (with gentle swirling every few minutes) until no bubbles came out of the resin.

After thawing the diluted crude extract, a 1.5 x 15 cm chromatography column (column volume = 26.51 mL) was prepared with 15 mL amylose resin. The column was washed with five column volumes (132.55 mL) of Column Buffer. The diluted crude extract was then loaded at a flow rate of no more than 1.875 mL/min. The column was then washed with 12 column volumes (318.12 mL) of Column Buffer at a flow rate of no more than 8.75 mL/min. The fusion protein was then eluted with 60 mL of Column Buffer + 10 mM maltose. Twenty-six 3-mL fractions were collected in glass culture tubes and stored at 4°C (New England BioLabs 2011).

A Bradford assay was performed to determine which fractions contained fusion protein before pooling the protein-containing fractions together. The concentration of the pooled fusion protein was determined by another Bradford assay, and the purity was confirmed by 8–16% acrylamide gradient SDS-PAGE.

8.1 Bradford Assay

A Bradford Assay using Coomassie Plus Reagent was used to determine protein concentration of each sample (**Figure 15**).

8.1.1 Standard Microplate Protocol

Five microliters of each standard or unknown sample (in duplicate) and the blanks (sample medium or water, in triplicate) were placed into the appropriate wells. One hundred fifty microliters of Bradford Reagent was added to each well and mixed on a 3D platform rotator (Fisher Scientific, Pittsburg, PA) for 30 seconds. The plate was removed from the shaker and incubated for 10 minutes at room temperature. The absorbance for each well was measured at 595 nm using a Microplate Autoreader (Bio-Tek Instruments, Winooski, Vermont). The average absorbance for the blanks was subtracted from the measurements for each individual standard and sample. A standard curve was prepared in Excel by plotting the average corrected absorbances for each BSA standard versus its concentration in μg/mL. The standard curve was then used to determine the protein concentration for each unknown sample (Thermo Fisher Scientific 2011 *Bradford*).

8.1.2 Micro Microplate Protocol

Seventy-five microliters of each standard or unknown sample (in duplicate) and the blanks (sample medium or water, in triplicate) were placed into the appropriate wells. Seventy-five microliters of Bradford Reagent was added to each well and mixed on a 3D platform rotator (Fisher Scientific, Pittsburg, PA) for 30 seconds. The plate was removed from the shaker and incubated for 10 minutes at room temperature. The absorbance for each well was measured at 595 nm using a Microplate Autoreader (Bio-Tek Instruments, Winooski, Vermont). The average absorbance for the blanks was subtracted from the measurements for each individual standard and sample. A standard curve was prepared in Excel by plotting the average corrected absorbances for each BSA standard versus its

concentration in μg/mL. The standard curve was then used to determine the protein

concentration for each unknown sample (Thermo Fisher Scientific 2011 *Bradford*).

8.2 SDS-PAGE

Tris/Glycine/SDS Running Buffer (10X, 25 mM Tris, 192 mM glycine, 0.1%

SDS, pH 8.3) was diluted 1:10 with deionized water and mixed well. The samples were

prepared by adding an equal amount of 2X Sample Buffer (either Laemmli, Laemmli +

5% β-mercaptoethanol, or Tricine) and heating them for five minutes at 98°C in a

Mastercycler Personal thermocycler (Eppendorf, Framingham, MA). The gel cassette was

placed into an electrophoresis chamber with 500 mL of running buffer and either 3, 5, or

10 μL of the samples and protein ladders were slowly loaded into their wells. The

electrophoresis chamber was covered and either 20 mA or 40 mA of current was applied

to the gel using a PowerPac 3000 Electrophoresis Power Supply (Bio-Rad, Hercules,

CA). Electrophoresis was performed for at least two hours until the sample buffer and

protein ladder neared the bottom of the gel.

The gel cassette was removed and rinsed under water to remove excess SDS

detergent. The gel was removed from the cassette and placed into a Tupperware container

for de-staining and staining. The gel was first covered with High Gel De-stain (35%

EtOH/MeOH, 10% Glacial Acetic Acid) and shaken on a Wave Action Rotator (Fisher

Scientific, Pittsburgh, PA) on setting 3 for at least 30 minutes at room temperature to fix

and de-stain the gel. The High Gel De-stain was then aspirated, and the gel was covered

with either 0.05% Coomassie Brilliant Blue Stain Solution (25% EtOH/MeOH, 10%

Glacial Acetic Acid) or SYPRO Ruby fluorescent stain. The gel was shaken overnight for

Coomassie Brilliant Blue or for at least three hours for SYPRO Ruby, after which the staining solution was aspirated.

If staining with Coomassie Brilliant Blue, the gel was covered with High Gel De-stain and shaken for at least one hour to remove most of the blue color. The High Gel De-stain was aspirated, and the gel was then covered with Low Gel De-stain (7.5% EtOH/MeOH, 10% Glacial Acetic Acid). The gel was shaken for at least one hour until most of the staining solution had been removed from the gel while the protein bands remained colored. If staining with SYPRO Ruby, the gel was covered with High Gel De-stain and shaken for 30–60 minutes to remove background stain.

After the staining and de-staining process, the gel was covered with 10% glacial acetic acid for preservation and scanned on a PharosFX Molecular Imager™ (Bio-Rad, Hercules, CA). If scanning a gel stained with Coomassie Brilliant Blue, an opaque, white sheet was placed underneath the gel prior to scanning. If scanning a gel stained with SYPRO Ruby, the gel was placed directly on the scanner.

8.3 Regenerating the Amylose Resin Column

The resin can be reused three to five times by regenerating it with the following sequence of washes at room temperature:

Sterile water:	3 column volumes (79 mL)
0.1% SDS:	3 column volumes (79 mL)
Sterile water:	1 column volume (27 mL)
Column Buffer:	3 column volumes (79 mL)
20% Ethanol:	2 column volumes (53 mL)

The column was washed at room temperature to prevent the 0.1% SDS from precipitating. After leaving some 20% EtOH in the column, the resin was transferred to a conical tube and stored at 4°C (New England BioLabs 2011).

9. Fusion Protein Cleavage

The fusion protein solution was diluted in Column Buffer (20 mM Tris-HCl, 200 mM NaCl, 1 mM EDTA) to a concentration of 1 mg/mL before performing a pilot experiment. Twenty microliters of 1 mg/mL fusion protein was mixed with 1 μL of 200 μg/mL Factor Xa protease (w/w ratio of 1%). Five microliters of fusion protein was placed in a separate tube with no protease as a control. The tubes were incubated at room temperature for 24 hours. At 2, 4, 8, and 24 hours, 5 μL of the reaction mixture was transferred to a separate tube, mixed with 5 μL 2X Laemmli Sample Buffer, and saved at 4°C. The fusion protein control was mixed with 5 μL 2X Laemmli Sample Buffer at 24 hours. The samples were then placed in a Mastercycler Personal thermocycler (Eppendorf, Framingham, MA) and heated to 98°C for 5 minutes before analysis by 8–16% acrylamide gradient SDS-PAGE (**Figures 22–25**) (New England BioLabs 2011).

Gel electrophoresis was also performed using a 16.5% Tris-tricine SDS-PAGE gel for better separation of proteins and peptides. Laemmli Sample Buffer (2X) + 5% β-mercaptoethanol was used for reduced conditions (**Figure 27**).

9.1 Denaturing the Fusion Protein

To assist cleavage of the BR-1 peptide from the maltose binding protein, the fusion protein was denatured through dialysis using FisherBrand™ regenerated cellulose

43

dialysis tubing (45 mm wide, 12–14 kDa molecular weight cutoff), first against 20

volumes of 20 mM Tris-HCl and 6 M guanidine hydrochloride, pH 7.4 dialysis buffer

solution for 24 hours at room temperature. The fusion protein was then dialyzed against

100 volumes of Column Buffer twice at room temperature for 24 hours each time (New

England BioLabs 2011).

9.1.1 Preparing the Dialysis Tubing

About 28 inches of dialysis tubing was cut, rolled up, and placed into a beaker

with 400 mL 2% sodium carbonate, 1 mM EDTA buffer. Ensuring that the tubing stayed

submerged, the solution was boiled for 20 minutes on a hot plate. The tubing was then

rinsed well with sterile dH_2O before placing it back into 400 mL 1 mM EDTA and

boiling for another 20 minutes. The tubing was rinsed again with sterile dH_2O,

submerged in sterile dH_2O, and stored at 4°C until use (Maniatis et al. 1982).

9.2 NanoDrop One UV-Vis

Samples that were used for the NanoDrop included: peptide bands from SDS-

PAGE, gel blank from SDS-PAGE, control band from SDS-PAGE, PBS blank, PBS +

0.1%/1%/5% SYPRO Ruby, and 1, 10, 25, 50, 75, and 100 µg/mL BR-1 peptide in PBS.

The NanoDrop One (Thermo Fisher Scientific, Waltham, MA) was turned on and

allowed to initialize before inserting a USB drive for exporting the data files. The UV-

Vis tab was selected and the desired wavelength of 214 nm for excitation of amide bonds

was entered. The head was then raised, and the pedestals were cleaned with sterile dH_2O

and a Kimwipe. Two microliters of PBS blanking solution was placed on the pedestal and

the head was lowered before selecting "Auto-blank." After blanking, the head was raised, and the pedestals were cleaned with a Kimwipe. Sample names were entered before loading two microliters and lowering the head. After the machine automatically read the sample, the pedestals were cleaned. After all the samples were read, the file was named, exported to the USB drive, and the pedestals were cleaned with sterile dH_2O and a Kimwipe (Thermo Fisher Scientific 2017).

9.2.1 Preparing the Peptide Sample from the Gel for NanoDrop Analysis

The portions of gel where peptide bands should have been present at the bottom of the protein cleavage sample lanes were excised using a scalpel and placed into a microfuge tube. An equal amount of gel not containing any proteins was excised from unused lanes to serve as background and placed into another microfuge tube. Six hundred microliters of PBS was added to each tube and the tubes were incubated overnight at 4°C. The two samples were syringe filtered using a 0.22 μm PES membrane syringe filter and placed into new microfuge tubes before use.

10. Statistical Analysis

Two-tailed paired t-tests were performed in Excel to determine statistical significance of the biotin incorporation assay data. One-tailed two-sample t-tests were performed on Excel to determine statistical significance of the ELISA data. The confidence interval was set at 95% confidence and statistical significance was determined when the p value was less than 0.05 for all tests.

D. Results

The BR-1 peptide selected by William (Bill) Rees was displayed on the pIII minor coat protein of the M13 filamentous phage clone HSA-6 and exhibited binding to human serum albumin (HSA) (Rees 2016). BR-1 is attached to the amino terminus of pIII via a Gly-Gly-Gly-Ser linker arm and the phage genome of clone HSA-6 was sequenced to yield the amino acid sequence for BR-1, Ala-Asn-His-His-Gln-Ala-Ser. Rees purchased synthetic BR-1 peptide from GenScript USA, biotinylated the peptide (now B-BR-1), and evaluated the peptide's binding specificity for HSA by performing ELISAs.

Additional BR-1 peptide was biotinylated for these studies and designated EP B-BR-1. The biotin was attached to the carboxy terminus of the peptide with a PEG_4 (poly(ethylene glycol)) linker arm using EDC (1-ethyl-3-(3-dimethylaminopropyl) carbodiimide) and biotin hydrazide. The use of the PEG_4 linker arm prevents the biotinylation from causing a conformational change in the peptide (Rees 2016; Thermo Fisher Scientific 2011 *EZ-Link*). The biotin would then allow attachment of avidin or streptavidin covalently bound to the enzyme horseradish peroxidase for detection in ELISAs. After biotinylation, the EP B-BR-1 sample was centrifuged in a 5-mL Zeba Spin Desalting Column to remove any salts and unreacted biotin. The desalted EP B-BR-1 sample was then dried in a vacuum evaporator (**Figure 7**) and resuspended in 1 mL MilliQ ultrapure water.

Figure 7: Vacuum Evaporator Setup. The biotinylated sample was inside a microfuge tube with the top removed and placed in a 15-mL conical tube. Aluminum foil was wrapped around the end to conduct and retain heat. A rubber stopper with a hole was trimmed and placed into the mouth of the vacuum Erlenmeyer. A wide thumb tack was used to create a vacuum seal as well as to equilibrate pressure when checking the sample for dryness.

The biotinylated sample was analyzed for biotin incorporated using a HABA (4'-hydroxyazobenzene-2-carboxylic acid)/avidin assay (Rees 2016; Thermo Fisher Scientific 2012). In the first attempt, the EP BR-1 sample had a low amount of biotin incorporated (0.002789 ± 0.010978 SEM mmol biotin/mmol BR-1). A second biotin incorporation assay was performed using all biotinylated samples to determine which sample had the highest amount of biotin incorporated (**Table 1**). All biotinylated BR-1 samples had low levels of incorporated biotin, yet two-tailed paired t-tests indicated that there were statistically significant differences in the amount of incorporated biotin between each sample. BR B-BR-1 had the highest amount of biotin incorporated (0.083184 ± 0.009412 SEM mmol biotin/mmol BR-1), which was statistically significantly higher than the FK, EP, and AH samples ($p < 1.50 \times 10^{-6}$). FK B-BR-1 had the second highest amount of biotin incorporated (0.004415 ± 0.035112 SEM mmol biotin/mmol BR-1), which was statistically significantly higher than the EP sample ($p < 2.87 \times 10^{-12}$) but not significantly higher than the AH sample ($p = 0.202$). AH BR-1 (-0.000006 ± 0.000152 SEM mmol biotin/mmol BR-1) and EP BR-1 had the lowest amount of biotin incorporated (-0.062462 ± 0.020253 SEM mmol biotin/mmol BR-1) and biotinylation was essentially undetectable using the HABA/Avidin assay. Despite the low amount of incorporated biotin in all the BR-1 peptide samples, the biotinylated peptides still showed activity in ELISA assays (**Figures 8 and 9**). The BR B-BR-1 peptide sample was selected for use in the remaining assays since it had the most biotin available.

Table 1: Biotin Incorporation Assay Of All Biotinylated BR-1 Samples	
Sample [a]	**Average Biotin Incorporated (mmol biotin/mmol BR-1) [b]**
FK B-BR-1[c]	0.004415 ± 0.035112
EP B-BR-1	-0.062462 ± 0.020253
BR B-BR-1[d]	0.083184 ± 0.009412
AH B-BR-1[e]	-0.000006 ± 0.000152

[a]All samples had an n = 10 ± SEM.
[b]Amount of incorporated biotin calculated from the HABA/Avidin Biotin Incorporation Assay (Methods 4.2).
[c]Kenney 2018.
[d]Rees 2016.
[e]Huber 2019.

The BR B-BR-1 peptide was tested for specificity of binding to HSA using two peptide ELISAs. The first peptide ELISA (**Figure 8**) used a polyvinyl chloride plate to which 1 µg HSA per well was bound with sodium carbonate buffer in one row of wells while another row was left alone. The wells were washed with PBST (PBS + 0.05% Tween-20), blocked with PBST + 1% Yeast Extract, and washed again before adding 1 µg BR B-BR-1 in PBST + 0.1% Yeast Extract sample buffer. The wells were washed, HRP/Streptavidin in sample buffer was added, and the wells were washed again before addition of TMB (3,3,5,5-Tetramethylbenzidine) substrate solution and measuring absorbance at 450 nm wavelength. The peptide ELISA was unable to detect binding to HSA and had all negative results except for the positive phage control. The HSA Test wells had an average absorbance of -0.007 ± 0.005 SEM at 450 nm while the No HSA wells had an average absorbance of 0.090 ± 0.162 SEM at 450 nm. A one-tailed two-sample t-test was performed and indicated that there was no statistically significant difference between the HSA Test and No HSA wells ($p = 0.2033$).
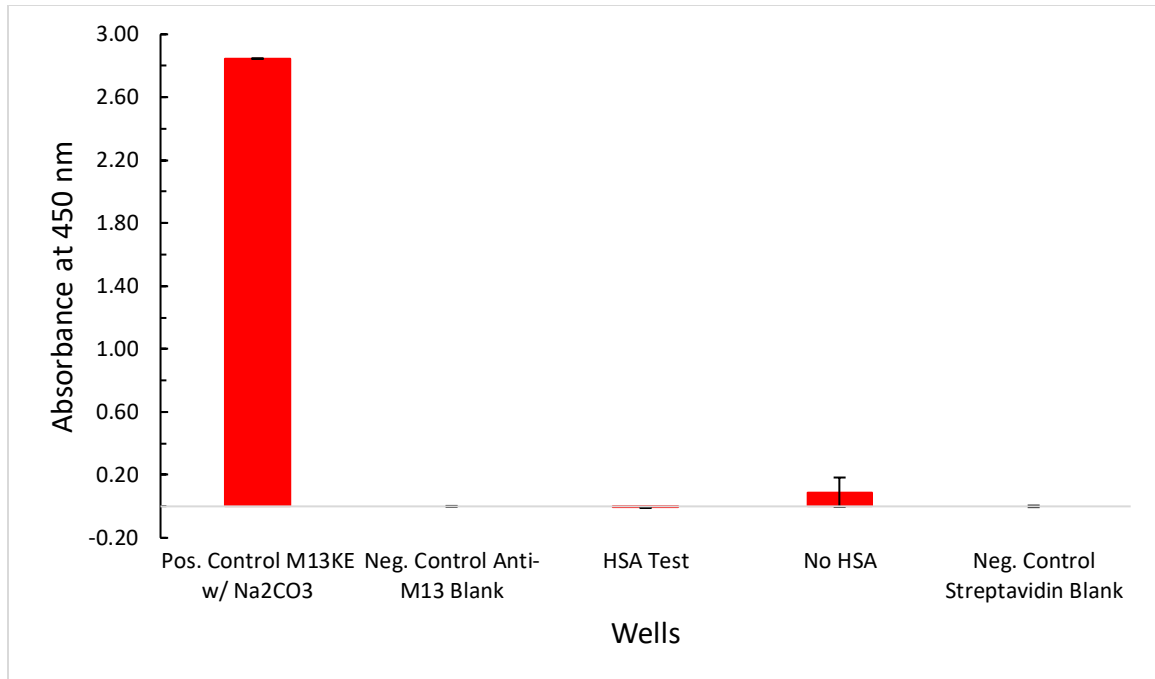
Figure 8: BR B-BR-1 Peptide ELISA Against HSA. One microgram HSA in 0.05 M Na$_2$CO$_3$, pH 9.6 was bound to a row of wells in a 96-well polyvinyl chloride assay plate. Wells were washed with PBST (PBS + 0.05% Tween-20) and blocked with PBST + 1% Yeast Extract. The blocked wells were washed and 1 μg BR B-BR-1 in PBST + 0.1% Yeast Extract was added. The wells were washed, and binding was demonstrated by the addition of HRP-Streptavidin, washing the wells, and addition of tetramethylbenzidine substrate solution. The reaction was stopped with 2 N H$_2$SO$_4$ and absorbance was measured at 450 nm. Positive control: M13KE phage (1 x 10^{10} pfu/mL in 0.05 M Na$_2$CO$_3$, pH 9.6). Negative controls: Phage Blank (No M13KE), Ab Blank (No HRP-Anti-M13), and Streptavidin Blank (No HRP-Streptavidin). All samples had an n = 3 ± SEM, except the positive control where n = 1. A one-tailed two-sample t-test was performed between the HSA and No HSA wells and concluded that there was no statistically significant difference (p = 0.2033).

The peptide ELISA was repeated (**Figure 9**) using all the biotinylated BR-1 samples (BR, FK, EP, and AH) to determine whether the BR B-BR-1 peptide sample had degraded in storage, which could have led to the ELISA's negative results (Huber 2019; Kenney 2018; Rees 2016). This ELISA used a MaxiSorp plate to test whether HSA would bind better to the plate's coating, as MaxiSorp plates are designed to bind to proteins with mixed hydrophobic and hydrophilic domains. The amounts of the BR, FK, and EP samples remained the same at 1 μg while the AH peptide amount was increased to 8 μg to test the effects of a higher amount of peptide in the assay.
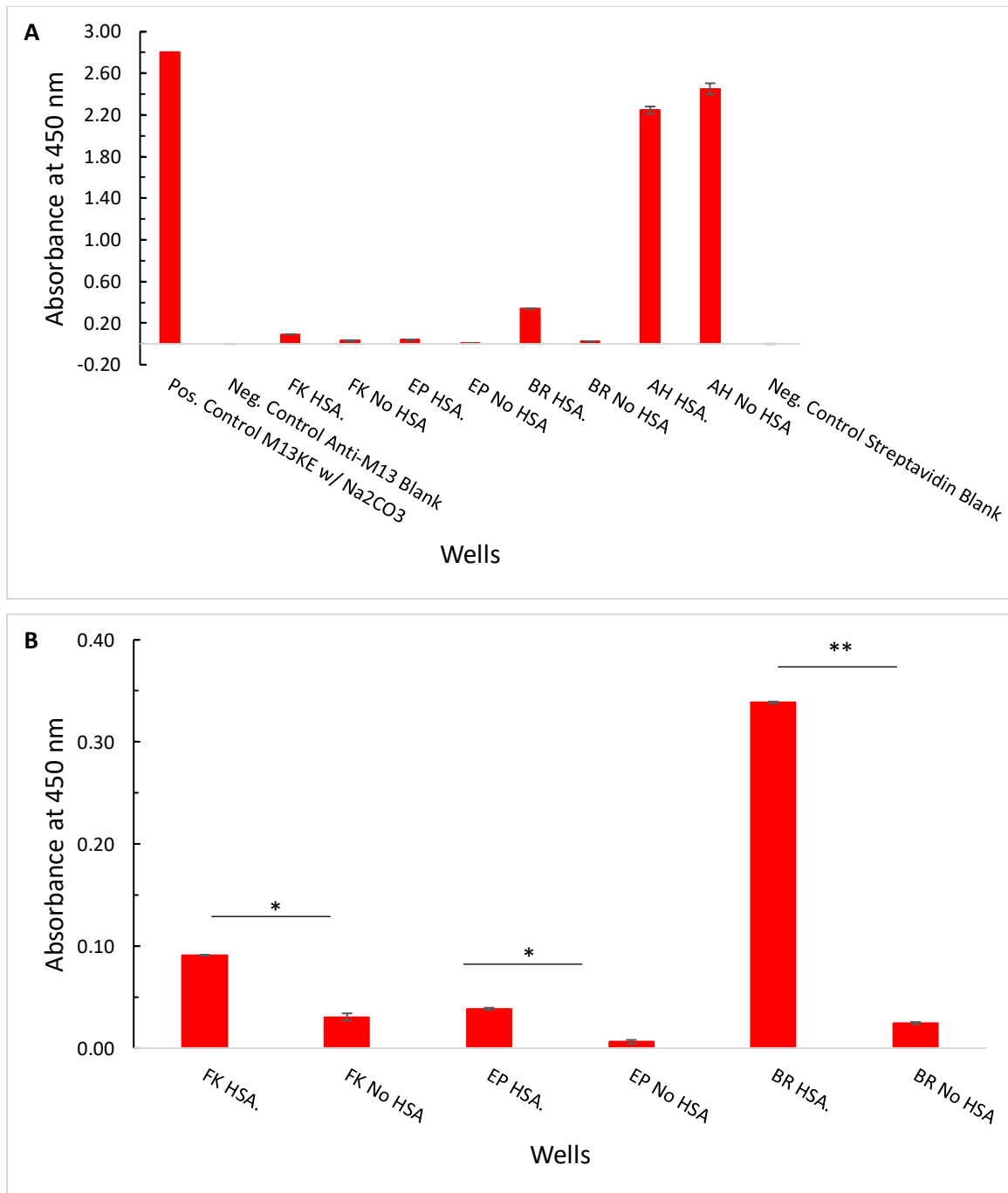
Figure 9: Peptide ELISA Against HSA Using All Biotinylated Peptide Samples. The ELISA was conducted as described in **Figure 8** with the following changes: A Nunc MaxiSorp plate was used, AH B-BR-1 peptide amount was increased to 8 μg. All samples had an n = 2 ± SD, except the positive control where n = 1 and the negative controls where n = 3. A) ELISA with controls. B) ELISA without controls and AH. A one-tailed two-sample t-test was performed between all sample HSA and No HSA wells

and there were statistically significant differences for the FK, EP, and BR samples between the HSA and No HSA wells (* = $p < 0.05$; ** = $p < 0.01$). There was no statistically significant difference for the AH sample ($p = 0.2537$).

The BR B-BR-1 sample had the highest binding to HSA compared to No HSA which was statistically significantly higher (BR HSA absorbance = 0.339 ± 0.001 SD, BR No HSA absorbance = 0.025 ± 0.001 SD, p = 0.0041). The FK sample had a higher absorbance in the FK HSA wells (0.091 ± 0.001 SD) than in the FK No HSA wells (0.031 ± 0.005 SD) with a statistically significant difference between them (p = 0.0428). The EP HSA wells had lower absorbances than the FK HSA wells at 0.039 ± 0.001 SD, and the EP No HSA wells had an average absorbance of 0.006 ± 0.003 SD, and the difference was statistically significant (p = 0.0256). The AH sample's result did not show increased binding in the presence of HSA, as the AH No HSA wells had a higher absorbance (2.451 ± 0.054 SD) than the AH HSA wells (2.247 ± 0.035 SD). There was no significant difference between the AH HSA and AH No HSA wells (p = 0.2537). Alexander Huber (2019) conducted the same ELISA in parallel using a polyvinyl chloride plate and achieved better results (the absorbances for the peptide samples were higher; data not shown) so it was decided that the polyvinyl chloride plates would be used for ELISAs instead of the MaxiSorp plates. Additionally, since the BR B-BR-1 sample was still binding to HSA, it was chosen for continued use in subsequent ELISAs.

The BR B-BR-1 peptide was also tested for specificity of binding to HSA using four competitive inhibition peptide ELISAS. In the first competitive inhibition peptide ELISA (**Figure 10**) one microgram HSA was bound with sodium carbonate buffer to a row of wells of a polyvinyl chloride assay plate. The wells were washed with PBST (PBS + 0.05% Tween-20), blocked with PBST + 1% Yeast Extract, and washed again. A second row of wells was also blocked to serve as preincubation wells in which different amounts of HSA (0.001, 0.01, and 0.1 μg HSA in PBST + 0.1% Yeast Extract sample

buffer) and BR B-BR-1 peptide (1 μg in sample buffer) were premixed and incubated at 37°C for 30 minutes. The peptide remaining in the supernatant was then transferred into the HSA test wells containing 1 μg bound HSA. The wells were washed, HRP/Streptavidin in sample buffer was added, and the wells were washed again before addition of TMB (3,3,5,5-Tetramethylbenzidine) substrate solution and measuring absorbance at 450 nm wavelength. HSA in the preincubation wells should bind to the peptide and decrease the amount of B-BR-1 available to bind to the HSA in the test wells.
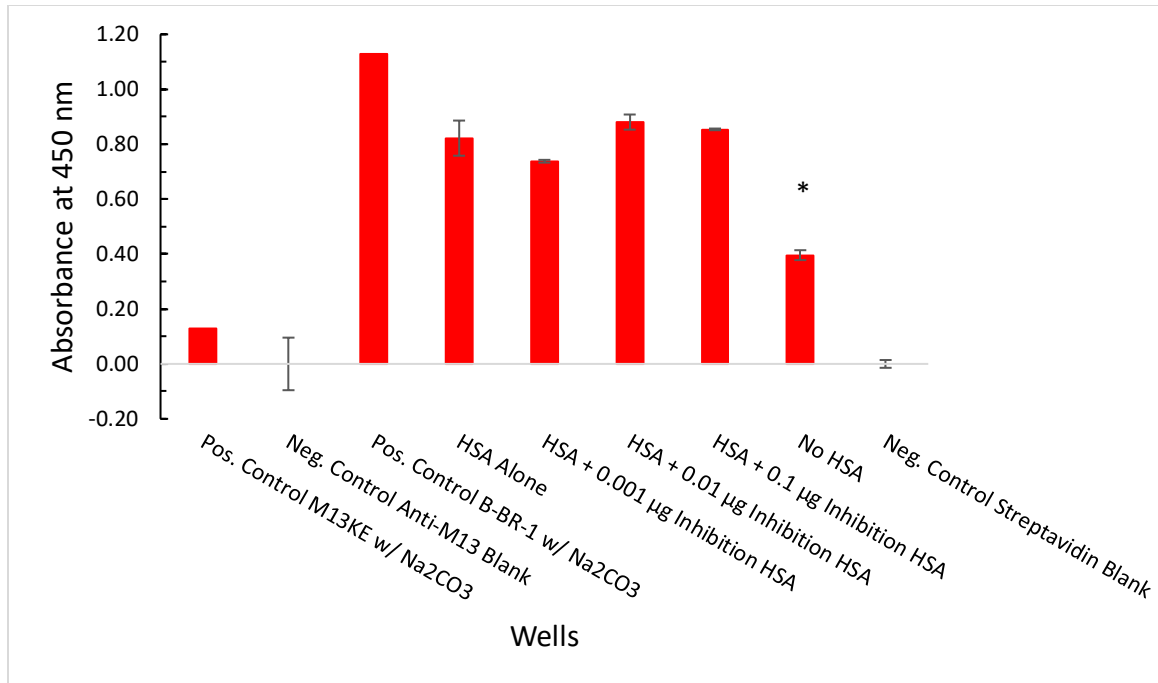
Figure 10: Competitive Inhibition With Soluble HSA And 1 μg BR B-BR-1 Peptide ELISA. One microgram HSA per well (test wells) in 0.05 M Na$_2$CO$_3$, pH 9.6 was bound to a row of wells in a 96-well polyvinyl chloride assay plate. Wells were washed with PBST (PBS + 0.05% Tween-20) and blocked with PBST + 1% Yeast Extract. A row of preincubation wells without HSA was also blocked. All wells were washed before mixing 0.001, 0.01, and 0.1 μg HSA (in PBS + 0.1% Tween-20 sample buffer) with 1 μg BR B-BR-1 (in sample buffer) in the preincubation wells. The preincubation wells were incubated at room temperature for 2 hours and then the HSA/B-BR-1 mixtures were transferred to the test wells containing 1 μg HSA bound to the plate. The mixtures were incubated for 2 hours at room temperature. The test wells were washed and binding of peptide to HSA in the wells was demonstrated by the addition of HRP-Streptavidin, washing the wells, and addition of tetramethylbenzidine substrate solution. The reaction was stopped with 2 N H$_2$SO$_4$ and absorbance was measured at 450 nm. Positive control: M13KE phage (1 x 10^{10} pfu/mL in 0.05 M Na$_2$CO$_3$, pH 9.6). Negative controls: Phage Blank (No M13KE), Ab Blank (No HRP-Anti-M13), and Streptavidin Blank (No HRP-Streptavidin). All samples had an n = 2 ± SD, except the positive controls where n = 1 and the negative controls where n = 3. A one-tailed two-sample t-test was performed between the HSA Alone and No HSA wells and concluded that there was a statistically

significant difference (p = 0.0381, * = p < 0.05). Another t-test was performed between the HSA Alone and HSA Inhibition wells and concluded that there were no statistically significant differences (p ≥ 0.2067).

The results were unexpected, as no downward trend in peptide binding in test wells was seen when the concentration of inhibiting HSA increased. The positive Biotin Control (absorbance = 1.127) and No HSA (absorbance = 0.396 ± 0.018 SD) wells worked as expected, indicating that the biotin/streptavidin interaction occurred with the HSA Inhibition wells and that there was little nonspecific binding of biotinylated peptide to the yeast extract block on the well walls. A one-way two-tailed t-test was performed between the HSA Alone and No HSA wells and concluded that the No HSA wells had statistically significantly lower absorbances than the HSA alone wells (p = 0.0381). It was observed, however, that the Phage Positive Control had low binding (absorbance = 0.129), possibly due to repeated freeze/thaw cycles that degraded the phage. The M13KE (control phage) microfuge tube in use was discarded and a new one was used for subsequent ELISAs.

The competitive inhibition peptide ELISA (**Figure 11**) was repeated with identical methods to **Figure 10**, but with increased amount of biotinylated peptide (10 μg BR B-BR-1) to determine whether a higher amount of peptide would lead to greater binding and higher absorbances.

Figure 11: Competitive Inhibition With Soluble HSA And 10 μg BR B-BR-1 Peptide ELISA. The ELISA was conducted as described in **Figure 10** with the following change: 10 μg BR B-BR-1 in PBS + 0.1% Tween-20 sample buffer mixed with 0.001, 0.01, and 0.1 μg HSA in sample buffer in the blocked preincubation wells, incubated for 2 hours at room temperature, and transferred to the testing wells containing 1 μg HSA bound to the plate. All samples had an n = 2 ± SD, except the positive controls where n = 1 and the

negative controls where n = 3. A) ELISA with controls. B) ELISA without controls. A one-tailed two-sample t-test was performed between the HSA Alone and No HSA wells and concluded that there was a statistically significant difference (p = 0.0065, ** = p < 0.01). Another t-test was performed between the HSA and HSA Inhibition wells and concluded that that there were no statistically significant differences (p ≥ 0.0518).

A downward trend in absorbance was seen in the assay as the concentration of inhibiting HSA increased (HSA Alone 0.610 ± 0.036 SD, HSA + 0.001 μg Inhibition HSA 0.468 ± 0.009 SD, HSA + 0.01 μg Inhibition HSA 0.438 ± 0.006 SD, HSA + 0.1 μg Inhibition HSA 0.395 ± 0.003 SD). However, a one-tailed two-sample t-test concluded that none of the HSA Inhibition wells were statistically significantly different from the HSA Alone wells ($p \geq 0.0518$). The Phage Positive Control gave a high absorbance of 2.287 as in other ELISAs with properly working M13KE phage stocks, while the Biotin Positive Control wells gave an even lower than expected absorbance of 0.352. A one-tailed two-sample t-test was performed between the HSA Alone and No HSA wells and concluded that the No HSA wells had an absorbance (0.182 ± 0.031 SD) that was statistically significantly lower than the HSA Alone wells ($p = 0.0065$).

The competitive inhibition peptide ELISA (**Figure 12**) was modified by binding the HSA in the preincubation wells to the plate with sodium carbonate buffer. The same amount of BR B-BR-1 peptide (1 μg in PBS + 0.1% Tween-20 sample buffer) from **Figure 10** was added to the preincubation wells before the depleted peptide solution from the inhibition wells was transferred to the test wells.
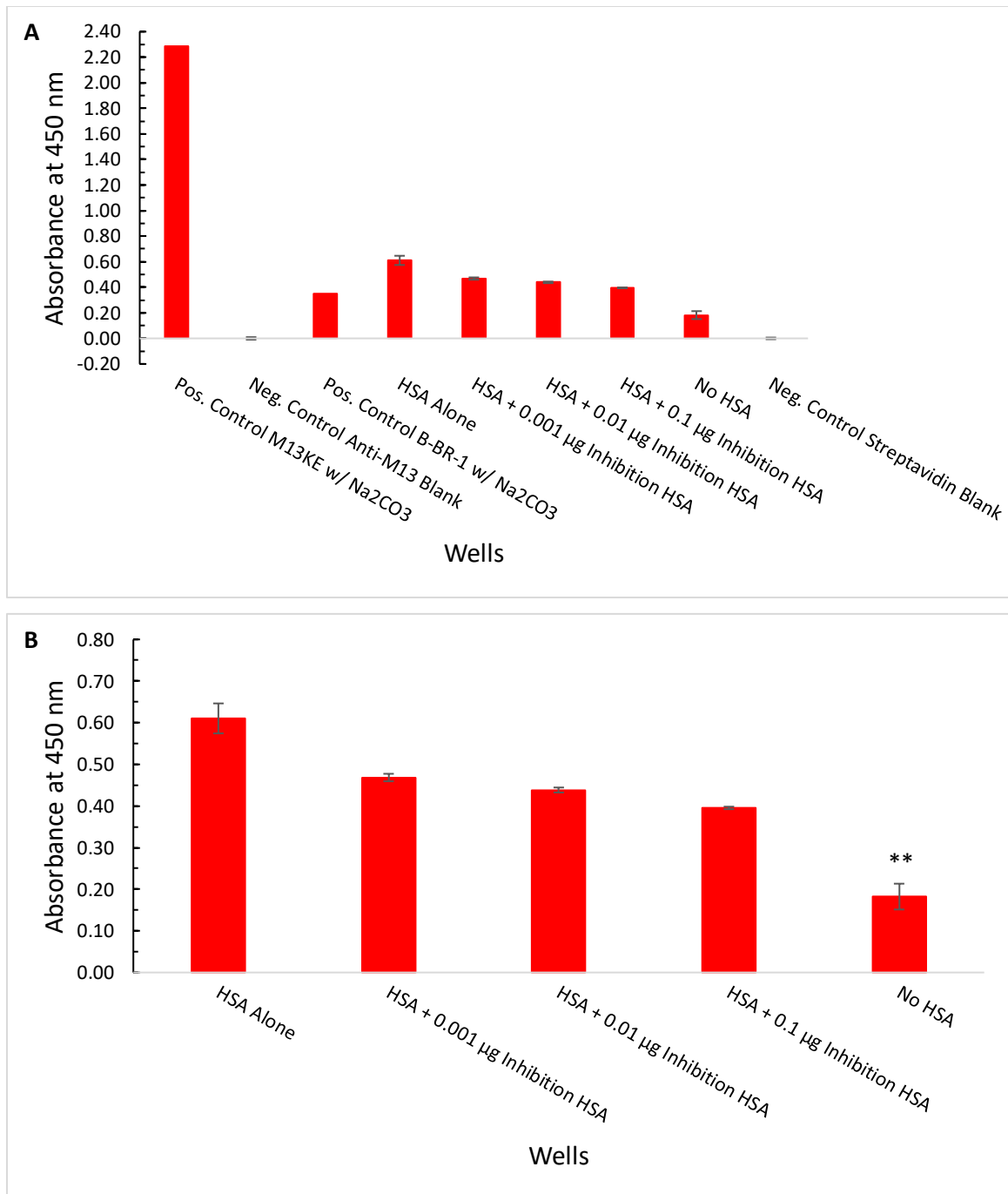
Figure 12: Competitive Inhibition With Bound HSA And 1 μg BR B-BR-1 Peptide ELISA. The ELISA was conducted as described in **Figure 10** with the following changes: 0.001, 0.01, and 0.1 μg HSA was bound to the preincubation wells with 0.05 M Na$_2$CO$_3$, pH 9.6; 1 μg BR B-BR-1 in PBS + 0.1% Tween-20 sample buffer added to preincubation wells and incubated for 2 hours at room temperature. The free BR B-BR-1 in the supernatant from the preincubation wells was then transferred to the testing wells

containing 1 μg HSA bound to the plate. All samples had an n = 2 ± SD, except the positive controls where n = 1 and the negative controls where n = 3. A) ELISA with controls. B) ELISA without controls. A one-tailed two-sample t-test was performed between the HSA Alone and No HSA wells and concluded that there was a statistically significant difference (p = 0.0206, * = p < 0.05). Another t-test was performed between the HSA and HSA Inhibition wells and concluded that that there were no statistically significant differences (p ≥ 0.4559).

There was no downward trend visible as the concentration of inhibition HSA increased, and all absorbance values were in approximately the same range (HSA Alone 0.184 ± 0.005 SD, HSA + 0.001 µg Inhibition HSA 0.178 ± 0.043 SD, HSA + 0.01 µg Inhibition HSA 0.198 ± 0.002 SD, HSA + 0.1 µg Inhibition HSA 0.180 ± 0.046 SD). A one-way two-tailed t-test was performed between the HSA Alone and HSA Inhibition wells and concluded that there were no statistically significant differences ($p \geq 0.0916$). The Phage Positive Control and Biotin Positive Controls gave strong absorbances (Phage absorbance = 2.228, Biotin absorbance = 0.982). A one-way two-tailed t-test was performed between the HSA Alone and No HSA wells and concluded that the No HSA wells had an absorbance (0.036 ± 0.015 SD) that was statistically significantly lower than the HSA Alone wells ($p = 0.0265$).

The previous competitive inhibition peptide ELISA with HSA bound to the preincubation wells was repeated (**Figure 13**) using a higher amount of peptide (2 µg BR B-BR-1).
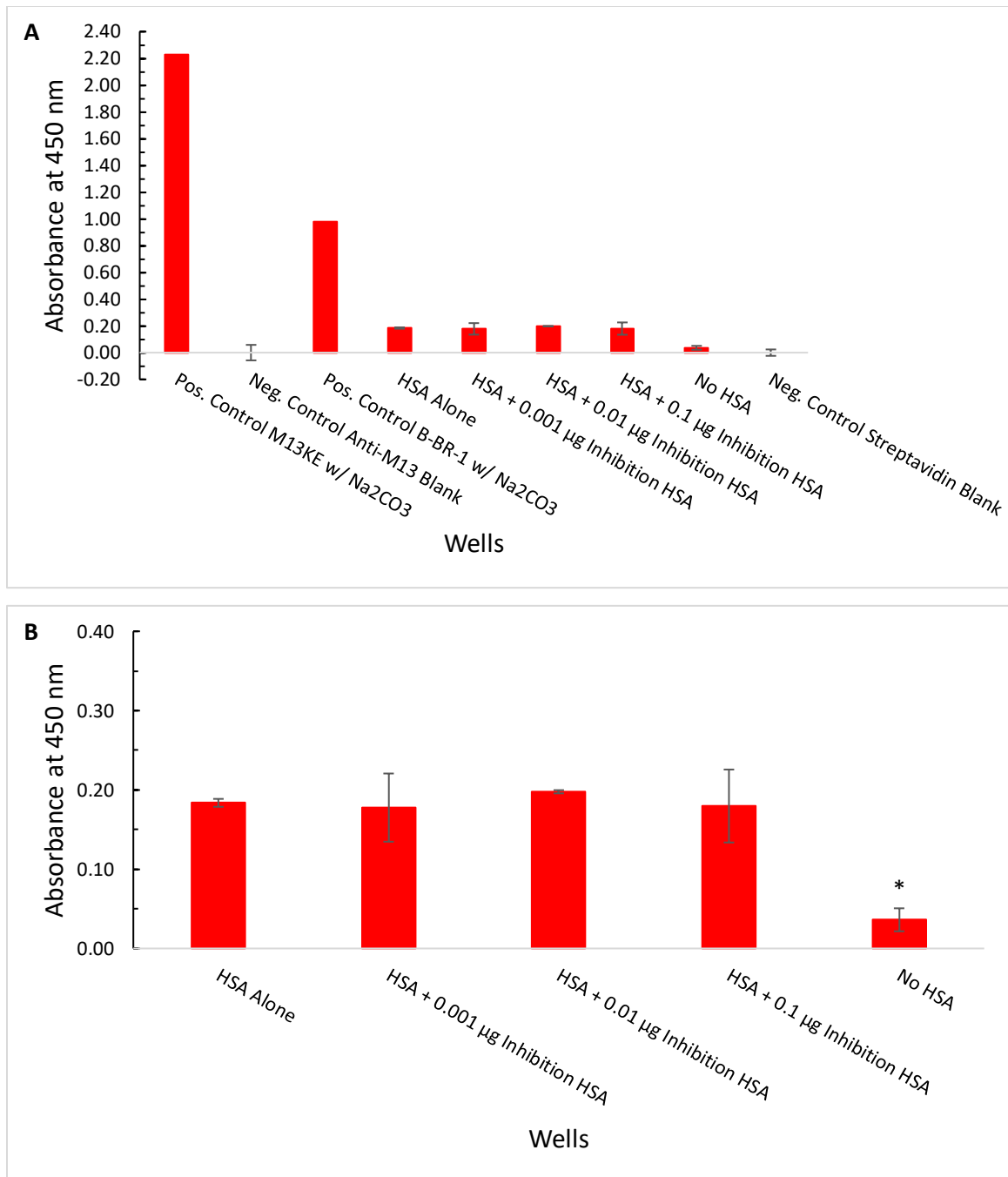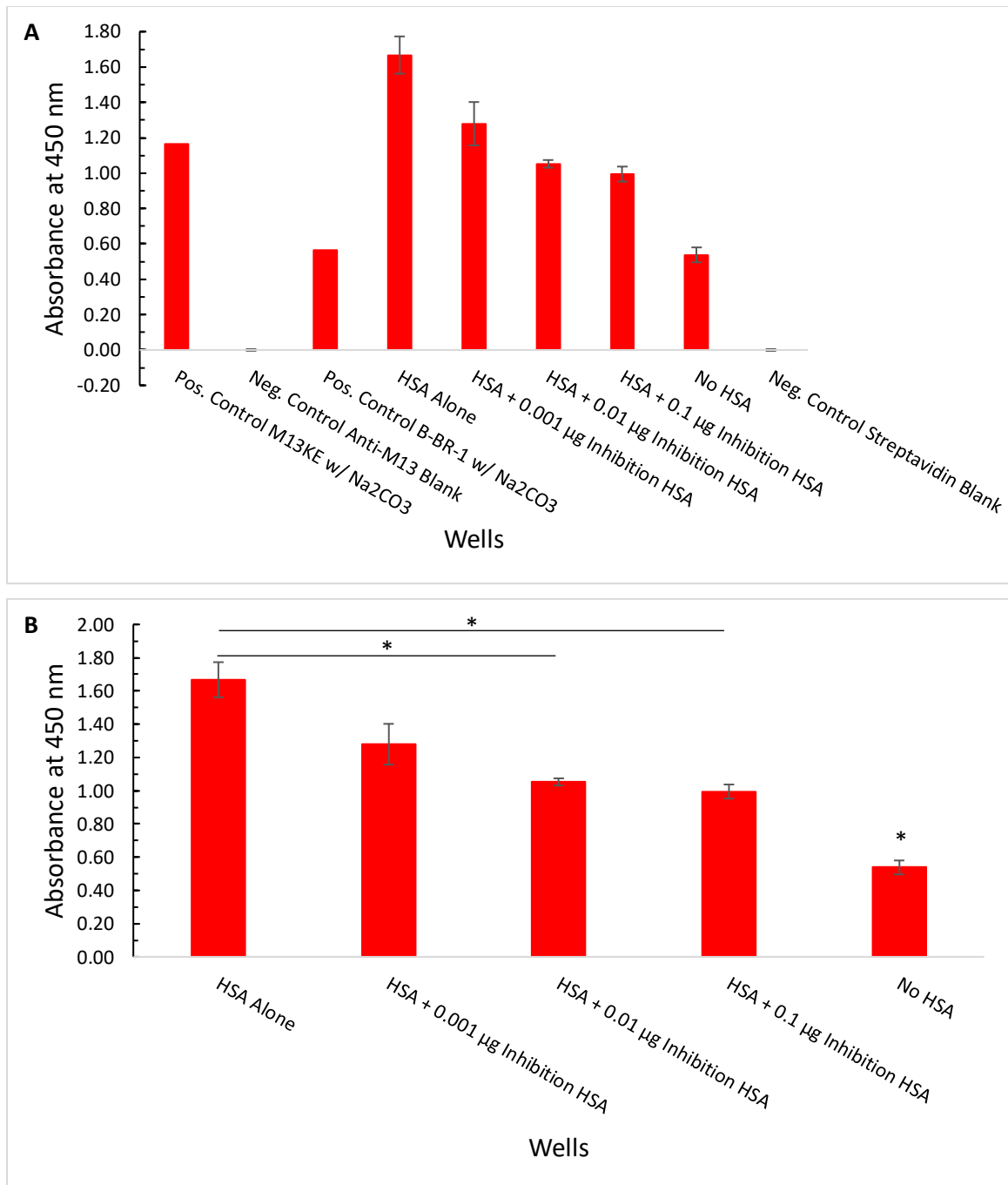
Figure 13: Competitive Inhibition With Bound HSA And 2 μg BR B-BR-1 Peptide ELISA. The ELISA was conducted as described in **Figure 12** with the following change: 2 μg BR B-BR-1 in sample buffer added to preincubation wells and transferred to the testing wells. All samples had an $n = 2 \pm SD$, except the positive controls where $n = 1$ and the negative controls where $n = 3$. A) ELISA with controls. B) ELISA without controls. A one-tailed two-sample t-test was performed between the HSA Alone and No HSA

wells and concluded that there was a statistically significant difference ($p = 0.0171$, $* = p < 0.05$). Another t-test was performed between the HSA Alone and HSA Inhibition wells and concluded that HSA + 0.01 µg Inhibition HSA/HSA + 0.1 µg Inhibition HSA wells were statistically different from the HSA Alone wells ($p \leq 0.0485$, $* = p < 0.05$) while the HSA + 0.001 µg Inhibition HSA wells were not ($p = 0.0706$).

A downward trend in absorbance was observed as the concentration of inhibiting HSA increased (HSA Alone 1.668 ± 0.106 SD, HSA + 0.001 µg Inhibition HSA 1.280 ± 0.123 SD, HSA + 0.01 µg Inhibition HSA 1.053 ± 0.022 SD, HSA + 0.1 µg Inhibition HSA 0.995 ± 0.042 SD). A one-way two-tailed t-test was performed between the HSA Alone and HSA Inhibition wells and concluded that the HSA + 0.01 µg Inhibition HSA and HSA + 0.1 µg Inhibition HSA wells were significantly different from the HSA Alone wells ($p \leq 0.0485$), but the HSA + 0.001 µg Inhibition HSA wells were not ($p = 0.0706$). The Phage Positive Control well gave a lower absorbance than previously observed (Phage absorbance = 1.166,), but it was enough to validate the assay. A one-tailed two-sample t-test was performed between the HSA Alone and No HSA wells and concluded that the No HSA wells had absorbances (absorbance = 0.538 ± 0.042) that were significantly different from the HSA Alone wells ($p = 0.0171$).

Specificity of peptide for HSA can also be demonstrated by showing increased binding of phage clones with increased concentration of phage. A phage ELISA (**Figure 14**) was performed with the HSA-6 phage clones (phage from which the BR-1 sequence was derived). The ELISA conditions used in previous studies included the use of Tris-buffered saline (TBS; 50 mM Tris-HCl, 150 mM NaCl) + 1% Casein as the blocking buffer and PBS wash buffer containing no detergent. The sample buffer was a 1:10 dilution of the blocking buffer in PBS to make PBS + 0.1% Casein. These conditions were used to replicate the original ELISA conditions from when the phage clone was first picked by William Rees (Rees, 2016).
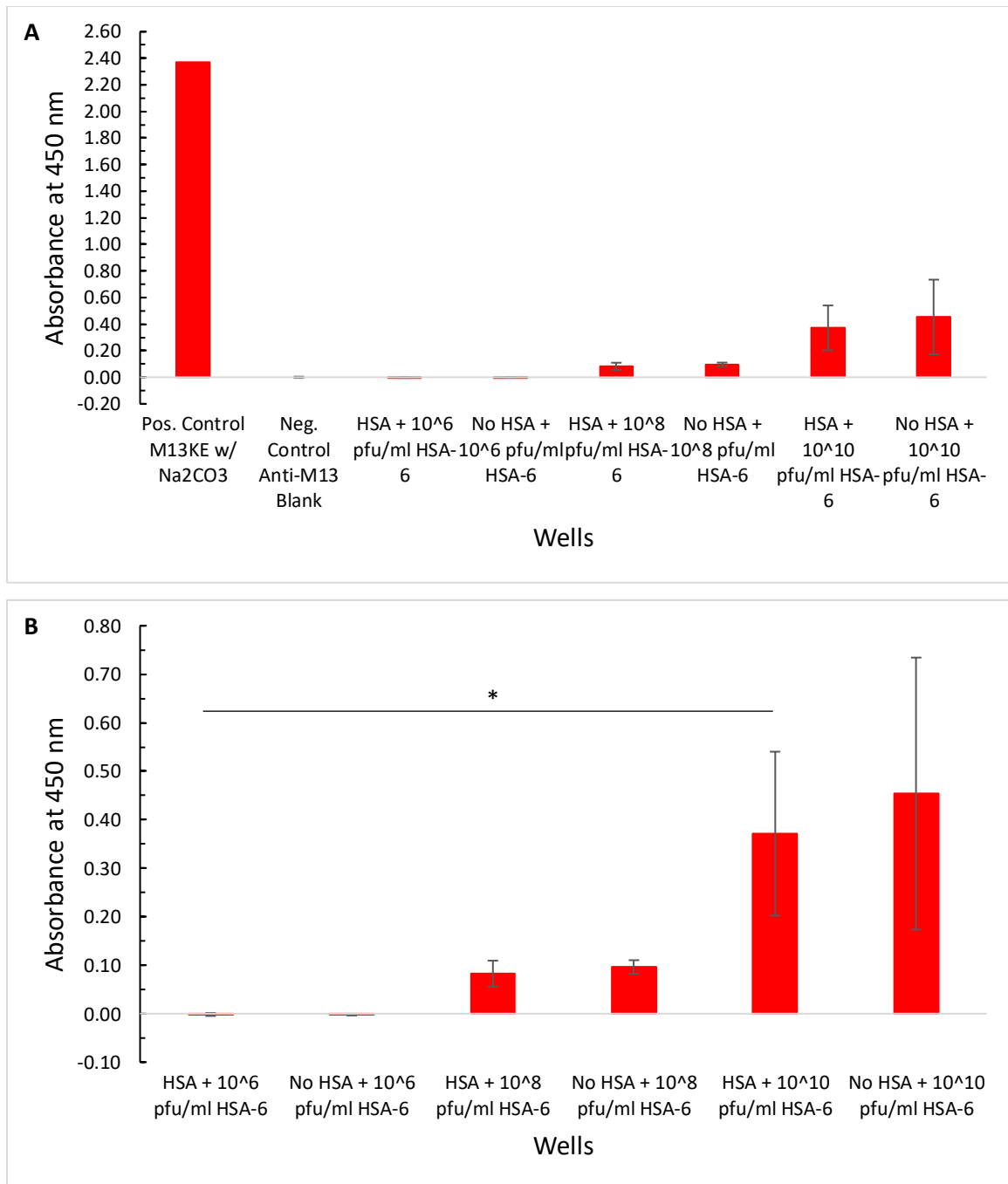
Figure 14: Phage ELISA. One microgram HSA per well in 0.05 M Na$_2$CO$_3$, pH 9.6 was bound to a row of wells on a 96-well polyvinyl chloride assay plate. The wells were washed with PBS and blocked with TBS + 1% Casein. The blocked wells were washed and increasing concentrations (10^6, 10^8, and 10^{10} pfu/mL) HSA-6 phage in TBS were added and incubated for 2 hours at room temperature. The wells were washed and binding of phage to HSA in the wells was demonstrated by the addition of HRP-Anti-

M13 (in PBS + 0.1% Casein sample buffer), washing the wells, and addition of tetramethylbenzidine substrate solution. The reaction was stopped with 2 N H_2SO_4 and absorbance was measured at 450 nm. Positive control: M13KE phage (1 x 10^{10} pfu/mL in 0.05 M Na2CO3, pH 9.6). Negative controls: Phage Blank (No M13KE), Ab Blank (No HRP-Anti-M13). All samples had an n = 2 ± SD, except the positive control where n = 1 and the negative controls where n = 3. A) ELISA with controls. B) ELISA without controls. A one-tailed two-sample t-test was performed between the HSA and No HSA wells for each phage dilution and concluded that there was no statistically significant difference for any dilution. Another t-test was performed between the HSA wells for each dilution and concluded that there was a significant difference between the 10^6 HSA wells and the 10^{10} HSA wells (p = 0.0395, * = p < 0.05) but not between the $10^6/10^8$ and $10^8/10^{10}$ HSA wells (p ≤ 0.1747).

The Phage Positive Control well worked properly and displayed a high absorbance of 2.371. The 10^6 pfu/mL HSA-6 phage dilution may have been too low to yield positive results since the 10^6 HSA and 10^6 No HSA wells had the same absorbance of -0.002 ± 0.003 SD. The 10^8 HSA-6 phage dilution may have also been too low, although the absorbances for the 10^8 HSA and 10^8 No HSA wells were detectable at 0.082 and 0.096, respectively. The absorbances did increase with increasing amount of phage (10^8 HSA 0.082 ± 0.027 SD, 10^8 No HSA 0.096 ± 0.014 SD, 10^{10} HSA 0.371 ± 0.169 SD, 10^{10} No HSA 0.454 ± 0.281 SD). However, a one-tailed two-sample t-test was performed between the HSA and No HSA wells for each phage dilution and concluded that there were no statistically significant differences at any dilution ($p \geq 0.0971$). A one-tailed two-sample t-test was performed between the HSA wells of each phage dilution and concluded that there was no statistically significant difference between the 10^6 and 10^8, and the 10^8 and 10^{10} HSA-6 HSA wells ($p \geq 0.1354$); however, there was a statistically significant difference between the 10^6 and 10^{10} phage HSA wells ($p = 0.0395$). It is possible that the titer and activity of the phage have declined with storage and the sample may need to be amplified and titered again.

To produce BR-1 peptide for use in a biosensor, protein production and purification of BR-1 peptide via the pMAL-c5X vector was performed. Lura-Bertani (LB) broth containing 20 μL 100 mg/mL ampicillin was inoculated with AH3 ER 2523 bacteria (BR-1 peptide in pMAL-c5X vector and transformed into *E. coli*, prepared by Alexander Huber, 2019) and incubated overnight at 37°C in a shaking incubator at 250 RPM. Ten milliliters of the overnight culture was used to inoculate 1 L of rich broth + glucose + ampicillin in a baffled 2-L Erlenmeyer flask. The culture was incubated at

37°C with 200 RPM shaking until the A_{600} reached 0.63 in the BioPhotometer. IPTG (0.3 mM) was added and the culture was divided into two 1-L Erlenmeyer flasks ($\approx$500 mL broth each). The flasks were then incubated at 37°C with 250 RPM shaking for two hours to allow cytoplasmic expression of the MBP-BR-1 fusion protein. After incubation, the culture was centrifuged, and the supernatant discarded. The cell pellet (4.54 g) was resuspended in approximately 5 mL of Column Buffer and frozen overnight at -20°C. The cells were thawed in cold water before placing the sample into an ice bath. A sonicator was used to lyse the cells with 15-second pulses. After each pulse, 5 µL of sonicate was taken and added to 1 mL Bradford reagent to monitor protein release (data not shown). The Bradford assay setup for sonicated cells containing fusion protein is shown in **Figure 15**.
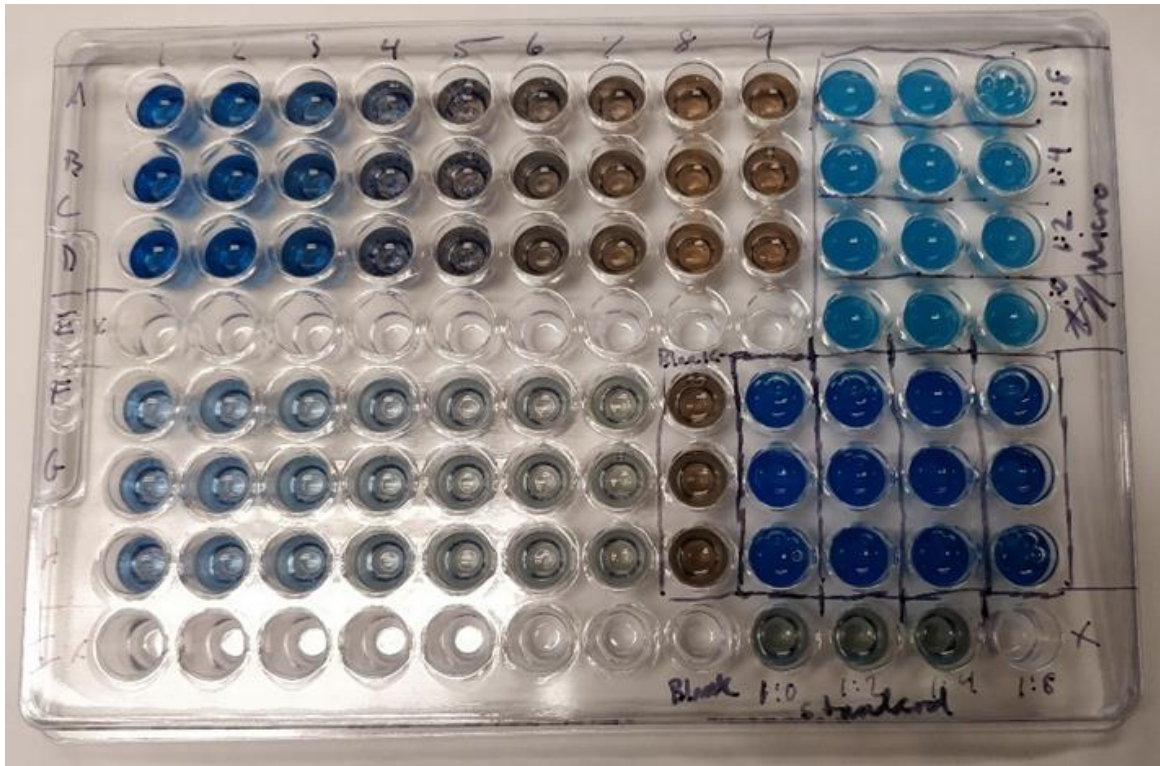
Figure 15: Bradford Assay of Sonicated AH3 ER 2523 Cells Containing BR-1 Peptide Expressed from the pMAL-c5X Vector. The left-hand side of the microtiter plate contains the BSA standards (top is the standard protocol, 0–2,000 μg/mL BSA, 5 μL sample + 150 μL Bradford reagent; bottom is the micro protocol, 0–25 μg/mL BSA, 75 μL sample + 75 μL Bradford reagent). The right-hand (with lines) are the cell lysates and blanks. Test: Cell lysate (undiluted, 1:2, 1:4, 1:8). Blank: dH$_2$O. The concentration of total protein in the lysate dilutions was calculated using BSA Standard curve (125–1,500 μg/mL detection limit) and BSA Micro Standard curve (1–25 μg/mL detection limit). Sample was added to Bradford reagent and the plate incubated at room temperature for 10 minutes before the absorption was measured at 595 nm.

A BSA Standard Curve was plotted (**Figure 16**) with a line of best fit and used to calculate the concentration of cell lysate after sonication. Two-fold serial dilutions of cell lysate had been prepared since the undiluted sonicate had a protein concentration that was beyond the detection limit of the assay. The calculated concentration of protein in the sonicate (**Table 2**) decreased in a stepwise manner. The undiluted lysate had a calculated concentration of 5,096 µg/mL, the 1:2 lysate dilution was 4,460 µg/mL, the 1:4 lysate dilution was 3,703 µg/mL, and the 1:8 lysate dilution was 3,503 µg/mL.

Figure 16: Bradford Assay BSA Standard Curve for Sonicated Cells. 125–1,500 μg/mL detection limit. Five microliters of standard or sample and the dH$_2$O blanks were mixed with 150 μL of Bradford reagent. All samples had an n = 3 ± SEM. The plate was incubated at room temperature for 10 minutes before the absorbance was read at 595 nm. Line of best fit y = 0.0003x + 0.0381, R^2 value 0.94.

Table 2: Calculated Concentration of Lysate from BSA Standard Curve	
Sample [a]	**Calculated Concentration (μg/mL)** [b]
Lysate	5,096
Lysate 1:2	4,460
Lysate 1:4	3,703
Lysate 1:8	3,503
[a]All samples had an n = 3 ± SEM. [b]Concentration of protein calculated from the Bradford Assay Standard Microplate Protocol (Methods 8.1.1).	

A BSA Micro Standard Curve was also plotted (**Figure 17**) with a line of best fit and used to calculate the concentration of cell lysate after sonication. The calculated concentration of sonicate was outside of the micro assay's detection limits for two samples (**Table 3**). The concentrations of the 1:4 and 1:8 lysate dilutions were able to be calculated as 796 µg/mL and 714 µg/mL, respectively. However, these calculated concentrations did not correlate with the concentrations calculated in **Table 2**.
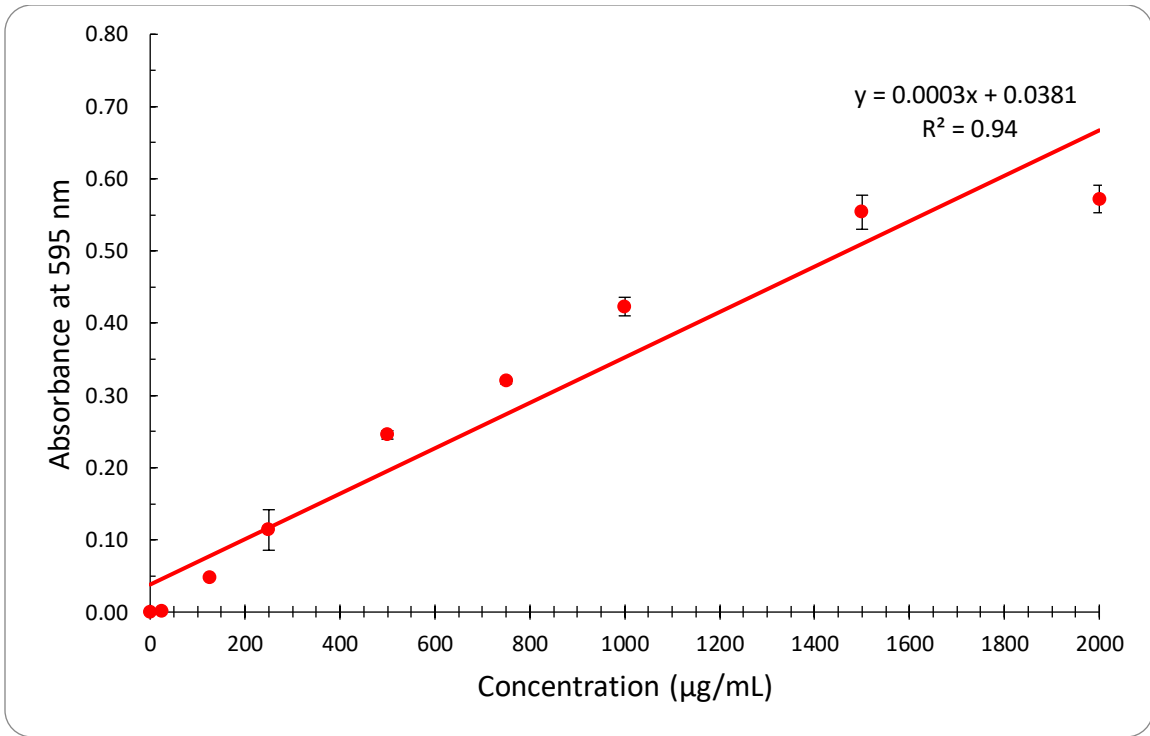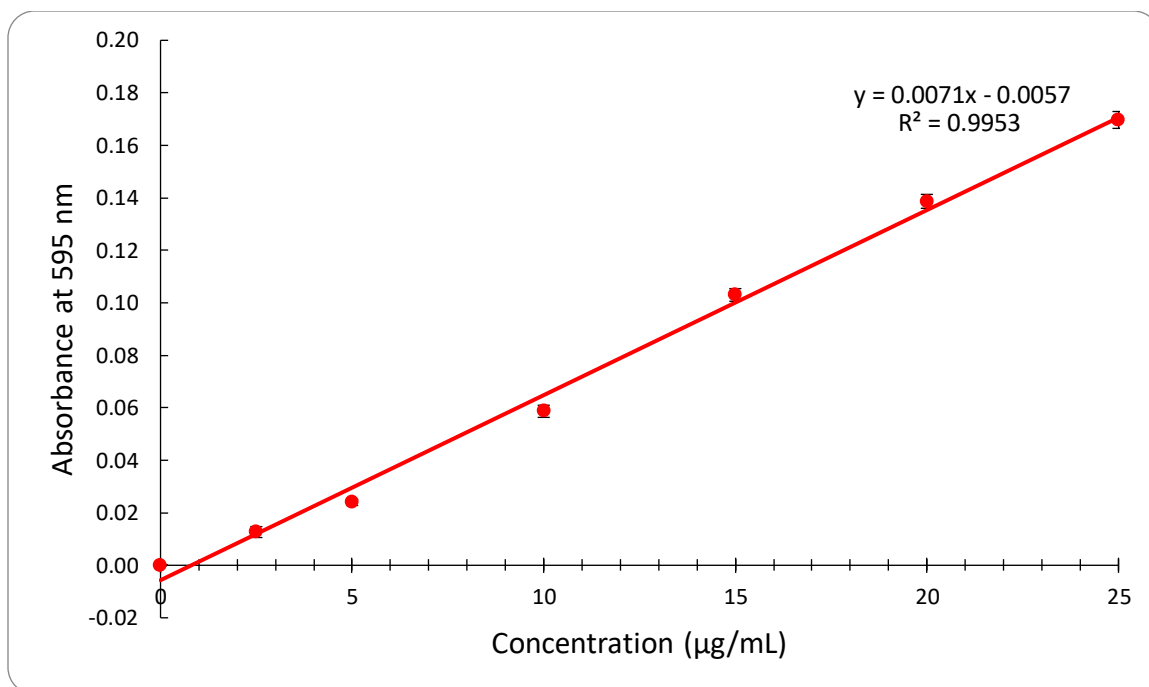
Figure 17: Bradford Assay BSA Micro Standard Curve for Sonicated Cells. 1–25 µg/mL detection limit. Seventy-five microliters of standard or sample and the dH_2O blanks were mixed with 75 µL of Bradford reagent. All samples had an n = 3 ± SEM. The plate was incubated at room temperature for 10 minutes before the absorbance was read at 595 nm. Line of best fit y = 0.0071x + 0.0057, R^2 value 0.9953.

Table 3: Calculated Concentration of Lysate from BSA Micro Standard Curve	
Sample [a]	Calculated Concentration (μg/mL) [b]
Lysate	Too high to measure
Lysate 1:2	Too high to measure
Lysate 1:4	796
Lysate 1:8	714
[a]All samples had an n = 3 ± SEM. [b]Concentration of protein calculated from the Bradford Assay Micro Microplate Protocol (Methods 8.1.2).	

Affinity purification of the fusion protein was performed using amylose resin affinity chromatography. The affinity chromatography equipment was then set up according to the diagram in **Figure 18**. The flow-through was collected in two flasks labeled Running Buffer 1 (equilibrating and loading sample) and 2 (from washing the column after loading sample) for analysis by SDS-PAGE. The AH3 MBP/BR-1 fusion protein was eluted using 60 mL of Column Buffer + 10 mM maltose. Twenty-six 2–3-mL fractions were collected.
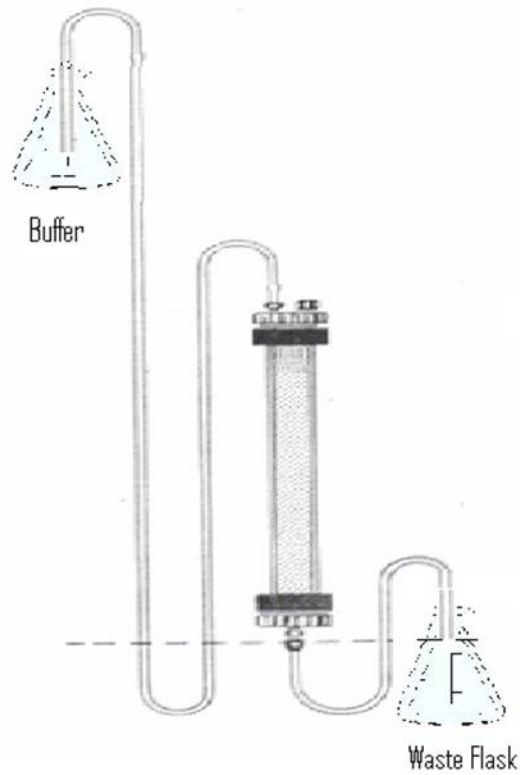
Figure 18: Affinity Chromatography. Running buffers were elevated in relationship to the chromatography column. The waste flask was placed below the bottom of the chromatography column. The tubing was looped so that the bottom of the loops was below the dashed line in the figure above. This setup prevented the chromatography column from running dry.

Fusion protein content of each fraction was tested by means of a Bradford assay and generation of a BSA standard curve with a line of best fit (**Figure 19**). The absorbance of each fraction mixed with Bradford reagent was graphed for visual representation of the elution curve (**Figure 20**). The absorbance of the elution fractions began increasing with fraction 4, reached a peak at fraction 7, and then tapered off after fraction 12. A small increase in absorbance was observed in fraction 19 but it was disregarded since the pMAL-c5X vector's instruction manual stated that the MBP fusion protein begins eluting around the fifth fraction and the bump was further along the elution curve.
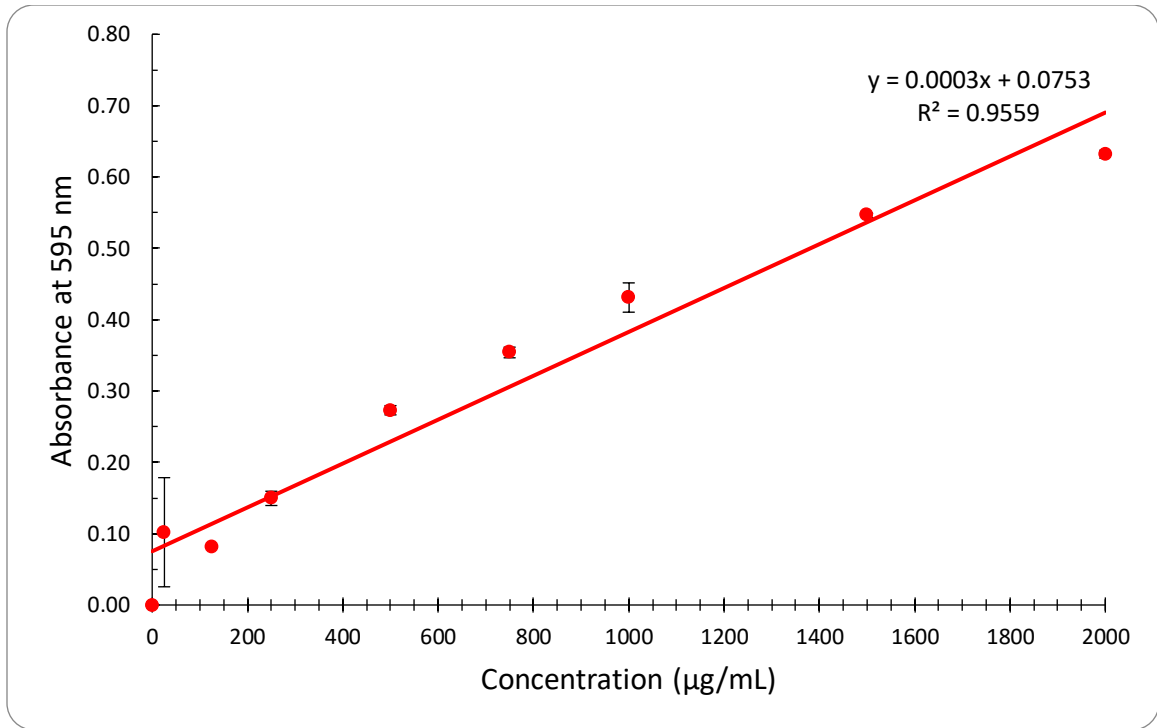
Figure 19: Bradford Assay BSA Standard Curve for MBP/BR-1 Fusion Protein Eluted Fractions. 125–1,500 µg/mL detection limit. Five microliters of standard or sample and the dH$_2$O blanks were mixed with 150 µL of Bradford reagent. All samples had an n = 2 ± SD. The plate was incubated at room temperature for 10 minutes before the absorbance was read at 595 nm. Line of best fit y = 0.0003x + 0.0753, R^2 value 0.9559.
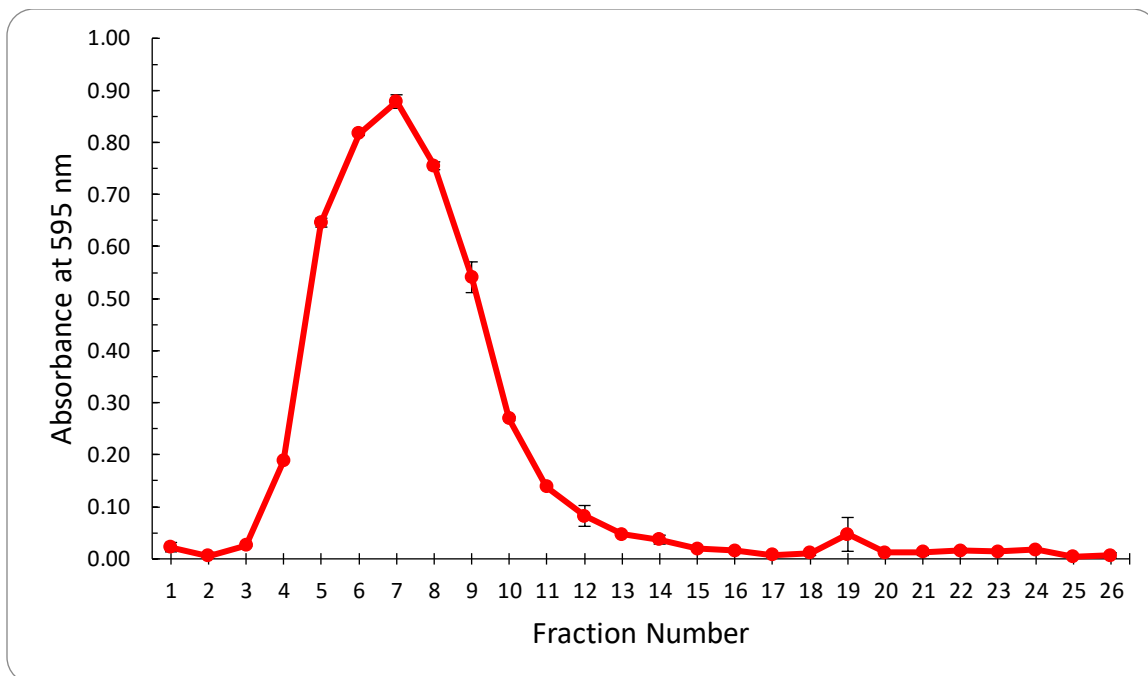
Figure 20: Elution Curve of MBP/BR-1 Fusion Protein. Each fraction collected was approximately 2–3 mL in volume. Five microliters of each sample and dH_2O blanks were mixed with 150 μL of Bradford reagent. All samples had an n = 2 ± SD. The plate was incubated at room temperature for 10 minutes before the absorbance was read at 595 nm. BSA was used to generate a standard curve for calculation of concentrations.

Each fraction's concentration was then calculated and placed into a chart (**Table 4**). Fractions 4–12 were pooled, and protein content determined using a Bradford assay. A BSA standard curve with a line of best fit was plotted to calculate the protein content of the pooled fractions (**Figure 21**). The concentration of the pooled AH3 MBP/BR-1 was calculated to be 2.23 mg/mL. The fusion protein was placed into microfuge tubes in 2-mL aliquots and stored at −20°C.

Table 4: Calculated Concentration of Fusion Protein from BSA Standard Curve			
Fraction Number [a]	**Calculated Concentration (μg/mL)** [b]	**Fraction Number** [a]	**Calculated Concentration (μg/mL)** [b]
1	−174	14	−128
2	−231	15	−184
3	−164	16	−198
4	379	17	−228
5	1,902	18	−211
6	2,476	19	−34
7	2,679	20	−205
8	2,266	21	−205
9	1,552	22	−198
10	649	23	−204
11	209	24	−191
12	26	25	−238
13	−34	26	−231
[a]All samples had an n = 2 ± SD. [b]Concentration of protein calculated from the Bradford Assay Standard Microplate Protocol (Methods 8.1.1).			

Figure 21: Bradford Assay BSA Standard Curve for Pooled Eluate. 125–1,500 µg/mL detection limit. Five microliters of sample and the dH_2O blanks were mixed with 150 µL of Bradford reagent. All samples had an n = 2 ± SD. The plate was incubated at room temperature for 10 minutes before the absorbance was read at 595 nm. Line of best fit y = 0.0003x + 0.0438, R^2 value 0.9615.
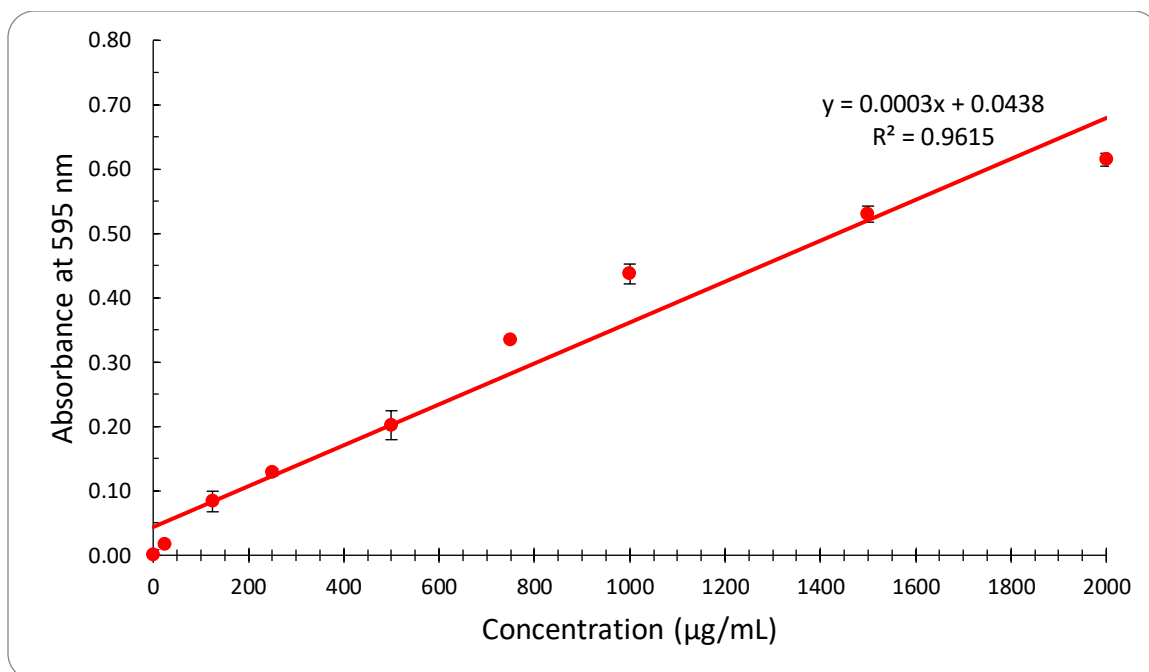
The pooled AH3 MBP/BR-1 fusion protein and Running Buffers 1 (equilibrating and loading sample) and 2 (from washing the column after loading sample) were then analyzed by SDS-PAGE for purity and molecular weight of the protein. Each sample was mixed with an equal volume of 2X Laemmli Sample Buffer and heated at 98°C in a thermocycler for 5 minutes. The samples were then loaded at three different volumes (10, 5, and 3 μL) to determine the best loading volume for subsequent electrophoresis gels. Precast Bio-Rad Criterion TGX gels (18-well comb, 30 μL volume/well, 1.0 mm thick, 8–16% acrylamide gradient) were used to separate the proteins. Twenty mA of current were applied to the gel for 2 hours before staining with Coomassie Brilliant Blue and scanning with a PharosFX bioimager (**Figure 22**). A 10–190 kDa protein ladder was placed into Lanes 1 and 11. Running buffer 1 from equilibrating and loading sample into the chromatography column was placed into Lanes 2, 8, and 14. Running buffer 2 from washing the column after loading sample was placed into Lanes 4, 10, and 16. Minute amounts of fusion protein were visible in Running Buffers 1 and 2 (Lanes 2 and 4). This fusion protein in the wash buffers could have resulted from the total amount of fusion protein being greater than the binding capacity of the amylose resin. Excess fusion protein would have then run off into the running buffer. Clear bands of the AH3 MBP/BR-1 were visible in the Eluate (Lanes 6, 12, and 18). This indicated that the MBP bound to the amylose resin and eluted with the maltose contained in the elution buffer. The 10 μL loading volume displayed a large band of fusion protein with some smearing, while the 5 μL loading volume displayed a more compact yet easily visible band. The 3 μL loading volume displayed a faint band.
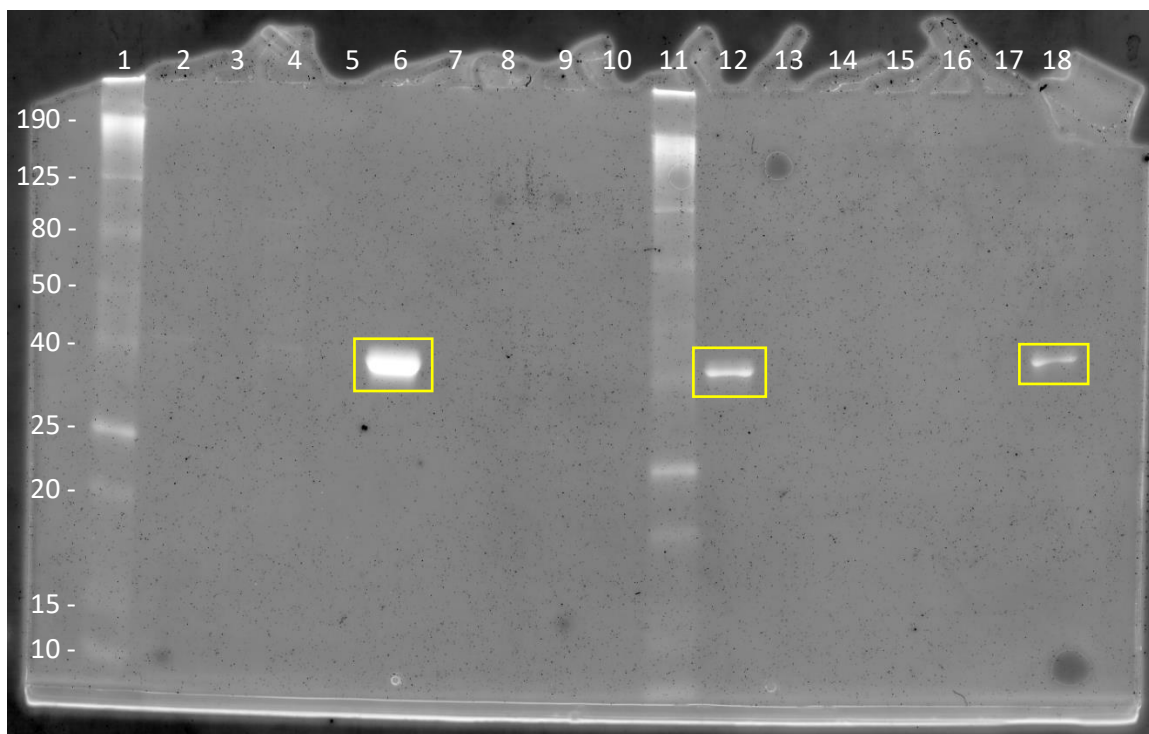
Figure 22: SDS-PAGE of Pooled Eluate Fractions and Running Buffers. Bio-Rad Criterion TGX 8–16% polyacrylamide precast gel. Stained with Coomassie Brilliant Blue. Samples mixed 1:1 with 2X Laemmli Sample Buffer. Ten microliters of ProSieve Color Protein Marker Ladder was placed into Lanes 1 and 11. Samples included running buffer 1 (equilibrating the column and loading sample) and 2 (from washing the column after loading sample), and eluate at three different volumes. Running buffer 1 is found in lanes 2, 8, and 14. Running buffer 2 is found in lanes 4, 10, and 16. MBP/BR-1 fusion protein eluate (AH3 MBP/BR-1 Eluate, MW ≈ 43 kDa) is found in lanes 6, 12, and 18. A 10 µL loading volume was used in Lanes 2, 4, and 6; 5 µL in Lanes 8, 10, and 12; and 3 µL in Lanes 14, 16, and 18. The yellow box indicates the presence of MBP/BR-1 fusion protein.

A pilot protein cleavage was performed using Factor Xa to determine the incubation time needed for maximum cleavage of the BR-1 peptide from MBP. Factor Xa typically cleaves after its preferred Ile-Glu/Asp-Gly-Arg sequence, although it may sometimes cleave after basic residues. Since the BR-1 peptide's amino acid sequence is located after the cleavage site, and the peptide does not contain the cleavage site, Factor Xa should be able to cleave the peptide and remove it from the MBP. After performing a pilot protein cleavage and preparing samples at different time points, two different (5 µL and 3 µL) sample loading volumes were used to determine if the expected MBP/BR-1 and MBP bands would be visible in the gel. Twenty milliamps of current was applied to the gel for two hours before staining with Coomassie Brilliant Blue and scanning with a PharosFX bioimager (**Figure 23**). The fusion protein bands were visible in all sample lanes at each time point, however, there was no distinction between uncut MBP/BR-1 (lanes 2 and 8) and MBP after cleavage. Some protein bands less than 43 kDa in size were visible in the lanes, possibly due to protein degradation while the pooled eluate was in storage at 4°C. The BR-1 peptide has a calculate molecular weight of 764 Da. No BR-1 peptide band was visible near the bottom of the gel in any of the reaction mixture lanes. The lack of peptide bands could be contributed to BR-1's small size and the gel's resolution of proteins 2 kDa or greater in size.

Figure 23: SDS-PAGE of Pilot MBP/BR-1 Fusion Protein Cleavage. Bio-Rad Criterion TGX 8–16% polyacrylamide precast gel. Stained with Coomassie Brilliant Blue. Samples mixed 1:1 with 2X Laemmli Sample Buffer. Ten microliters of ProSieve Color Protein Marker Ladder was placed into Lanes 1 and 7. A 5 μL loading volume was used in Lanes 2–6, 3 μL in Lanes 8–12. Lanes 2 and 8: 0 hr (control, no protease). Lanes 3 and 9: 2 hr cleavage mixture. Lanes 4 and 10: 4 hr cleavage mixture. Lanes 5 and 11: 8 hr cleavage mixture. Lanes 6 and 12: 24 hr cleavage mixture. The yellow box indicates the presence of either MBP/BR-1 fusion protein (MW ≈ 43.2 kDa) or MBP (MW ≈ 42.5 kDa).

The gel was de-stained to remove as much Coomassie Brilliant Blue as possible before staining with SYPRO Ruby to obtain a higher sensitivity for protein detection and a greater resolution of the protein bands (Bio-Rad Laboratories n.d.). The gel was scanned again using the PharoxFX bioimager (**Figure 24**). The expected BR-1 peptide band was still absent after staining the gel with SYPRO Ruby. Many more protein bands were now visible in every sample lane, indicating that there could be protein degradation occurring during storage of the AH3 MBP/BR-1 fusion protein. The lack of a 764 Da protein band could be due to the Factor Xa protease losing enzyme activity. Upon examining the Factor Xa microfuge tube, it was observed that the protease had already been expired for one year. New protease was ordered and used in a second pilot protein cleavage experiment.
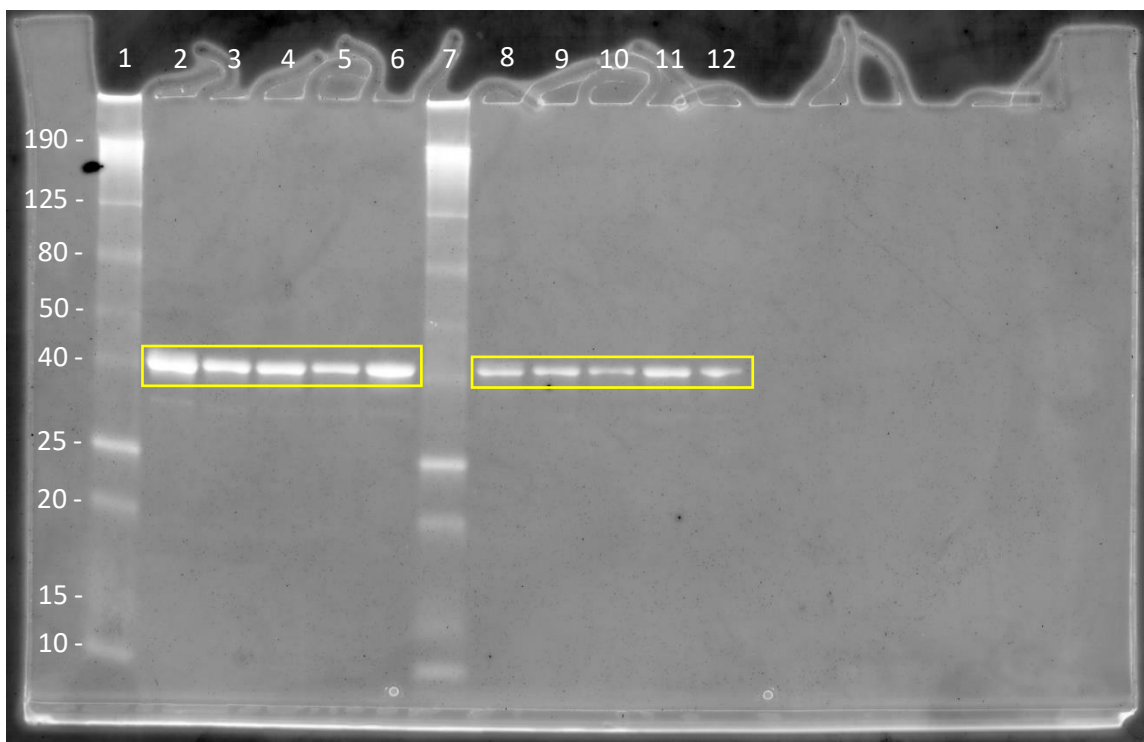
Figure 24: SDS-PAGE of Pilot MBP/BR-1 Fusion Protein Cleavage. Bio-Rad Criterion TGX 8–16% polyacrylamide precast gel from Figure 23 stained with SYPRO Ruby. Samples mixed 1:1 with 2X Laemmli Sample Buffer. Ten microliters of ProSieve Color Protein Marker Ladder was placed into Lanes 1 and 7. A 5 μL loading volume was used in Lanes 2–6, 3 μL in Lanes 8–12. Lanes 2 and 8: 0 hr (control, no protease). Lanes 3 and 9: 2 hr cleavage mixture. Lanes 4 and 10: 4 hr cleavage mixture. Lanes 5 and 11: 8 hr cleavage mixture. Lanes 6 and 12: 24 hr cleavage mixture. The yellow box indicates the presence of either MBP/BR-1 fusion protein (MW ≈ 43.2 kDa) or MBP (MW ≈ 42.5 kDa).

Digestion with the new Factor Xa is shown in **Figure 25**. The samples were prepared as above and 3 µL of each were loaded into another Bio-Rad Criterion TGX 8–16% acrylamide gradient gel. Twenty milliamps of current was applied to the gel for two hours before staining with SYPRO Ruby and scanning with a PharosFX bioimager. The previously observed bands from protein degradation were no longer visible, indicating that the new Factor Xa protease did not produce nonspecific cleavage of the AH3 MBP/BR-1 fusion protein. The fusion protein bands were defined, although there was still no distinction between the MBP/BR-1 fusion protein and MBP after cleavage. No BR-1 peptide bands were visible at the bottom of the gel.
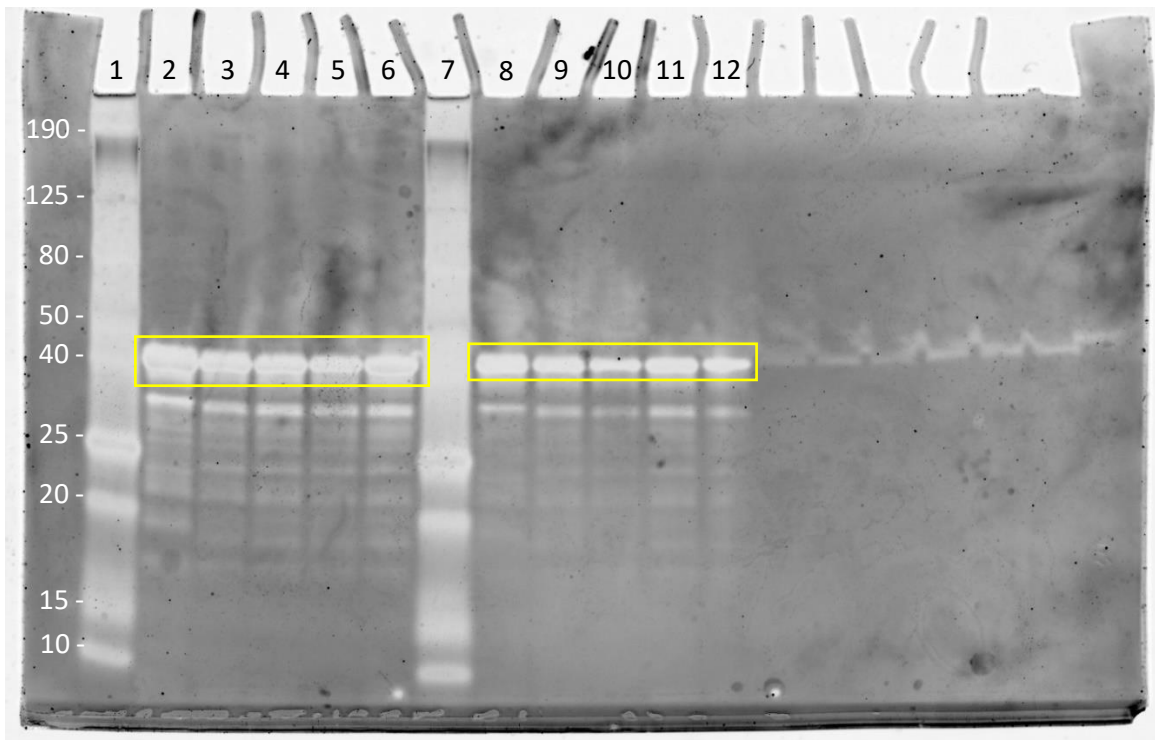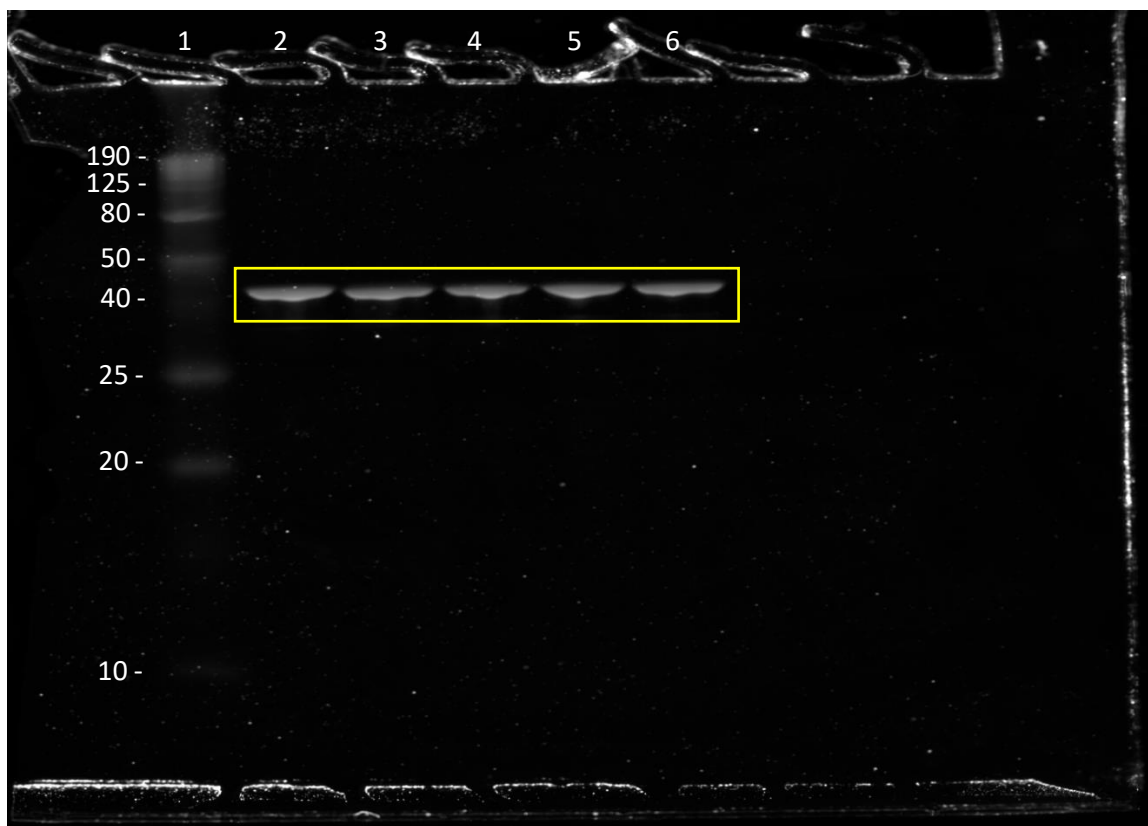
Figure 25: SDS-PAGE of Pilot MBP/BR-1 Fusion Protein Cleavage, New Protease. Bio-Rad Criterion TGX 8–16% polyacrylamide precast gel. Stained with SYPRO Ruby. Samples mixed 1:1 with 2X Laemmli Sample Buffer. Ten microliters of ProSieve Color Protein Marker Ladder was placed into Lane 1. A 3 µL loading volume was used in Lanes 2–6. Lane 2: 0 hr (control, no protease). Lane 3: 2 hr cleavage mixture. Lane 4: 4 hr cleavage mixture. Lane 5: 8 hr cleavage mixture. Lane 6: 24 hr cleavage mixture. The yellow box indicates the presence of either MBP/BR-1 fusion protein (MW ≈ 43.2 kDa) or MBP (MW ≈ 42.5 kDa).

The AH3 MBP/BR-1 fusion protein was dialyzed against 20 volumes of 20 mM Tris-HCl and 6 M guanidine hydrochloride, pH 7.4 dialysis buffer solution for 24 hours to increase access to the cleavage site for the protease by denaturing the fusion protein. Denaturing should have removed any protein folding and linearize the protein, as suggested by the pMAL-c5X expression vector's instruction manual (New England BioLabs 2011). After dialysis of the AH3 MBP/BR-1 fusion protein, a pilot cleavage with the new protease was repeated. To increase visualization of the protein bands, a Bio-Rad Criterion Tris-Tricine Precast Protein Gel (16.5% polyacrylamide) with a resolution of at least 1 kDa was used. The samples were prepared as above, with the addition of 5% β-mercaptoethanol in the Laemmli sample buffer to break disulfide bonds and separate Factor Xa into 27.7 kDa and 15.7 kDa subunits, before loading 10 μL of each into the lane. Factor Xa has a total molecular weight of 42.3 kDa while the MBP has a molecular weight of 42.5 kDa. (New England BioLabs 2011). The 10 μL loading volume was used to increase the possible amount of BR-1 peptide that would be present at the bottom of the gel. Forty milliamps of current was applied to the gel for four hours to speed up electrophoresis (due to a higher 16.5% polyacrylamide density since there is no 8−16% polyacrylamide gradient) before staining with SYPRO Ruby and scanning with a PharosFX bioimager (**Figure 26**). Enhancing the contrast of the scanned image showed that many nonspecific protein bands were visible alongside the MBP/BR-1 fusion protein (yellow box) and protein ladder bands. In addition, a possible BR-1 peptide band was faintly visible at the bottom of the gel (red box).
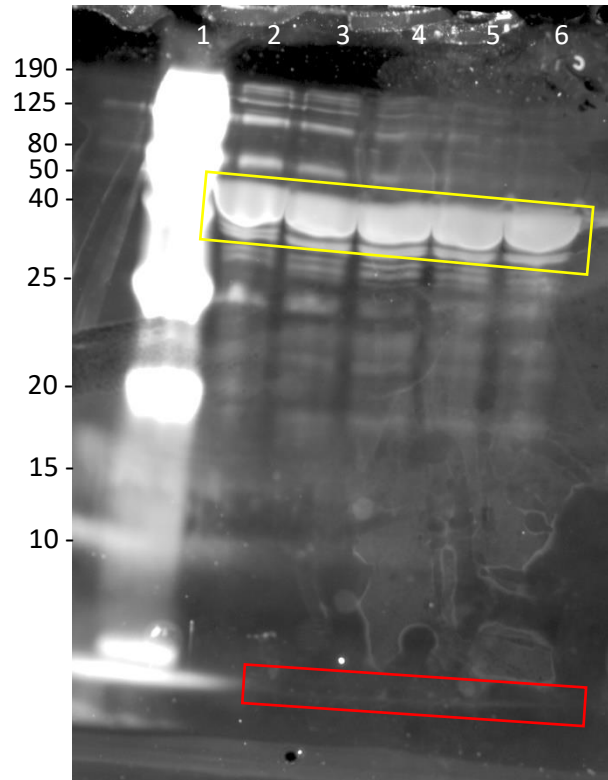
Figure 26: SDS-PAGE of Pilot MBP/BR-1 Fusion Protein Cleavage, New Protease and Dialyzed Fusion Protein. Bio-Rad Criterion Tris-Tricine 16.5% polyacrylamide precast gel. Stained with SYPRO Ruby. Samples mixed 1:1 with 2X Laemmli Sample Buffer + 5% β-mercaptoethanol (Lanes 2–6). Ten microliters of ProSieve Color Protein Marker Ladder was placed into Lane 1. A 5 μL loading volume was used in Lanes 2–6. Lane 1: 0 hr (control, no protease). Lane 3: 2 hr cleavage mixture. Lane 4: 4 hr cleavage mixture. Lane 5: 8 hr cleavage mixture. Lane 6: 24 hr cleavage mixture. The yellow box indicates the presence of either MBP/BR-1 fusion protein (MW ≈ 43.2 kDa) or MBP (MW ≈ 42.5 kDa). The red box indicates a faint line where the BR-1 peptide (MW ≈ 764 Da) could be.

Measuring absorbance of peptide in gel samples would require cutting out bands that might contain SPYRO Ruby dye. To determine if the dye would affect light absorbance used to measure protein concentration, several solutions of PBS containing SYPRO Ruby were prepared and analyzed by UV-Vis (PBS blank). The UV-Vis absorption spectra for the PBS + SYPRO Ruby samples are shown in (**Figure 27)**. SYPRO Ruby generates an absorption spectrum that would interfere with NanoDrop One readings when detecting peptide concentration. The PBS + 0.1% SYPRO Ruby sample had a peak absorption of 0.498 at 190 nm, whereas PBS + 1% SYPRO Ruby and PBS + 5% SYPRO Ruby samples had peak absorptions of 0.937 at 195.5 nm and 3.720 at 196.5 nm, respectively.
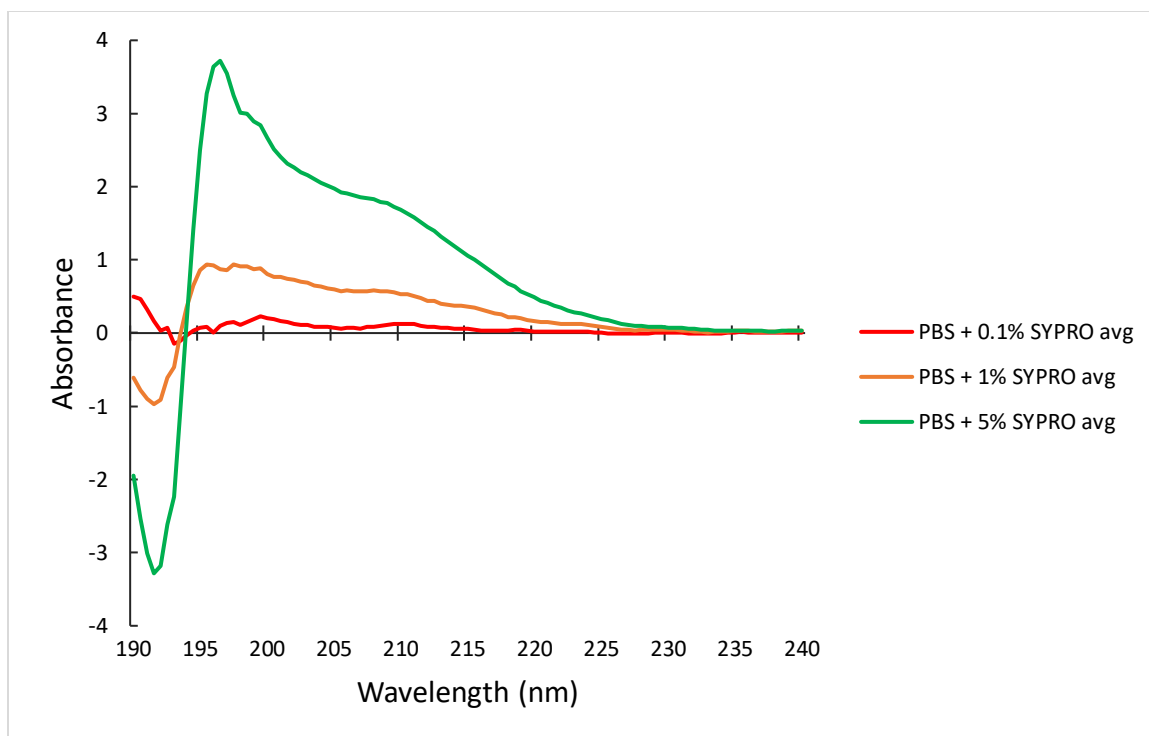
Figure 27: UV-Vis SYPRO Ruby Effects Spectrum. Different solutions of PBS containing 0.1%, 1%, and 5% SYPRO Ruby dye. All samples had an n = 3 ± SEM. Absorbances were measured on a NanoDrop One by UV-Vis from 190–850 nm using PBS as the blanking solution. The 190–240 nm absorption spectra of the averaged sample values are shown.

To determine whether the cleaved BR-1 peptide was present in the SDS-PAGE gels after protein cleavage, another pilot protein cleavage was performed, and the gel was run with no dye (Coomassie or SPYRO Ruby) added. A 0-hour (control) protein cleavage mixture (30 μg MBP/BR-1 in 20 mM Tris-HCl, 200 mM NaCl, 1 mM EDTA Column Buffer + no protease) and a 24-hour protein cleavage mixture (30 μg MBP/BR-1 + 0.3 μg Factor Xa protease in Column Buffer) were added 1:1 to 2X Laemmli Sample Buffer. The samples were heated to 98°C for 5 minutes before loading onto an 8–16% acrylamide gradient SDS-PAGE gel. The gel was electrophoresed and the area that should contain BR-1 peptide and Laemmli sample buffer dye was excised. Bands containing Laemmli sample buffer dye, but no BR-1 peptide, and gel portions with no proteins or dye were excised and incubated in PBS overnight. All the samples were syringe filtered and their absorbances measured on a NanoDrop One by UV-Vis from 190–850 nm wavelength with PBS as a blank. The absorption spectra are shown in **Figure 28**. The SDS-PAGE peptide plus dye bands had a peak absorbance of 12.391 ± 0.151 SEM at 204 nm and an absorption of 4.716 ± 0.027 SEM at 214 nm. The control bands (dye with no peptide) had a peak absorbance of 12.674 ± 0.100 SEM at 201.5 nm and an absorption of 4.844 ± 0.041 SEM at 214 nm. The gel background (gel alone) had a peak absorbance of 13.184 ± 0.122 SEM at 203 nm and an absorption of 5.140 ± 0.027 SEM at 214 nm.
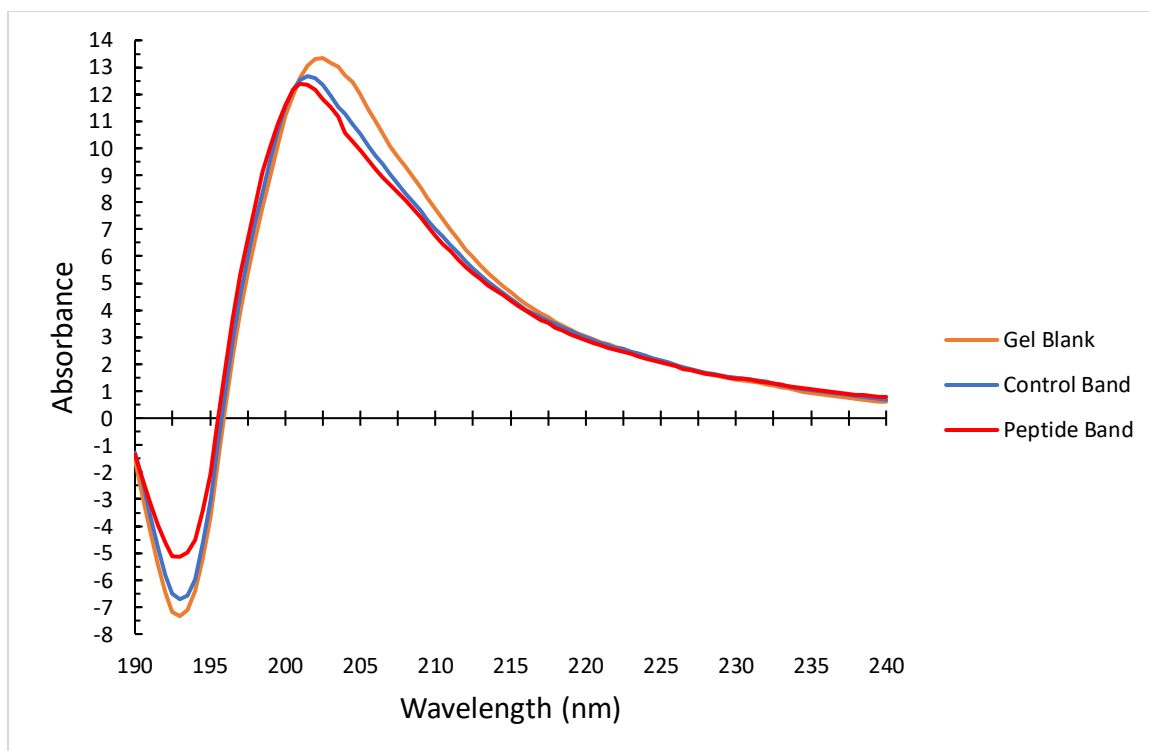
Figure 28: UV-Vis SDS-PAGE Peptide Detection, Peptide Bands Spectra. The bands that were thought to contain BR-1 peptide (and loading dye) were excised from an SDS-PAGE gel, incubated in 600 μL PBS overnight at 4°C, and filtered with a 0.22 μm PES syringe filter. The same was done to a control portion of gel that contained no proteins (but contained loading dye = control band) and a portion of gel without loading dye (gel blank). All samples had an n = 5 ± SEM. Absorbances were measured on a NanoDrop One by UV-Vis from 190–850 nm using PBS as the blanking solution. The 190–240 nm absorption spectra of the averaged sample values are shown.

The gel background absorbances were subtracted from the peptide bands and control bands absorbances to give the spectra minus gel background effects shown in **Figure 29**. The peptide band had a new peak absorbance of 2.200 at 193 nm and an absorption of −0.401 at 214 nm. The control band had a new peak absorbance of 0.673 at 192.5 nm and an absorption of −0.296 at 214 nm. The control bands absorbances were also subtracted from the peptide bands absorbances to give the spectra minus control bands and any effects caused by the Laemmli sample buffer dye (**Figure 30**). The peptide bands had a final peak absorbance of 1.584 at 193.5 nm and an absorption of −0.105 at 214 nm.
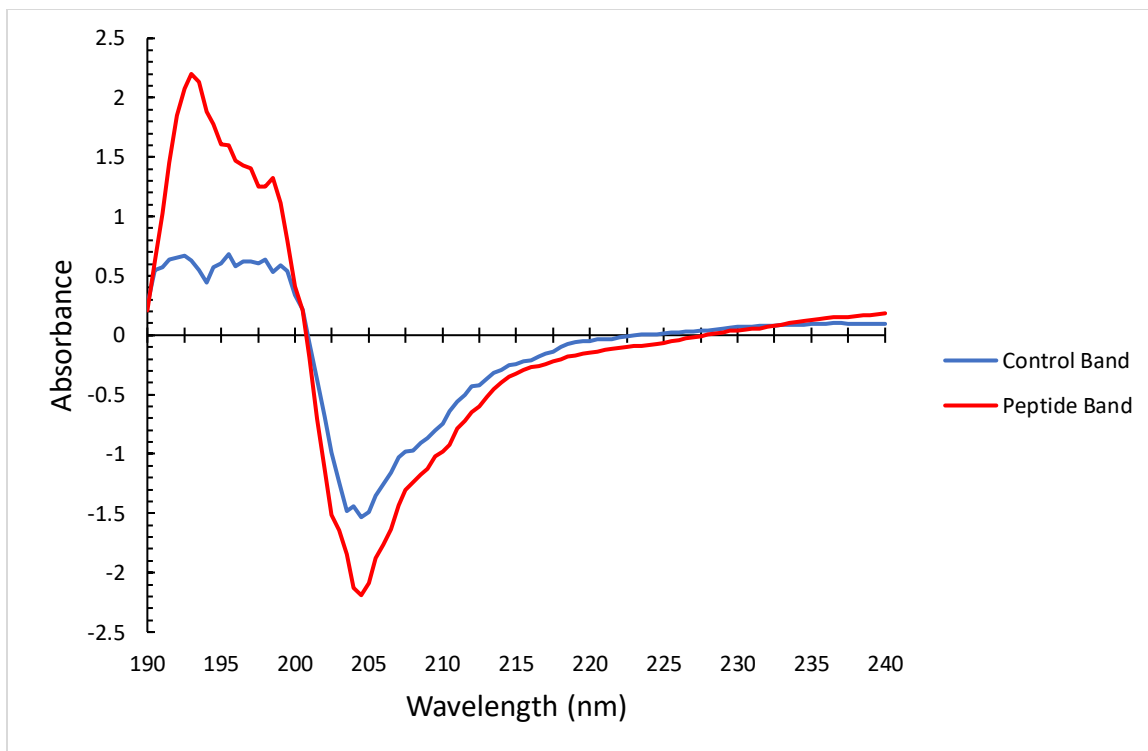
Figure 29: UV-Vis SDS-PAGE Peptide Detection, Peptide Band Spectra, minus gel background. Peptide band = peptide in gel containing loading dye. Control band = gel containing loading dye but no peptide. Gel background = section of dye with no dye or peptide. This data is from Figure 28 with the gel background absorbance subtracted.
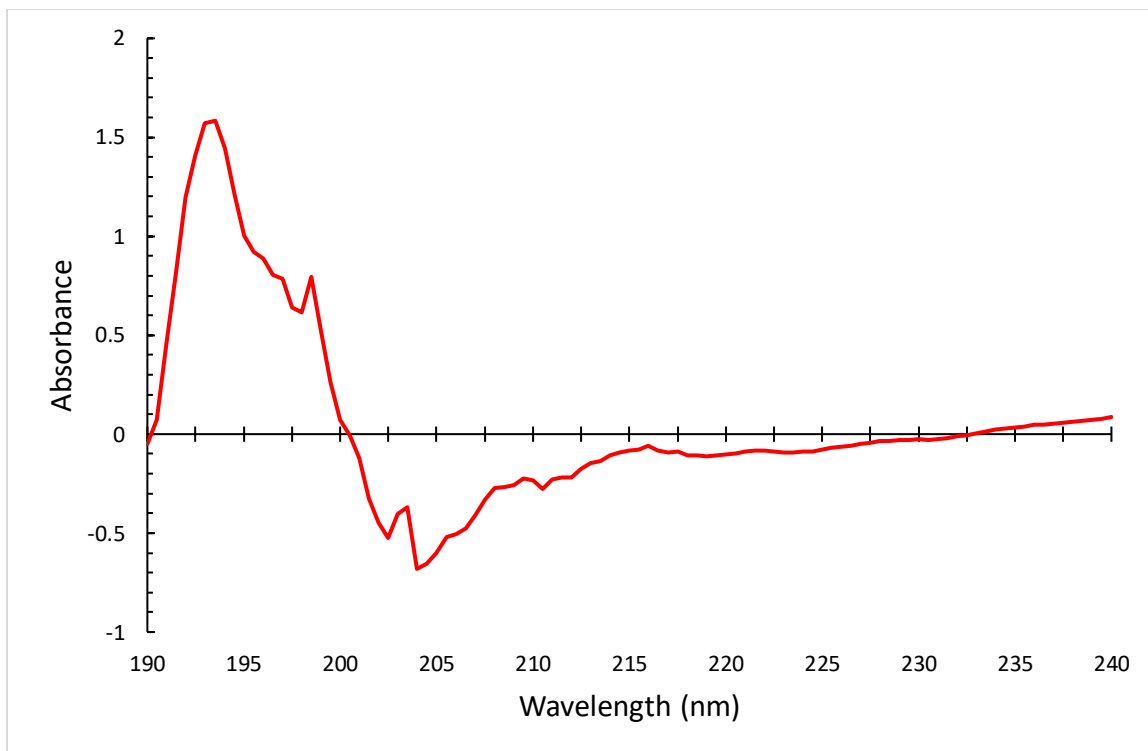
Figure 30: UV-Vis SDS-PAGE Peptide Detection, Peptide Bands Spectra, minus gel background and control band. Peptide band = peptide in gel containing loading dye. Control band = gel containing loading dye but no peptide. Gel background = section of dye with no dye or peptide. This data is from Figure 28 with both the gel background and control band absorbances subtracted.

Several dilutions of BR-1 peptide were prepared in PBS and analyzed by UV-Vis (PBS blank) in order to generate a standard curve for calculation of BR-1 peptide concentration from the protein cleavage SDS-PAGE gel. The UV-Vis absorption spectra for the BR-1 peptide in PBS samples are shown below (**Figure 31**). The absorbance values of the BR-1 peptide increased as the concentration of peptide increased. The peak absorbances and wavelength for each BR-1 peptide sample were as follows: 1 µg/mL BR-1, 2.021 ± 0.045 SEM at 191 nm; 10 µg/mL BR-1, 1.792 ± 0.104 SEM at 191 nm; 25 µg/mL BR-1, 0.500 ± 0.017 SEM at 200.5 nm; 50 µg/mL BR-1, 0.944 ± 0.014 SEM at 202 nm; 75 µg/mL BR-1, 1.415 ± 0.025 SEM at 200.5 nm; and 100 µg/mL BR-1, 1.881 ± 0.013 SEM at 202 nm.
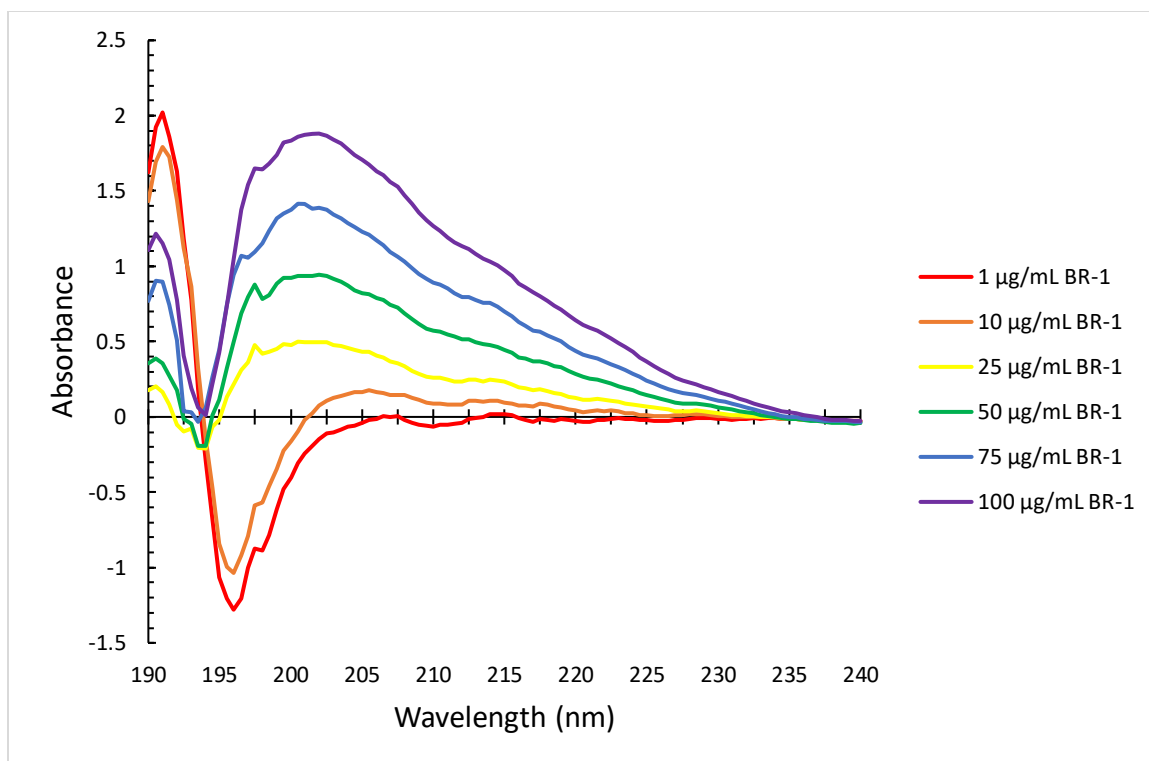
Figure 31: UV-Vis BR-1 Standards Spectra. Different solutions of PBS containing 1, 10, 25, 50, 75, and 100 µg/mL BR-1 peptide. All samples had an n = 5 ± SEM. Absorbances were measured on a NanoDrop One by UV-Vis from 190–850 nm using PBS as the blanking solution. The 190–240 nm absorption spectra of the averaged sample values are shown.

The BR-1 peptide samples' absorbances at 214 nm were graphed to create a standard curve in order to calculate the concentration of BR-1 peptide contained in the SDS-PAGE peptide sample (**Figure 32)**. The absorbances at 214 nm for each BR-1 peptide sample were as follows: 1 µg/mL BR-1, 0.015 ± 0.014 SEM; 10 µg/mL BR-1, 0.110 ± 0.009 SEM; 25 µg/mL BR-1, 0.248 ± 0.013 SEM; 50 µg/mL, 0.477 ± 0.0064 SEM; 75 µg/mL, 0.756 ± 0.012 SEM; and 100 µg/mL BR-1, 1.034 ± 0.0067 SEM. The line of best fit had an equation of $y = 0.0102x - 0.0033$ with a strong R^2 value of 0.9982. The concentration of BR-1 peptide was unable to be calculated since the peptide sample from the peptide detection in a gel (**Figure 30)** had an absorption of –0.105 at 214 nm which was outside the detection limits of the BR-1 standard curve.
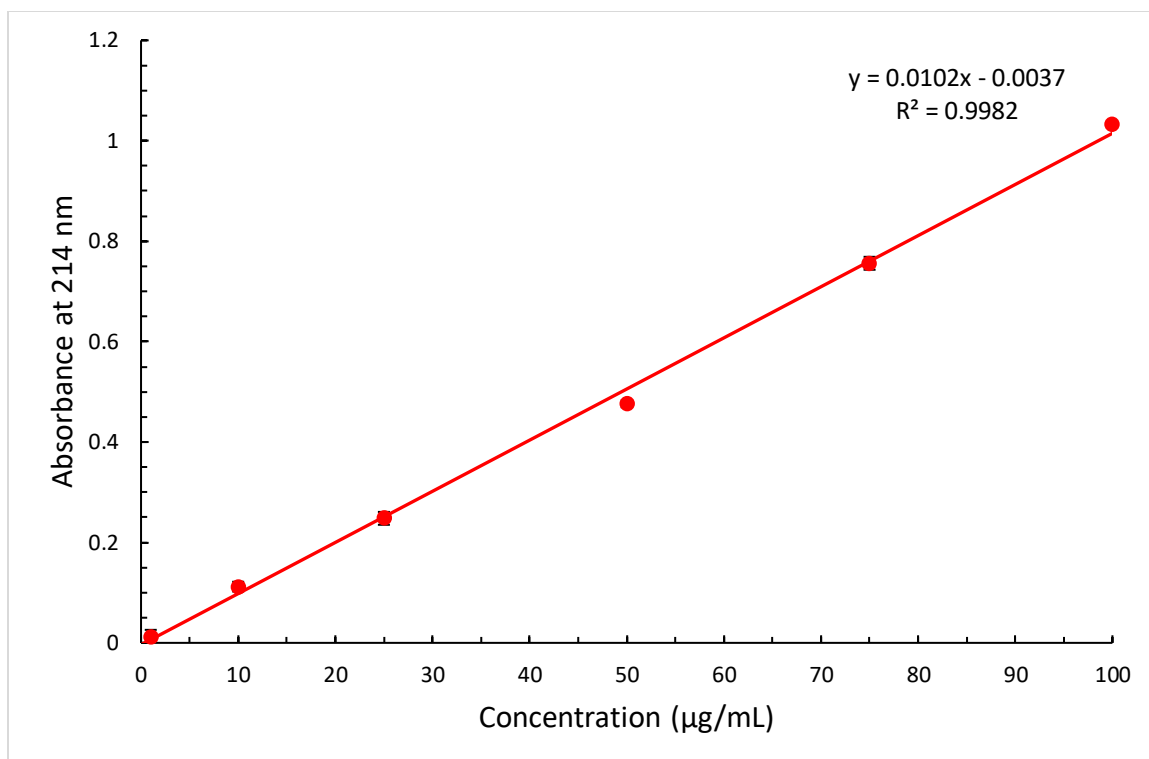
Figure 32: UV-Vis Absorbance at 214 nm for BR-1 Standard Curve. where different solutions of PBS containing 1 μg/mL, 10 μg/mL, 25 μg/mL, 50 μg/mL, 75 μg/mL, and 100 μg/mL BR-1 peptide. All samples had an n = 5 ± SEM. Absorbances were measured on a NanoDrop One by UV-Vis at 214 nm using PBS as the blanking solution. Line of best fit y = 0.0102x - 0.0037, R^2 value 0.9982.

E. Discussion

Biosensors have been extensively researched to diagnose illnesses, monitor patient health and disease markers, and detect environmental and/or food contaminants that could cause harm (as reviewed in Yang et al. 2015). Current research in the development of biosensors have traditionally used hybridoma technology to produce large antibodies which are specific for virtually any target of interest. However, those proteins may have shorter half-lives compared to smaller peptides and are more expensive and time-consuming to produce when compared to phage display (Elgundi et al. 2017; as reviewed in Nagaraju et al. 2015). Phage technology can produce smaller antibody fragments or peptides that retain antibody-like affinities and specificities for their targets of interest. Phage display is much quicker, cost-effective, and reduces or even eliminates safety issues and immune responses caused by using animal-sourced proteins in humans (Hey 2017). A novel peptide that is highly specific, smaller in size, more durable, and less expensive to produce is needed for incorporation into a blood biosensor that can detect injury in military and law enforcement personnel. Identification and production of a peptide that is specific for HSA will facilitate the development of a blood biosensor that uses functionalized carbon nanotube-coated threads which will be woven into a textile fabric.

In this project, a peptide that bound to human serum albumin (HSA) and was discovered using phage display technology (Rees 2016) was evaluated for specificity to HSA. The peptide BR-1 is displayed on the pIII minor coat protein of M13 filamentous phage clone HSA-6 (from the Ph.D.-7 phage display library; New England BioLabs 2016). The phage DNA was sequenced, and the corresponding peptide was purchased

from GenScript (Piscataway, NJ). Biotinylation of the peptide and enzyme-linked immunosorbent assays (ELISAs) were optimized by Sheila Sang (Sang 2014). A pMAL-c5X expression vector was created by Alexander Huber and Dr. Jonathan Caguiat (Huber 2019). Gel electrophoresis and UV-Vis spectrophotometry were used in this thesis to further evaluate BR-1 specificity for HSA and the peptide's viability in a protein production and purification process. The findings of this thesis suggest that biotinylated BR-1 peptide binds specifically to HSA as demonstrated in inhibition ELISA assays (**Figures 9–13**). The findings also confirmed that the BR-1 peptide can be produced and purified as a fusion protein via the pMAL-c5X vector (**Figures 20, 22**), yet protein cleavage techniques and purification of the resulting peptide still need to be developed (**Figures 23–25, 29**). Thus, the first hypothesis of this thesis: 1) the BR-1 peptide will be found to bind to HSA with high specificity, has been supported by the data. The second hypothesis: 2) that the BR-1 peptide can be produced through use of the pMAL-c5X expression vector, has been partially satisfied, as the fusion protein has been produced, but more work is needed to produce pure peptide. We have not yet produced the pure peptide to accomplish the third hypothesis: 3) that the BR-1 can be attached to functionalized SWCNTs and tested for preferential binding to HSA over other substances.

The phage display library and techniques used in this project have been used successfully by other laboratories. Wu et al. utilized phage display and a New England BioLabs Ph.D.-12 M13 phage library to find a series of peptides which bound to alanine aminotransferase (ALT; Wu et al. 2011). ALT in blood is an indicator for liver damage and the "gold standard" biomarker for hepatotoxicity. Phage clones selected in this study

were tested by indirect enzyme-linked immunosorbent assay (ELISA) very similar to the one used in our study. ALT5-8 clones were found to have a dose-dependent affinity for ALT, characterized for binding kinetics, and incorporated into a biosensor. The biosensor was tested using electrical impedance spectroscopy (EIS) in which ALT, streptavidin, and BSA were used to study the selectivity of the peptide. Although some nonspecific binding of the streptavidin and BSA was observed, ALT bound strongly to the biosensor with nanomolar affinity (Kd = 20.1±0.6 nM) and a limit of detection of 92 ng/mL. Wu et al. successfully used phage display and ELISAs to select and test specificity of a peptide toward a target and incorporated the peptide into a biosensor.

The development of a biosensor for HSA has been pursued by other laboratories. Shim and coworkers developed a simple HSA biosensor utilizing cotton yarn dip coated in polyelectrolyte solutions of either Nafion-ethanol or poly(sodium 4-styrene sulfonate) (PSS) containing SWCNTs and MWCNTs (Shim et al. 2008). The coated yarn was then functionalized using an IgG antibody that was specific for HSA. The cotton thread gained the ability to conduct electrical signals with a resistivity as low as 20 Ω/cm. where the Nafion-stabilized CNTs were two orders of magnitude more conductive than the PSS-stabilized CNTs. The adsorbed nanotubes seamlessly covered the cotton yarn, with the smaller SWCNTs creating a tighter network than the MWCNTs. The coated yarn exhibited strength that was at least twice as strong as the original cotton thread while retaining flexibility and softness, qualities which are desirable for incorporation into a wearable biosensor. Upon exposure of PSS-stabilized SWCNTs with anti-HSA IgG to solutions of HSA and BSA, the functionalized yarn was able to sensitively and selectively bind HSA in concentrations as low as 119 nM with a signal drop of 2,980 Ω

compared to baseline while concentrations of BSA as high as 30 µM only produced a

maximum signal drop of 1,100 Ω from baseline.

These methods of producing an HSA biosensor are like the process developed by

Dr. Pedro Cortes and performed by Amy Olszewski (Cortes et al. 2013; Olszewski 2013).

In these studies, the sequence of a peptide demonstrated to be specific for HAS, a protein

in human blood, by Adams et al (1989) and Pingali et al (1996), The peptide chain had

been selected based on panning results obtained by Pingali et al. where they found a

peptide with sequence CAQCHTVEK that bound to albumins. Pingali et al. synthesized a

peptide analog to remove the cysteine residues and simplify immobilization of the

peptide during high-performance affinity chromatography, resulting in a sequence of

GAQGHTVEK. The GK-1 peptide (GAQGHTVEK) was purchased from NEO Biolabs

(Cambridge, MA) and used as the specific binding element towards HSA in the

development of a biosensor. The peptide was attached to carboxylated MWCNTs through

EDC cross-linking and the MWCNT-peptide complex was coated onto cotton threads

through a dipping process. The resulting semi-conductive threads were successfully

evaluated for binding to HSA by measuring their changes in electrical resistance when

exposed to different liquid media and analytes such as coffee, a sweat surrogate, and

apple juice. The thread-CNT-peptide apparatus was demonstrated to show increased

resistance upon binding to HSA over other substances (Cortes et al. 2013; Olszewski

2013; Shim et al. 2008). GK-1 was shown to bind with specificity to HSA over several

other solutions and analytes by ELISA.

To produce a novel peptide that could be used in a patented product, phage

display has been used in this laboratory to select for phage clones displaying peptides that

bind specifically to human serum albumin (HSA; Huber 2019; Rees 2016; Sang 2014).

The Ph.D.-7 phage display library from New England Biolabs utilizes a filamentous M13

phage vector, M13KE, which displays five copies of a seven-amino acid peptide fused on

the amino terminus of the pIII minor coat protein. Since the peptide is short in length, it

does not affect infectivity of the phage and thus allows the phage genome to contain one

copy of a fusion pIII gene. The library has a clone diversity of 10^9 individual clones

where the heptamer is attached to the amino terminus of pIII by a short Gly-Gly-Gly-Ser

linker. The M13KE phage is a coliphage specific for male bacteria that have an F

plasmid. The *E. coli* strain ER2738 (F' *proA$^+$B$^+$ lacI^q Δ(lacZ) M15 zzf::Tn10(Tet^R)/fhuA2

glnV Δ(lac proAB) thi-1 Δ(hsdS-mcrB)5*) that comes in the Ph.D.-7 phage display kit is an

F+ strain that grows quickly and contains a transposon encoding for tetracycline

antibiotic resistance, resulting in all bacteria grown in tetracycline to be F$^+$. The F

plasmid encodes for the sex pilus used between bacteria for conjugation. The M13 phage

takes advantage of this sex pilus by binding to it with the pIII minor coat protein. Plating

the ER2738 strain on Luria-Bertani (LB) plates with tetracycline or growing them in LB

broth with tetracycline allows selective growth of the F+ bacteria for use in phage display

(New England BioLabs 2016).

Sheila Sang screened the Ph.D.-7 phage display library from New England

BioLabs using surface panning to select for HSA-specific phage (Sang 2014), isolating

eight clones (designated HSA-1 through HSA-8) after performing three rounds of

panning. Sang used this pool of phage clones to develop an indirect ELISA assay with

horseradish peroxidase (HRP) conjugated to anti-M13 antibody and using 3,3',5,5'-

tetramethylbenzidine (TMB) colorimetric substrate. The best results for the indirect M13

ELISA assay were obtained by using polyvinyl chloride plates with a casein block.

William Rees also used the Ph.D.-7 phage display library and surface panning to select for HSA-specific phage, isolating ten clones (designated HSA-1 through HSA-10) after performing three rounds of panning, without amplification after the first two rounds (Rees 2016). Rees performed indirect M13 ELISA assays and determined that HSA-6 had the highest binding to HSA. HSA-6 was selected for DNA purification and sequencing. The sequence from phage clone 6 was used for peptide synthesis (GenScript, Piscataway, NJ) and further analysis. The synthesized peptide ANHHQAS, designated BR-1, was biotinylated (renamed B-BR-1) and its affinity for HSA was confirmed using indirect M13 ELISA assays with streptavidin-HRP and TMB colorimetric substrate. Rees tested B-BR-1 against other albumin homologs such as bovine serum albumin (BSA), chicken serum albumin (CSA), chicken egg white albumin/ovalbumin (OVA), and rabbit serum albumin (RbSA). BR BR-1 displayed preferential binding to HSA over OVA and BSA but similar binding to HSA, CSA, and RbSA. Rees also tested B-BR-1 against other solutions of urine, sweat, coffee, and whole blood. B-BR-1 displayed significant binding to HSA compared to all other solutions, yet it did not bind to whole blood. The lack of binding to human blood was unexpected, as HSA is the protein in the highest concentration in human blood. These studies need to be repeated and the lack of binding to human blood resolved prior to producing a sensor for human blood.

Alexander Huber performed ELISAs to further test the specificity of B-BR-1 for HSA (Huber 2019). He performed multiple competitive inhibition ELISAs and, upon encountering unusually negative results, began troubleshooting the use of reagents and the amount of biotin that had been incorporated onto the peptide. Huber and Pham used

different block, wash, and sample buffers in addition to microtiter plates of several types of plastics until the ELISAs had been optimized. Huber and Pham also conducted a biotin incorporation assay on all biotinylated BR-1 peptide samples to determine which sample had the highest amount of biotin. It was concluded that all samples had relatively low amounts of biotin, so the sample with the highest amount was used for subsequent ELISAs.

Although the amount of biotin incorporated into the various BR-1 peptide samples tested in this study was low (**Table 1**), the peptides were able to bind to avidin when used in assays (**Figures 9–13**). The low incorporation of biotin could be attributed to degradation of the peptide during storage, so the BR-1 peptide may need to be replaced in the future. Biotinylation of a polypeptide is used with enzyme-conjugated avidin to aid in protein detection and purification. Biotin's smaller size in comparison to globular proteins (which minimizes interference with the protein of interest), a valeric acid side change that allows easy derivatization and conjugation to other chemical structures, and strong interaction with avidin make it desirable as a protein label. Avidin binds with high affinity to biotin. The enzyme conjugated to the avidin can then be used to produce a color change that indicates peptide binding. Biotinylation typically occurs by chemical means where a spacer arm can be used to further decrease any possible steric hindrance from the biotin molecule. Solubility of the protein of interest can be increased when uncharged reactive groups are present. Additionally, biotinylating with a spacer arm can also prevent aggregation of the biotinylated protein when stored for long periods of time (Thermo Fisher Scientific Biotinylation).

A possible confounding factor of this project's biotinylation process is the

mechanism through which biotin is conjugated to the BR-1 peptide. The BR-1 peptide is fused via its carboxy terminus and a Gly-Gly-Gly-Ser linker arm to the amino terminus of the pIII minor coat protein of the HSA-6 phage that had been selected through William Rees' biopanning procedure (New England BioLabs 2016; Rees 2016). The amino terminus of the peptide is thus exposed when the peptide-pIII fusion binds to its target molecule. When biotin is attached to BR-1 using Biotin Hydrazide and EDC chemistry, the carboxy terminus of the peptide is similarly fused via a PEG4 linker arm to the hydrazide group of the EDC molecule (Thermo Fisher Scientific 2011 EZ-Link, **Figure 4**). When the BR-1 peptide is attached to carboxylated SWCNTs via EDC chemistry without a linker arm in the future, however, the amino terminus of the peptide will be fused and the carboxy terminus will be exposed. Although the reversal of BR-1 may not result in significant changes to its ability to bind to HSA, the difference in attachment of the peptide may result in steric hindrance that could cause differences in binding to the HSA target. Thus, further testing of the peptide with an amino terminus fusion and in the absence of a linker arm should be performed to more thoroughly evaluate BR-1 as a candidate for blood biosensor production.

Enzyme-linked immunosorbent assays (ELISAs) are evaluative procedures which utilize a target bound to a plate, and a ligand covalently bound to an enzyme that catalyzes the conversion of a colorimetric, fluorescent, or chemiluminescent substrate. Several ELISA assays have been developed and widely used, including indirect and competitive ELISAs. An indirect ELISA assay measures the concentration of a primary detection agent and requires an antigen and secondary detection agent that is conjugated to an enzyme. A microtiter well is first coated with the target antigen followed by the

addition of the primary detection agent to be measured. The primary agent binds to the antigen and the unbound agent is washed away. A secondary detection agent (specific for the primary agent) conjugated to an enzyme is then added to the well to bind to the primary agent. The excess secondary agent-enzyme conjugate is likewise washed away before the enzyme substrate is added to produce a reaction. The concentration of product (colored, fluorescent, or luminescent) formed by its reaction with the enzyme is then determined by using a plate reader, and the concentration of product is thus inferred to be the same as the concentration of primary agent bound (Owen et al. 2013).

The peptide and phage ELISAs used in this thesis were both indirect ELISAs measuring binding of the biotinylated BR-1 peptide and HSA-6 phage to HSA (Fi**gures 8–14**). Although the blocking, washing, and sample buffers were different for the two assays, due to working with a peptide versus working with a phage, these ELISAs both had the HSA target bound to the plate using sodium carbonate buffer. The B-BR-1 peptide and HSA-6 phage acted as the primary detection agent while streptavidin-horseradish peroxidase and anti-M13-horseradish peroxidase acted as the secondary agents, respectively. Tetramethylbenzidine (TMB) was used to indirectly measure binding of the peptide or phage to the HSA target and the reaction was stopped with 2N H_2SO_4. While the first peptide ELISA using the BR B-BR-1 peptide sample indicated that the peptide had no binding activity (**Figure 8**, $p = 0.2033$), the peptide ELISA with all the B-BR-1 samples did demonstrate that an increased amount of the AH biotinylated peptide yielded greater absorbances (**Figure 9**). The BR B-BR-1 sample had significantly greater binding to HSA than in the No HSA wells (**Figure 9**), and there was a correlation between the amount of biotin incorporated into the peptide (**Table 1**) and the biotinylated

peptide's binding to HSA (**Figure 9**). The phage ELISA, on the other hand, was unable to determine statistical significance of binding to HSA wells over the No HSA negative control wells (**Figure 14**, $p \geq 0.0971$), although a 10^4-fold higher amount of phage yielded greater absorbances. These results suggest that a greater amount of peptide should be used in future ELISAs to more adequately determine statistical significance of binding to the HSA test wells over binding to the HSA negative control wells.

In competitive ELISA assays, the concentration of ligand is measured instead. The primary detection agent is first incubated in a solution of ligand and then added to a ligand-coated microtiter well. In this method, increasing the amount of ligand in the first solution decreases the amount of free primary agent that can bind to the ligand in the well. After washing off the excess primary agent and ligand solution, a secondary agent (specific for the primary agent) conjugated to an enzyme is then added to the well and binds to the primary agent. The excess is washed off, the substrate is added and reacts with the enzyme, and the concentration of product is then measured using a plate reader to give the concentration of ligand. If the concentration of ligand in the first solution was high, the final concentration of detection agent binding to the well is lower (Owen et al. 2013).

The competitive inhibition peptide ELISAs in this study had HSA bound to the test wells with sodium bicarbonate and utilized a preincubation step with either solutions of B-BR-1 peptide and increasing amounts of soluble HSA (**Figures 10 and 11**) or wells that had increasing concentrations of HSA bound to the plate with solutions of B-BR-1 peptide added (**Figures 12 and 13**). Both types of preincubation decreased the amount of free peptide available to bind to the HSA target wells. Thus, as the amount of HSA

increased in the preincubation wells, the amount of B-BR-1 peptide that was transferred

and bound to the HSA testing wells and the subsequent absorbances decreased (**Figures**

11 and 13). The results of the HSA inhibition assay were not significant when soluble

HSA was used to decrease B-BR-1 transferred to the test wells, although the amount of

binding decreased as the amount of competing HSA increased. However, significant

inhibition was seen when 0.01 and 0.1 µg bound HSA was used to remove B-BR-1 from

solution prior to transfer to the test wells. This data is a stronger indicator of peptide

specificity for HSA than that from indirect ELISAs (**Figure 9**). This assay could be used

in future studies to test the ability of other molecules (BSA, etc.) to bind to B-BR-1.

It is interesting that bound HSA was more successful at inhibiting B-BR-1 binding to

HSA in the test wells than soluble HSA. It is possible that conformational changes in

HSA may have occurred in the preincubation wells and test wells when HSA was bound

to the wells, influencing the parts of the HSA available to bind to peptide. It should be

noted that native HSA is in suspension in blood, so it would be prudent to ensure that the

peptide is binding to free-floating albumin and not a conformationally strained form of

the albumin when used in a blood biosensor. This data may explain why BR-1 did not

bind well to human blood and indicates that we may need to reevaluate the form of HSA

used in both the biopanning wells and ELISAs. Biotinylated HSA could be used to bind

HSA to avidin coated plates in the panning wells. This might select for phage clones with

peptides that bind to soluble HSA. However, using biotinylated HSA in ELISAs could

not be done without developing a method to detect BR-1 binding that did not involve the

use of a biotinylated peptide, as enzyme conjugated to avidin would bind to the

biotinylated HSA as well as bind to the biotinylated peptide.

The results of this and previous theses concerning BR-1 binding to HSA may not be representative of day-to-day conditions. As described in Fasano et al.'s review of HSA's ligand binding properties, multiple factors such as pH, allosteric modulation, competition for binding sites, and the conformational changes HSA undergoes can affect the peptide's binding to the albumin. HSA is formed by three homologous domains that are made of two separate helical subdomains, providing multiple sites for compounds to bind. Research has been performed on Sudlow's sites and fatty acid (FA) sites utilizing aromatic carboxylates, the anticoagulant warfarin, ibuprofen, long-chain fatty acids, heme, the thyroid hormone thyroxine, benzodiazepines, the anesthetics propofol and halothane, and other compounds. For example, heme allosterically modulates warfarin binding to HSA by decreasing the amount of warfarin that can bind. Warfarin also allosterically modulates heme binding to HAS and similarly decreases the amount of heme that can bind. In addition, genetic mutations in the HSA gene affect ligand binding and may cause problems in a future blood biosensor (Fasano et al. 2005).

Ogata et al. provide a demonstration of conditions in which HSA binding to a target can be affected by the nature of the solvent. A monolithic, two-electrode electrochemical biosensor was developed by coating two gold plates with a composite containing M13 phage and an electronically conductive polymer poly(3,4 ethylenedioxythiophene), or PEDOT. The biosensor was intended for use in detecting albuminuria in patients. Phage had been selected to bind HSA and, upon binding of the biosensor to HSA, an increase in electrical impedance was measured by electrical impedance spectroscopy. The biosensor was able to detect HSA concentrations from 100 nM to 5 μM using PBS as the solvent. The Hill coefficient of $h = 1.0 \pm 0.2$ indicated that

there was no cooperativity in binding between the phage and HSA. When the biosensor was tested with urea as the solvent, however, the sensitivity was decreased by an order of magnitude and the Hill coefficient indicated negative cooperativity in binding. Thus, utilizing solutions such as PBS to replicate physiological conditions may not be representative of those found in whole blood, especially if the patient has a disease or is taking medication that can alter HSA's structure and ability to bind ligands (Ogata et al. 2017).

To produce a biosensor for commercial applications, we will need a method of producing the peptide in bulk. Huber started the work to produce our own peptide using the pMAL-c5X expression vector to fuse the BR-1 peptide to maltose-binding protein for production in the Fagan laboratory. Two primers were designed that were complementary to the pMAL-c5X vector. One of the primers also contained the BR-1 DNA sequence. Polymerase chain reaction (PCR) of the vector with these primers resulted in the incorporation of the peptide sequence into the vector (Huber 2019). Huber transformed ER2523 *E. coli* with the modified pMAL-c5X vector, cultured the bacteria, and then performed a plasmid preparation and digestion with EcoRI to sequence the DNA and confirm the peptide's amino acid sequence. The first modification of the pMAL-c5X vector almost succeeded. There was a change in the peptide's terminal codon base pairs which caused only six of the seven amino acids to be properly introduced into the vector. After graduating from Youngstown State University and submitting his thesis, Huber continued to work on the project by repeating the pMAL-c5X modification. The amino acid sequence was then completed with all seven amino acids encoding the BR-1 peptide present. A cost analysis performed by Huber indicated that the cost of producing more

than 100 mg of BR-1 peptide with the pMAL-c5X protein production and purification system was less than purchasing the peptide from a company.

Protein production and purification of the BR-1 peptide for use in a blood biosensor was initiated in this thesis. The AH3 ER 2533 *E. coli* bacteria transformed and prepared by Alexander Huber (2019) via the pMAL-c5X expression vector containing the MBP (maltose binding protein)/BR-1 fusion protein was grown in culture. Expression of the fusion protein was successfully induced in the bacteria and separated by affinity column chromatography with minimal amounts of loss in the running buffers from equilibrating, loading, and washing the column (**Figures 20** and **22**). The loss could be attributed to having a large amount of fusion protein that saturated the amylose resin and ran off into the running buffers. The BR-1 peptide, however, was unable to be visibly detected after removing it from the MBP protein in pilot protein cleavage experiments where SDS-PAGE stained with Coomassie Brilliant Blue and SYPRO Ruby were used for analysis (**Figures 23–25**). Although the inability to visually detect the BR-1 peptide bands at the bottom of the electrophoresis gels (**Figures 23** and **24)** could have been attributed to degradation of Factor Xa protease, new protease in **Figure 25** also did not yield visible peptide bands.

It was suggested by the pMAL-c5X expression vector's instruction manual to dialyze the fusion protein in order to increase Factor Xa's ability to access the preferred cleavage site Ile-Glu/Asp-Gly-Arg (New England BioLabs 2011). The reducing agent β-mercaptoethanol in 2X Laemmli sample buffer was included in **Figure 26** to break Factor Xa's disulfide bonds and separate the 42.3 kDa protease into 26.7 and 15.7 kDa subunits for better visualization of either the 43.2 kDa MBP/BR-1 fusion protein or 42.5 kDa

MBP during gel electrophoresis. After staining with SYPRO Ruby, the presence of a faint line in **Figure 26** indicated that BR-1 peptide could have been contained in the SDS-PAGE gel, although many nonspecific protein bands were present when the image contrast was enhanced. It is possible that repeated freeze-thaw cycles of the same fusion protein aliquot led to protein degradation, as the presence of similarly sized bands in **Figures 24** and **26** (ranging from 18–39 kDa) in all of the protein cleavage lanes was consistent. Despite careful loading of the samples onto the gels (no sample was visibly lost in the running buffer), contamination with the protein ladder was most visible within three lanes of the ladder when using SYPRO Ruby protein stain (**Figure 26**). No such contamination was observed when Coomassie Brilliant Blue was used in **Figure 22**. This difference in visualization of nonspecific protein bands confirmed that SYPRO Ruby is a more sensitive stain for protein detection.

The difficulty visualizing the BR-1 peptide following SDS-PAGE gel electrophoresis may be due to the peptide's small size of 764 Da and the protein production and purification process performed in this thesis (Rees 2016). A study by Haq et al. utilized the pMAL-c5X expression vector to produce a bioactive porcine myostatin (MSTN) propeptide in *E. coli*. Wild-type porcine MSTN propeptide (pMSTNProW) and mutant porcine MSTN (pMSTNProM) cDNA fragments were amplified, digested, and ligated into the pMAL-c5X vector. The vectors were transformed into the bacteria and sequenced to ensure proper fusion of the MSTN propeptide to maltose binding protein (MBP). Expression of the fusion proteins was induced, the proteins were purified, and the fusion protein was dialyzed and cleaved similarly to the methods used in this thesis (see Methods and Results above for Protein Purification from Bacterial Cytoplasm) with

several changes: transformed cells were grown to an A_{600} of 0.7–0.8 (instead of 0.63); IPTG was added to a final concentration of 0.2 mM (instead of 0.1 mM IPTG); inclusion of a Complete Mini Protease Inhibitor Cocktail Tablet (Roche, Mannheim, Germany) before sonication of the cells; use of a 2.5 x 10 cm chromatography column (instead of a 1.5 x 15 cm column); and dialysis of the MBP-pMSTNPro fusion protein against 100 volumes of Factor Xa reaction buffer consisting of 20 mM Tris, 100 mM NaCl, 2 mM $CaCl_2$, pH 7.5 at 4°C overnight with two changes during dialysis (instead of 20 volumes of 20 mM Tris-HCl, 6 M guanidine hydrochloride, pH 7.4 at room temperature for 24 hours with swirling, then twice with 100 volumes 20 mM Tris, 200 mM NaCl, 1 mM EDTA, pH 7.5 Column Buffer at room temperature for 24 hours with swirling); and incubation of 1 nm Factor Xa protease with 50 ng MBP-pMSTNPro fusion protein at 4°C for 24 hours (instead of 0.2 μg Factor Xa protease with 20 μg MBP/BR-1 fusion protein at room temperature for 24 hours). Haq et al. examined the protein cleavage mixture with a 12.5% SDS-PAGE gel (stained with Coomassie Brilliant Blue) which showed complete disappearance of the 75 kDa MBP-pMSTNPro fusion protein. They saw the appearance of two protein bands of around 43 and 29 kDa which corresponded to MBP (43 kDa) and pMSTNPro (29 kDa). Western blot analysis was used to identify each protein band with anti-MBP antibody and anti-MSTNPro antibody and confirmed their identities. Haq et al.'s cleaved protein was much larger in size than BR-1 and easier to visualize with SDS-PAGE, and their conditions for both dialysis and protein cleavage were done at temperatures which slowed down any protein degradation that could occur. Inclusion of a protease inhibitor cocktail may have also prevented degradation of the fusion protein during sonication of the cells and subsequent chromatography, dialysis, and protein

cleavage. The methods performed in this thesis could be optimized to use lower temperatures and include a protease inhibitor for future experiments to better evaluate the BR-1 peptide's ability to be produced via the pMAL-c5X expression vector (Haq et al. 2013).

Peptide detection by UV-Vis spectrophotometry following elution of peptide from the SDS-PAGE gel in this study was unable to confirm the presence of cleaved BR-1 peptide. The SDS-PAGE gel had higher absorbances than the control bands (Laemmli sample buffer dye) and peptide bands (BR-1 + Laemmli sample buffer dye) from ≈200–224 nm wavelength in the absorption spectrum (**Figure 27**). There was a noticeable difference between the control bands' and peptide bands' absorbances upon subtraction of the gel's background absorbances to remove any influence from the SDS-PAGE gel material, although the control bands' absorbances were still higher from ≈200–233 nm wavelength (**Figure 28**) which was likely attributable to the Laemmli sample buffer dye. The control bands' absorbances were subtracted from those of the peptide bands to remove the influence of the Laemmli sample buffer dye (**Figure 29**). The peptide bands still had negative absorbances from ≈200–233 nm wavelength. Since 30 µg of MBP/BR-1 fusion protein was present in the protein cleavage sample, and the fusion protein has a molecular weight of 43,246 Da while the BR-1 peptide has a molecular weight of 764 Da, and the SDS-PAGE gel was incubated in 600 µL of PBS, the maximum concentration of BR-1 peptide that could have been detected by UV-Vis spectrophotometry was 0.88 µg/mL. However, the concentration of BR-1 peptide at 214 nm was unable to be calculated since all the BR-1 standards had positive absorbances (**Figure 32**). Thus, cleavage of the BR-1 peptide from the MBP/BR-1 fusion protein was

unable to be confirmed.

A study by Conibear et al. examined the accuracy of several peptide/protein detection methods such as amino acid analysis, gravimetric analysis, nuclear magnetic resonance (NMR) spectroscopy, and UV-Vis spectrophotometry at 214 and 280 nm wavelengths in detecting small, cyclic, disulfide-rich peptides. All peptides used either were synthesized using *tert*-butyloxycarbonyl (Boc) or fluorenylmethyloxycarbonyl (Fmoc) chemistry or were extracted from the flowering plant *Oldenlandia affinis*. Upon comparison of the peptide concentrations determined by amino acid analysis and gravimetric, NMR-, and UV-Vis-based methods, all methods consistently over- or under-estimated the concentration of all five peptides studied. The concentrations calculated from UV-Vis absorbance measurements were of particular interest to this thesis. Absorbance measurements at 214 nm gave calculated concentrations about 35% lower than the amino acid analysis results, while the measurements at 280 nm gave calculated concentrations 30–300% higher. The reversed-phage high performance liquid chromatography (RP-HPLC) concentration values were closest to the values obtained from amino acid analysis, although the limiting factor for this detection method is the amount of standard with known concentration, extinction coefficient, and very similar or identical amino acid composition to the peptides being studied. RP-HPLC, however, required dilution of the samples, took up to one hour for analysis, and used equipment that was more expensive than the equipment needed for UV-Vis spectrophotometry. NMR spectroscopy was more accurate than the UV-Vis methods and was able to use a standard without the same amino acid composition or extinction coefficient as the peptide samples being analyzed. The disadvantages to NMR are that the equipment is expensive,

the method is much more complex to perform and optimize, and the NMR signals must be well-resolved for accurate calculation of peptide concentration (Conibear et al. 2012).

It is likely that the UV-Vis method for quantifying the peptide produced would work for us if contaminating electrophoresis products were removed prior to analysis. In future studies the fusion product will be digested and then the mixture put over a size exclusion chromatography column to remove any maltose binding protein and Factor Xa protease. The effluent from the column will be dialyzed extensively against water to remove any salts and other contaminants. The dialyzed effluent will be lyophilized and weighed to give an amount of peptide present. The peptide will be resuspended in a small volume of water and the UV-Vis measurement repeated. It is hoped that this method will allow purification of the peptide for future studies.

In conclusion, this thesis project was able to successfully demonstrate specificity of the biotinylated BR-1 peptide for human serum albumin (HSA). Although the biotinylated EP B-BR-1 sample was unable to give positive results in a peptide ELISA, a biotin incorporation assay was performed and showed that the BR B-BR-1 peptide sample had the most mmol biotin incorporated per mmol BR-1 peptide. The BR peptide sample was used in subsequent competitive inhibition peptide ELISAs. After optimization of the ELISA methods, specific binding of the BR-1 peptide to HSA was demonstrated. Protein production and purification followed using the AH3 ER 2523 *E. coli* (transformed with a pMAL-c5X vector encoding MBP/BR-1 fusion protein; prepared by Alexander Huber, 2019) and successfully produced a fusion protein that was purified by affinity chromatography using an amylose resin. Protein cleavage of the fusion protein to release BR-1 peptide was performed. However, due to the small size of the peptide, we

were unable to detect free peptide following SDS-PAGE gel electrophoresis. Several parameters such as temperature, dialysis solutions, and peptide detection methods can be changed in future experiments to optimize and ensure successful production of a small, durable, and specific peptide suitable for incorporation into a wearable blood biosensor. ELISAs should also be performed against albumin homologs and other substances to further validate BR-1's specificity for HSA, and the peptide will be used to functionalize carbon nanotubes that will then be used to produce sensing threads such as those tested by Dr. Pedro Cortes and Amy Olszewski (Cortes et al. 2013; Olszewski 2013). Our work will continue toward the development of a blood biosensor which can be worn by military and law enforcement personnel to detect injury, decrease response times of medical personnel, and potentially increase the survivability of those who protect and serve our country.

F. References

Adams P.A., Goold R.D., Thumser A.A. Heme-peptide/protein interactions: the binding of heme octa and undecapeptides, and microperoxidase-8 and -11, to human serum albumin. *J Inorg Biochem* 1989; 37: pp. 91–103.

Barbas C.F., Burton D.R., Scott J.K., Silverman G.J. *Phage display: A laboratory manual*. 2001. New York: Cold Spring Harbor Laboratory Press.

Barozzi M., Manicardi A., Vannucci A., Candiani A., Sozzi M., Konstantaki M., Pissadakis S., Corradini R., Selleri S., Cucinotta A. Optical fiber sensors for label-free DNA detection. *J Lightwave Technol* 2017; 35(16): pp. 3,461–3,472.

Bazan J., Calkosinski I., Andrzej G. Phage display—A powerful technique for immunotherapy. *Hum Vaccines Immunother* 2012; 8(12): pp. 1,817–1,828.

Bikiaris D., Vassiliou A., Chrissafis K., Paraskevopoulos K.M., Jannakoudakis A., Docoslis A. Effect of acid treated multiwalled carbon nanotubes on the mechanical, permeability, thermal properties and thermo-oxidative stability of isotactic polypropylene. *Polym Degrad Stab* 2008; 93(5): pp. 952–967.

Bio-Rad Laboratories, Inc. *SYPRO Ruby Protein Stains*. Instruction Manual. n.d. California: Bio-Rad Laboratories, Inc.

New England BioLabs, Inc. *Protein Tools: pMAL Protein Fusion & Purification System*. Instruction Manual. 1.2. 2011. Massachusetts: New England BioLabs, Inc.

Campbell N.A., Mitchell L.G., Reece J.B. *Biology: concepts and connections*. 3rd ed. 2000. California: Benjamin/Cummings.

Chung C.T., Niemela S.L., Miller R.H. One-step preparation of competent Escherichia
coli; transformation and storage of bacterial cells in the same solution. *Proc Natl Acad Sci USA* 1989; 86; pp. 2,172–2,175.

Conibear, A.C., Daly, N.L., Craik, D.J. Quantification of small cyclic disulfide-rich peptides. *Biopolymers* 2012; 96(6): pp. 518–524.

Cooper T.G. *The tools of biochemistry*. 1977. New York: John Wiley and Sons, Inc.

Cortes P., Olszewski A., Fagan D. "Blood detection using biological modified CNTs." AIChE MESD. 2013 Annual Meeting of The American Institute of Chemical Engineers, Materials Engineering and Sciences Division; 2013 Nov 3–8; San Francisco, CA. Youngstown (OH): Youngstown State University. pp. 1–8.

Dennis M.S., Zhang M., Meng Y.G., Kadkhodayan M., Kirchhofer D., Combs D., Damico L.A. Albumin binding as a general strategy for improving the pharmacokinetics of proteins. *J Biol Chem* 2002; 27(38): pp. 35,035–35,043.

Fasano M., Curry S., Terreno E., Galliano M., Fanali G., Narciso P., Notari S., Ascenzi P. The extraordinary ligand binding properties of human serum albumin. *Life* 2005; 57(12); 787–796.

Fischer C., Fraiwan A., Choi S. A 3D paper-based enzymatic fuel cell for self-powered, low-cost glucose monitoring. *Biosens Bioelectron* 2016; 79: pp. 193–197.

Gao Y., Kyratzis I. Covalent immobilization of proteins on carbon nanotubes using the cross-linker 1-ethyl-3-(3-dimethylaminopropyl)carbodiimide—a critical assessment. *Bioconjugate Chem* 2008; 19(10): pp. 1,945–1,950.

Grieshaber D., MacKenzie R., Vörös J., Reimhult E. Electrochemical biosensors - Sensor principles and architectures. *Sensors* 2008; 8(3): pp. 1,400–1,458.

Haq, W.Y., Kang S.K., Lee S.B., Kang, H.C., Choi, Y.J., Lee, C.N., Kim Y.S. High-level

soluble expression of bioactive porcine myostatin propeptide in E. coli. *Appl*

Microbiol Biotechnol 2013; 97: pp. 8,517–8,527.

Hey, A.S. Safety and general considerations for the use of antibodies in infectious

diseases. *Adv Exp Med Biol* 2017; 1053: pp. 265–294.

Huber A.D. *Purification of phage-displayed HSA-specific peptide for biosensor*

production. M.S. thesis. Youngstown State University, Youngstown, 2019.

Electronic.

Holzinger M., Baur J., Haddad R., Wang X., Cosnier S. Multiple functionalization of

single-walled carbon nanotubes by dip coating. *Chem Commun* 2011; 47: pp.

2,450–2,452.

Kenney, F.E. *Biosensor production by conjugation of HSA-specific peptide to*

functionalized nanotube fiber. M.S. thesis. Youngstown State University,

Youngstown, 2018. Electronic.

Maniatis T., Sambrook J., E.F. Fritsch. *Molecular cloning: a lab manual*. 1982. New

York: Cold Spring Harbor Laboratory Press.

McKnight M., Agcayazi T., Kausche H., Ghosh T., Bozkurt A. "Sensing textile seam-line

for wearable multimodal physiological monitoring." IEEE EMBC. 38th Annual

International Conference of the IEEE Engineering in Medicine and Biology

Society (EMBC); 2016 Aug 16–20; Orlando, FL. Raleigh (NC): North Carolina

State University. pp. 311–314.

Merriam-Webster. "Biosensor." In: Merriam-Webster Dictionary. Rev. Ed. Springfield

    (MO): Merriam-Webster; Updated 2018 Aug 21; Accessed 2018 Oct 1.

    https://www.merriam-webster.com/dictionary/biosensor.

Nagaraju K., Reddy R., Reddy N. A review on protein functionalized carbon nanotubes. *J*

    Appl Biomater Funct Mater 2015; 13(4): pp. e301–e312.

New England BioLabs, Inc. *Protein Tools: pMAL Protein Fusion & Purification System*.

    Instruction Manual. 1.2. 2011. Massachusetts: New England BioLabs, Inc.

New England BioLabs, Inc. *Protein Tools: Ph.D.^{TM} Phage Display Libraries*. Instruction

    Manual. 2.1. 2016. Massachusetts: New England BioLabs, Inc.

Ogata A.F., Edgar J.M., Majumdar S., Briggs J.S., Patterson S.V., Tan M.X., Kudlacek

    S.T., Schneider C.A., Weiss G.A., Penner R.M. A virus-enabled biosensor for

    human serum albumin. *Anal Chem* 2017; 89(2); pp. 1,373–1,381.

Olszewski A.L. *Synthesis, biological functionalization, and integration of carbon*

    nanotubes for bio-sensing textiles. M.S. thesis. Youngstown State University,

    Youngstown, 2013. Electronic.

Owen J.A., Punt J., Stranford S.A., Jones P.P. *Kuby Immunology*. 7th ed. 2013. New

    York: W. H. Freeman and Company.

Patton A.J., Poole-Warren L.A., Green R.A. Mechanisms for imparting conductivity to

    nonconductive polymeric biomaterials. *Macromol Biosci* 2016; 16: pp. 1,103–

    1,121.

Peters T. *All about albumin: biochemistry, genetics, and medical applications*. 1996.

    California: Academic Press.

Pierce Biotechnology, Inc. *Protein stability and storage*. Technical resource. 2003.
Illinois: Pierce Biotechnology, Inc.

Pingali A., McGuinness B., Keshishian H., Fei-Wu J., Varady L., Regnier F. Peptides as
affinity surfaces for protein purification. *J Mol Recognit* 1996; 9: pp. 426–432.

Rahbarnia L., Farajnia S., Babaei H., Majidi J., Verisi K., Tanomand A., Akbari B. Invert
biopanning: a novel method for efficient and rapid isolation of scFvs by phage
display technology. *Biologicals* 2016; 44: pp. 567–573.

Rakonjac J., Fen J., Model P. Filamentous phage are released from the bacterial
membrane by a two-step mechanism involving a short c-terminal fragment of pIII.
J Mol Biol 1999; 289: pp. 1,253–1,265.

Rees W. *Identifying peptides that bind to human serum albumin using phage display for
the development of sensors that detect injury in military personnel*. M.S. thesis.
Youngstown State University, Youngstown, 2016. Electronic.

Russell P.J., Wolfe S.L., Hertz P.E., Starr C., McMillan B. *Biology: the dynamic science*.
1st ed. 2008. California: Brooks/Cole.

Sang S.J. *The use of phage display to identify specific peptide ligands*. M.S. thesis.
Youngstown State University, Youngstown, 2014. Electronic.

Sato A.K., Sexton D.J., Morganelli L.A., Cohen E.H., Wu Q.L., Conley G.P., Streltsova
Z., Lee S.W., Devlin M., DeOliveira D.B., et al. Development of mammalian
serum albumin affinity purification media by peptide phage display. *Biotechnol
Prog* 2002; 18: pp. 182–192

Shim B.S., Chen W., Doty C., Xu C., Kotov N.A. Smart electronic yarns and wearable

      fabrics for human biomonitoring made by carbon nanotube coating with

      polyelectrolytes. *Nano Lett.* 2008; 8(12): pp. 4,151–4,157.

Sidhu S.S. Engineering M13 for phage display. *Biomol Eng* 2001; 18: pp. 57–63.

Thermo Fisher Scientific, Inc. *Coomassie Plus (Bradford) Assay Kit*. Instruction Manual.

      2011. Rockford: Pierce Biotechnology.

Thermo Fisher Scientific, Inc. *EZ-Link® Hydrazide Biotins*. Instruction Manual. 2011.

      Rockford: Pierce Biotechnology.

Thermo Fisher Scientific, Inc. *HABA*

4´-hydroxyazobenzene-2-carboxylic acid. Instruction Manual. 2012. Rockford: Pierce

      Biotechnology.

Thermo Fisher Scientific, Inc. *NanoDrop Micro-UV/Vis Spectrophotometers: NanoDrop*

      One User Guide. Instruction Manual. 2017. Rockford: Thermo Fisher Scientific,

      Inc.

Thermo Fisher Scientific, Inc. *Pierce® Graphite Spin Columns*. Instruction Manual.

      2011. Rockford: Pierce Biotechnology.

Thermo Fisher Scientific, Inc. *Pierce® Protein Methods: Biotinylation*. n.d. [accessed 15

      Apr 2020]. <https://www.thermofisher.com/us/en/home/life-science/protein-

      biology/protein-biology-learning-center/protein-biology-resource-library/pierce-

      protein-methods/biotinylation.html>

Thermo Fisher Scientific, Inc. *Procedure for using EDC for coupling haptens to a carrier*

      protein. Instruction Manual. 2011. Rockford: Pierce Biotechnology.

Thermo Fisher Scientific, Inc. *Zeba™ spin Desalting Columns*. Instruction Manual. 2013. Rockford: Pierce Biotechnology.

Willats W.G.T. Phage display: practicalities and prospects. *Plant Mol Biol* 2002; 50: pp. 837–854.

Wu J., Park J.P., Dooley K., Cropek D.M., West A.C., Banta S. Rapid development of new protein biosensors utilizing peptides obtained via phage display. *PLoS One* 2011; 6(10): e24948.

Yang N., Chen X., Ren T., Zhang P., Yang D. Carbon nanotube based biosensors. *Sens Actuators B Chem* 2015; 207: pp. 690–715.